GROUNDWATER RECHARGE ESTIMATION OF THE MALEWA CATCHMENT, NAIVASHA -KENYA

by

Angella Graham

APRIL 1998

GROUNDWATER RECHARGE ESTIMATION OF THE MALEWA CATCHMENT NAIVASHA -KENYA

BY

ANGELLA GRAHAM

THESIS SUBMITTED IN PARTIAL FULFILLMENT OF THE REQUIREMENTS FOR THE AWARD OF MASTER OF SCIENCE DEGREE IN ENVIRONMENTAL SYSTEM ANALYSIS AND MONITORING.

TO

INTERNATIONAL INSTITUTE FOR AEROSPACE SURVEY AND EARTH SCIENCES (ITC), WATER RESOURCES DEPARTMENT, ENSCHEDE, THE NETHERLANDS,
APRIL 1998

BOARD OF EXAMINERS

Prof. Dr. Ir. J. C. Van Dam (Chairman)
Delft University of Technology
Prof. Dr. A.M.J. Meijerink (Head of Department, WRS)
I.T.C. Enschede
Dr. D. Kovacs (Director of Studies)
I.T.C. Enschede
Dr. R. Becht (Supervisor)
I.T.C. Enschede
Dr. M. Lubczynski
I.T.C. Enschede

To my Mother- Loretta, Father - Cleveland, Sisters - Mitzie and Marcia and my nephew Kyle. Thanks for all your support and prayers.

TABLE OF CONTENTS

List of Figures

List of Tables

List of Appendices

ABSTRACT

Groundwater recharge is that amount of surface water which reaches the permanent water table either by direct contact in the riparian zone or by downward percolation through the overlying zone of aeration. It is this quantity which may in the long term be available for abstraction and which is therefore of prime importance in the assessment of any groundwater resource.

Groundwater recharge quantification to the Lake Naivasha is very important as there is a growing demand placed on the present available water resources. The lake currently supports intensive irrigation-based agriculture, geothermal power, fishery and tourist industries. Because of its shallow nature it is subject to considerable variation in water level.

This study uses the analysis of baseflow in an attempt to quantify groundwater recharge in the Malewa catchment. A soil water budget "WTRBLN" was also used to validate the results obtained by baseflow analysis. EC routing was used to evaluate groundwater inflow into the catchment.

These results indicate that baseflow vary between 60 and 290 mm/year. An average annual baseflow contribution of 60 mm/year was calculated as inflow to the Lake Naivasha.. This represents approximately 8% of the effective rainfall that occurs over the catchment. Total inflow, that is, baseflow and surface inflow to the lake was estimated to be 137 mm/year.

Acknowledgements

I wish to express my sincere gratitude to Dr. R. Becht, my supervisor, for directing me towards the study of Groundwater Recharge Estimation of the Malewa Catchment, and for his support. Special thanks are also due to Dr. M. Lubczynski and Dr. D.Kovacs for their critical comments on my draftscripts. I would like to thank Dr. A.S.M. Gieske for his tremendous assistance and support with the Mortons Model. I am grateful to my Director of Studies Dr. C. Mannaerts for his continuous support.

I very much appreciate the support of the following people in Kenya:

The staff of the Water Resources Assessment Project (WRAP) who gave us tremendous assistance in the field.

The Kenyan Netherlands Wetlands Training Programme, especially Mr. Bas van Helvoort, who provided substantial logistic support.

The staff and administration of Kenya Wildlife Service(KWS)- Naivasha who made their facilities available to us.

I am grateful to the Dutch Government and all the other organizations responsible for the financially support that enabled me to pursue my studies here. Special mention must be made of the Water Resources Division who granted me the time to pursue this course of Study.

Thanks to all my Msc. colleagues who have assisted me along the way. I thank the members of my immediate family and my extended church family for all their love and support through prayer. Above all I thank the Creator who guided me all the way.

1. INTRODUCTION

Naivasha is the only freshwater lake in the Central Rift Valley. The lake and its environ are important because of their biological diversity and the lake functions as a freshwater resource. It supports intensive irrigation-based agriculture, geothermal power production, fishery and tourist industries. Because of its shallow nature, the lake is subject to considerable variation in water level which may have significant consequences.

Increasing water demand with the development of this area has resulted in pressure on the water resources sector of the government to establish the Lake Naivasha Management Plan, which aims at developing a methodology to model and monitor lake level changes.

Groundwater resources investigations previously carried out in this area, aimed to integrate remotely sensed data and ground data using a GIS to assess water level changes on three lakes in the Central Kenyan Rift Valley, Naivasha, Elmenteita and Nakuru. The database was used to implement a hydrological model capable of accurately predicting annual average lake level changes for these lakes.

This study applies remote sensing in conjunction with point data over the Naivasha area to assess and quantify recharge from the Malewa Catchment.

1.1 Study Aims and Methods

The aim of the study is to elucidate surficial information obtained by Remote Sensing and fieldwork in conjunction with collected meteorological point data to:

(i) Evaluate the spatial variation of groundwater recharge from the Malewa Catchment.

(ii) Quantify recharge from baseflow analysis and the "WTRBLN" model, using new and previously existing data and extrapolation of data from the adjoining project areas

Methods:-Geophysics (largely unsuccessful)
- Remote sensing -TM bands
- GIS
- Waterbalance-climatological data)

1.2 Previous Work:

The main hydrogeological work done in the area is summarized in a final report entitled Monitoring Lakes in Kenya: An Environmental Analysis Methodology for Developing Countries. This report aimed to develop a methodology to model and monitor lake level changes on three Rift Valley lakes in Kenya. The report contains information on the general geology, hydrogeology and climatological data of the area. A hydrological mathematical model was implemented to provide a simulation of lake level changes. This model was fairly successful and has a sufficiently flexible structure to permit adaptation.

A report entitled" Geological, volcanological and hydrogeological controls on the occurrence of geothermal activity in the area surrounding Lake Naivasha, Kenya"contains information on geology, hydrogeology (physical and chemical), petrology and geothermal sources. The aim of this report was to provide a detailed geological and geothermal mapping of the Longonot volcano and surroundings in the central Rift Valley. A reconnaissance sampling of surface waters over the whole length of the Rift Valley was done.

The report "Studies of Lake Naivasha, Kenya and its Drainage Area" provided information on the geology, climatological data, vegetation, and the water budget of the lake.

In "A Three Phase Environmental Impact Study of Recent Developments Around Lake Naivasha" the ecology of the lake and its environs was studied. The aim of the report was to study the environment impact of the lake to ensure sustainable use of the resource in the future.

A systematic geological survey of the study area is covered in Report Number 55 entitled "Geology of the Naivasha Area.

Available maps are shown in Table 1.2a

Table 1.2a Available Maps

Map	Sheet	Title	Date	Map Scale	Source
Topographic	SA-37-1	Nyeri	1981	1:250000	Survey of Kenya
Topographic	133/2	Naivasha	1975	1:50000	UK Ordnance Survey Overseas Survey Department maps
Topographic	120/3	Kipipri	1975	1:50000	UK Ordnance Survey Overseas Survey Department maps
Topographic	119/4	Gilgil	1975	1:50000	UK Ordnance Survey Overseas Survey Department maps
Topographic	119/3	Nakuru	1974	1:50000	UK Ordnance Survey Overseas Survey Department maps
Geological		Geological Map of Longonot Volcano,The Greater Olkaria And Eburru Volcanic Complexes, And Adjacent Areas	1988	1:100,000	Government of Kenya Ministry of Energy Geothermal Section
Soil		Exploratory Soil Map Of Kenya	1980	1:1000,000	Republic of Kenya, Ministry of Agriculture Kenya Soil Survey, Nairobi

A qualitative description of the geology and hydrogeological environment can be obtained from the reports listed in Table 1.2b.

Table 1.2b Available Reports

Report Title	Authors	Year
Geology of the Naivasha Area	Thompson, A.O. and Dodson, R.G.,	1963
Studies of Lake Naivasha, Kenya and its Drainage Area	Ase,L.E., Sernbo, K. and Per, S.	1986
Geological, volcanological and hydrogeological controls on the occurrence of geothermal activity in the area surrounding Lake Naivasha, Kenya	Clarke, M.C.G.,Woodhall, D.G., Allen, D. and Darling, G.	1990
A Three Phase Environmental Impact Study of Recent Development Around Lake Naivasha - Phase I	Lake Naivasha Riparian Owners Association	1993
Monitoring Lakes in Kenya: An Environmental Analysis Methodology for Developing Countries	Stuttard, M., Hayball, J., Narciso, G., Carizi, G., Suppo, M., Catani, R., Isavwa, L., Baraza, J., Oroda, A.	1995
Lake Naivasha Management Plan	Lake Naivasha Riparian Owners Association	1996

1.3 Methodology

1.31 Primary Methodology

In the field the ABEM Terrameter (which measures earth resistivity) was used in an attempt to determine soil moisture distribution in different soil type and ground cover and to establish the soil rooting depth of the unsaturated zone. This was done as resistivity measurements are sensitive to soil moisture and decreases with increasing moisture. Soil texture also influences resistivity where resistivity increases in clayey soil as opposed to sandy soil with little moisture.

Measurements were done in areas representing the main ground cover type and in different soil type. Here a three-layered earth model was assumed in which the upper layer is thin and moist, the second layer is relatively moist and drier and the third layer

where the soil approaches field capacity. Below this it was assumed that the water table would occur. These assumptions were based on the standard one-dimensional earth model.

A resistivity logger was used in auger holes was used in an attempt to verify the findings of the soundings. Hence for several locations, soundings were made using the ABEM Terrameter, auger holes were drilled and the down-the hole geophysics device was used to verify the findings. Soil samples were also collected and a soil moisture sensor (Theta probe, Delta T) was used to determine the water content. Resistivity profiling were also done across different cover type to detect changes in soil moisture distribution across different ground cover.

Analysis of this findings did not yield the results expected as no change in the soil moisture distribution was noted, among different cover type and soil, in the interpretation of the resistivity data and curves. Furthermore the results of the soundings could not be verified due to malfunctioning of several of the equipment.

1.32 Secondary Methodology

As a result of the unsuccessful attempt at quantifying groundwater recharge with the aid of geophysics, a modified waterbalance Model of Thornethwaite and Mather (WTRBLN-Donker 1988) and the analysis of streamflow were used in an attempt to quantify groundwater recharge. These model involved the use of meteorological data, soil characteristics and landcover type. Baseflow separation was done in an attempt to quantify recharge from the gauged areas of the catchment. Electrical Conductivity routing was also done in an attempt to calculate groundwater inflow into the basin.

1.33 Procedure

The methodology applied in the study can be divided into three phases.

Phase I) Pre-Fieldwork
Major activity involved:
-Digitizing Drainage, Contour lines, Water bodies, Roads, Geology, Soil etc. Aerial photographs and existing geological maps were used to determine areas of interest.

-TM images were georeferenced to the Universal Transverse Mercator (UTM) international coordinate system . Image processing (correction, information extraction) was done using Ilwis - Integrated Land and Water Management Information System" software.

- Testing and configuration of Data Logger and Sensors.

Phase2) Fieldwork

The major tasks executed during this period include:

- Fieldcheck of various attributes and classifications prepared in the preceding step,
- Identification of landuse/landcover types
- Institutions were visited in an attempt to gather information (meteorological, stream discharge, soil, landuse etc.)
- Augering to assess the texture of the upper part of the soil and to find the depth of the rooting zone.
- Electrical Conductivity (EC) routing of the River Malewa and its tributaries.
- Installation of a semi-permanent Logging semi-permanent logging station on the property at Kenya Wildlife Service (KWS). Three temperature sensors, three relative humidity sensors and a rain gauge were installed above ground and three resistance sensors and a theta probe was installed underground.

Phase 3) Post-Fieldwork

In this phase all the data collected was analyzed in the framework of a water budget to arrive at a point estimate of groundwater recharge from the Malewa catchment.

Fig 1.3 overleaf shows a project activity flow chart.

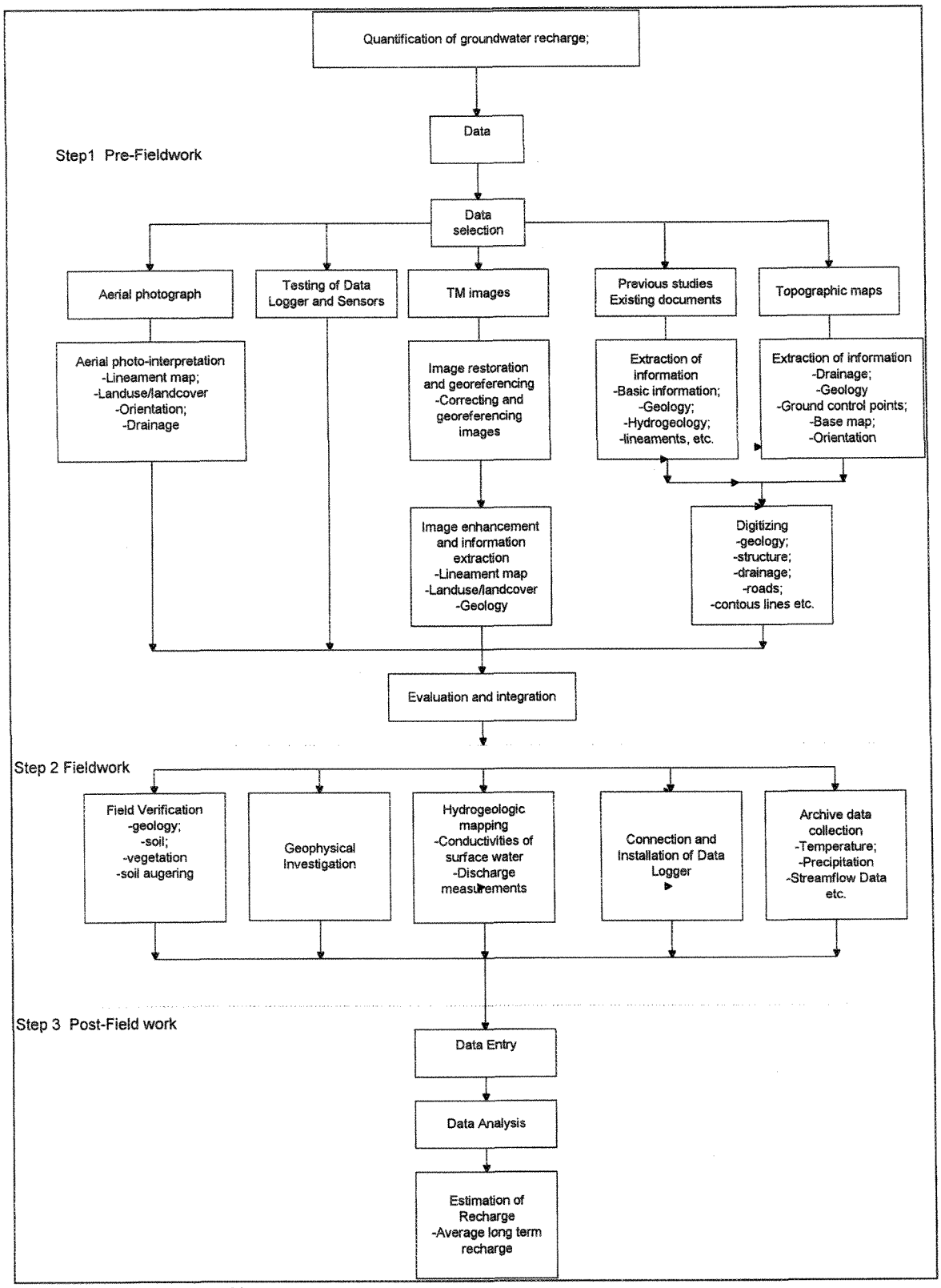

Fig. 1.3 Project Activity Chart

2.0 PROJECT AREA

2.1 Location

The study area is situated in Naivasha - Kenya within the East African section of the Rift Valley, 70 km north-west of Nairobi (Fig.2.1a). The area is located in UTM Zone 37 South lying between coordinates 148491, 9983010 mm North and 245000, 9897500 mm East. The area is bounded by latitude 0 ° 09′ S and 0° 55′ S and by longitudes 35° 50′ E and 36 ° 42′ E. This section of the Rift valley is confined by the Nyandarua Mountains (formerly the Aberdares) to the east (elevated to over 3,960m) and the Mau Escarpment to the west (exceeding 3,000m), to the South by Mount Longonot (exceeding 2400m) and to the North by the Menengai Crater (exceeding 2100m) (Fig. 2.1b). The width of the Rift Valley within this region varies between 45 and 70 km.

2.2 Size and Physiography of the Basin

The basin may be described as a graben which is defined by major NNW-SSE trending faults. The floor of the basin is gently sloping and is highest in the central portion between Nakuru and Lake Naivasha where it is almost 2000m amsl and decreases in altitude northwards to 300m amsl and southwards to 600m amsl.

The River Malewa drainage basin covers an area of 1553 km^2. About 73 % of the area is situated within the Kinangop Plateau and lies at levels between 2100-2700 m amsl (Fig. 2.1b). 22 % of the area lies between an altitude of 2700-3900 m above mean sea level. These area are the hills and slopes of the Nyandarua Range. The remaining 5% is located at altitudes of less than 2100 m above mean sea level. These areas are located in the vicinity of the lake.

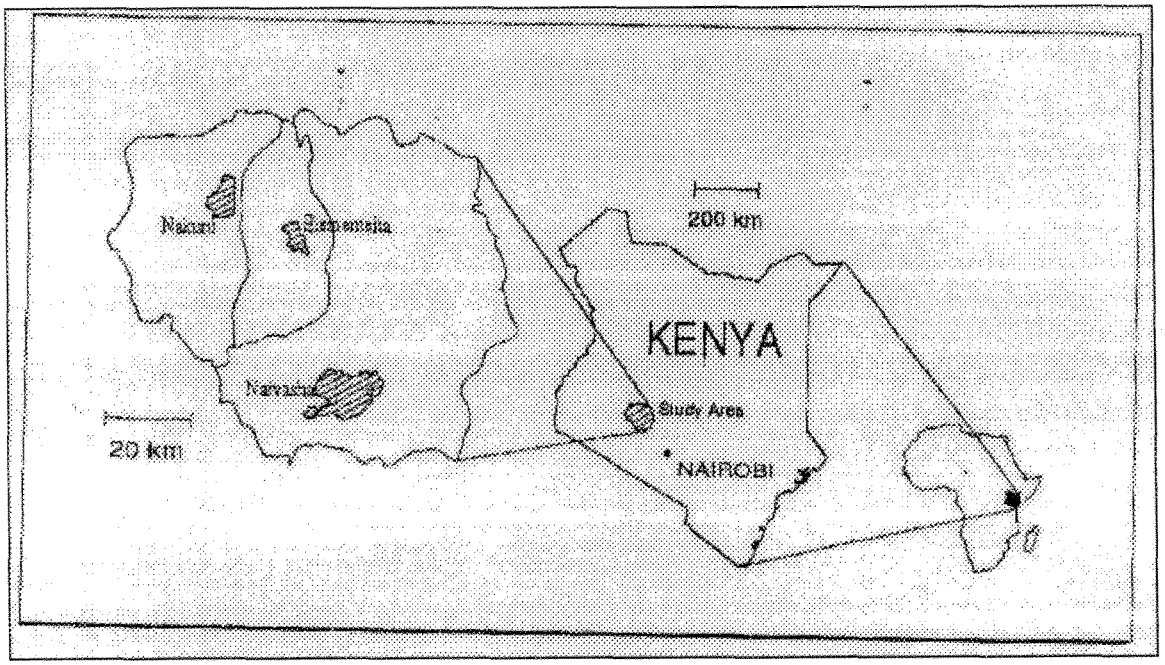

Fig. 2.1a Location of the Study Area (adapted from "Monitoring Lakes in Kenya: An Environmental Analysis Methodology for Developing Countries" by Stuttard et al., 1995).

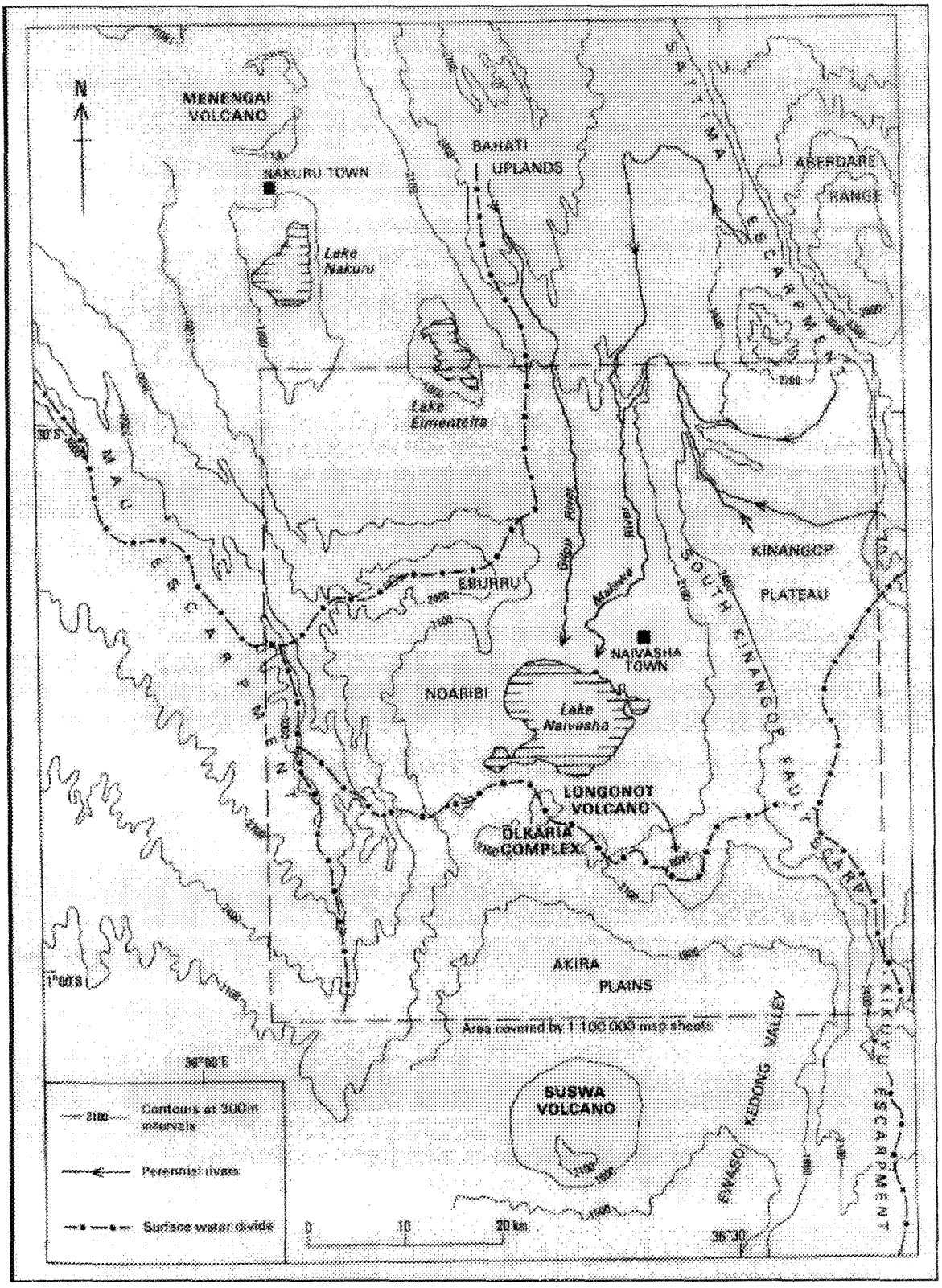

Fig. 2.1b Physiography of the Central Rift Valley (adapted from "Monitoring Lakes in Kenya: An Environmental Analysis Methodology for Developing Countries" by Stuttard et al., 1995).

2.3 Geomorphology

The study area is situated within the large African Rift System and its geological evolution has influenced the geomorphology and hydrogeology in the area. Two major geomorphological groups can be observed.

(1) The Rift Margins :

These are North- South oriented and comprised of the Mau Escarpment in the west and the Kinangop Plateau in the east.

The Kinangop Plateau lies in the south-eastern part of the area between the Aberdare range and the Rift floor (Fig. 2.1b). It is a broad flat plain ranging in height from 2379 m to a maximum elevation of about 2740 m above mean sea level. Its western margin is defined by the north-north-west trending South Kinangop fault scarp which ranges in height from 100 m to 240 m. It is deeply incised by the tributaries of Malewa river. Gorges of depths 61 and 122m have been formed along the northern edge of the area. Along much of its length, this scarp has very steep or vertical rock face above less steep talus slopes. The crest of the scarp is between 500 and 600 m high relative to the rift floor , but is separated from the floor by a series of downfaulted platforms.

The north-north-west trending Mau Escarpment forms the western edge of the Naivasha basin. It attained a maximum elevation of just over 3080m at some localities but is over 3000m for 36 km of its length within the map area, decreasing in height both north and south. Rifting has produced down-faulted platforms which separate the Mau Escarpment from the rift floor proper.

(2) Rift floor plains:

The Rift floor forms part of the Gregory Rift Valley. It is diverse in its structures and topography where numerous volcanic cones and crater, scarps and lakes are found. It reaches its highest elevation (near 2000 m) in the vicinity of Elmenteita and Naivasha. High points are formed by Mount Longonot and Eburru, both of which rise over 2745 m above mean sea level. On the western and south-western shores of the Lake Naivasha numerous volcanic craters exist.

The Lake Naivasha dominates the Naivasha basin. The lake covers an area of approximately 145 km^2 and stands at an elevation of 1882.4 m amsl (October 1997). The lake is smooth floored and has a mean depth of 4.7 m

2.4 Drainage Network

The lake Naivasha catchment area covers an area of approximately 3387 km2 and is drained by two major rivers, Malewa and Gilgil (Fig. 2.1b). These rivers are perennial in nature.

The River Malewa drainage basin comprises approximately 23% of the Naivasha basin. The river rises on the western slopes of the Nyandarua range (Aberdares) at an altitude of 3,400 m. The small streams flow westwards and develop into four main tributaries - the Mugutyu, the Turasha, Kitiri and Makungi. All four flow north-south before turning west and joining the Malewa. The Turasha is the most important tributary and joins the Malewa approximately 8 km east of Gilgil Town (Fig.2.4). The tributaries of the Malewa river form a very dense dendritic drainage pattern except in the Kipipiri area and where they have a radial pattern due to the conical shape of the volcano. These rivers however tend to disappear before entering the lake.

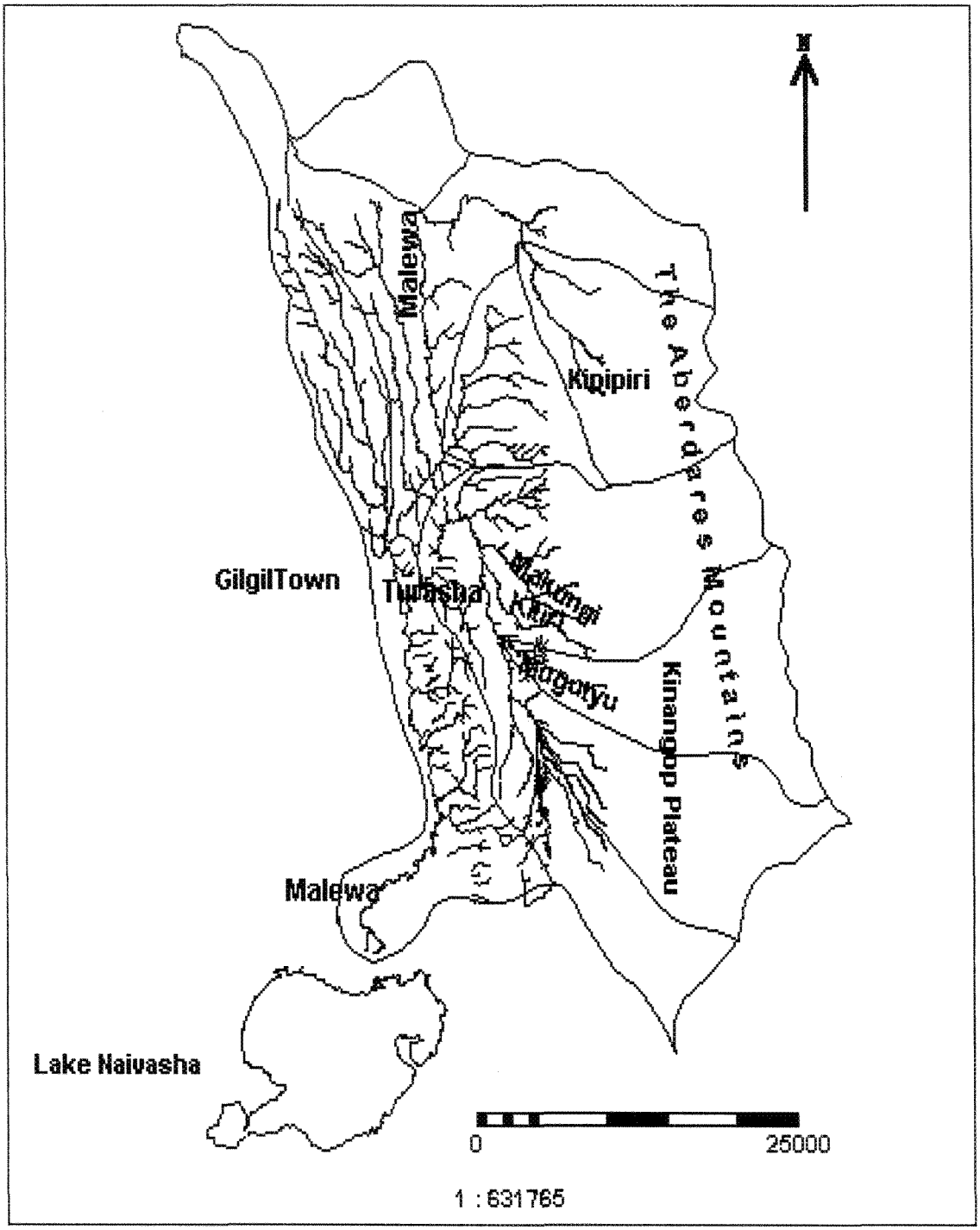

Fig. 2.4 The Malewa River and its major Tributaries.

2.5 Climate

2.5.1 The Tropical Climate of Kenya

The tropical climate of Kenya is characterized by large diurnal temperature variations, small variations of the mean monthly air temperature throughout the year and by seasonal rainfall regimes. Kenya's equatorial position also results in the number of daylight hours being more or less constant all year round.

The seasonal moisture regime of the Rift valley is characterized by two rainy seasons following both equinoxes. The period of maximum rainfall, the so-called "long rains" occurs from March to May and is followed by a short dry season from June to September. The "short rains" from October to December are followed by a short dry season which lasts from January to February.

This seasonal pattern of precipitation reflects the seasonal shifts of the ITCZ (Inter-Tropical Convergence Zone) and of the wind systems. The atmospheric circulation patterns are governed by four main surface currents:

- the NE monsoon from November to the end of April , carrying drier air masses from Egypt and Sudan.
- the SE monsoon from June to the end of October , carrying moister maritime air.
- the SW monsoon or Congo air which may affect western Kenya from June to October.
- "easterlies" which are dominant at the coast during the dry season July to September

2.5.2 The Climate of the Study Area

The Study Area is subject to the same general circulation patterns and associated rainfall regimes as the rest of the country. Climatic conditions are quite diverse due to considerable differences in altitude and landforms. There are primarily two types of climatic conditions which exist in the study area. These refer to the semi-arid climate of the Rift-Floor and the wet conditions which exists on the upper catchment areas of The Aberdares.

2.5.3 Temperature

Generally temperature over the study area is quite diverse due to considerable differences in altitude and landforms. The East African Meteorological Department calculated a decrease in temperature of 0.56 ^{0} C for every 100m of increase in elevation.

Temperature data was obtained from the station Nakuru and Nyeri. These stations lie outside the study area but represent the nearest stations from which climatological data was available. The station at Nakuru represents the western area of the catchment and includes areas such as Turasha and Ol Kalou and the Nyeri station represents the eastern section of the catchment (The Aberdares and The Kinangop Plateau). The data set covers the period 1994-1997 and was obtained from the National Climatic Data Centre (NCDC) from the Internet. Temperature data for the period 1994-1997 was available as daily maximum, minimum and mean temperature. The daily data has been processed to estimate monthly temperatures for the area.

Table 2.6 Maximum, Minimum and Mean Temperatures (°C)- Nakuru

STATION													
NAKURU	Date	JAN	FEB	MAR	APR	MAY	JUN	JUL	AUG	SEP	OCT	NOV	DEC
Mean Max.	1994-1997	28.12	28.92	27.56	26.29	26.53	25.89	25.02	24.95	27.36	27.18	26.63	25.83
Mean Min	1994-1997	10.36	10.89	11.52	12.15	12.56	12.49	12.19	10.79	11.72	12.42	13.08	11.53
Mean	1994-1997	19.95	20.27	19.08	18.13	17.97	17.37	16.96	17.58	17.65	17.46	17.08	16.70
Highest Max.	1994-1997	28.76	29.31	29.87	30.42	30.98	31.53	32.09	32.65	33.20	33.76	34.31	34.87
Lowest Min.	1994-1997	9.69	9.67	9.26	11.38	11.40	11.86	10.87	5.87	9.42	10.24	10.93	6.05

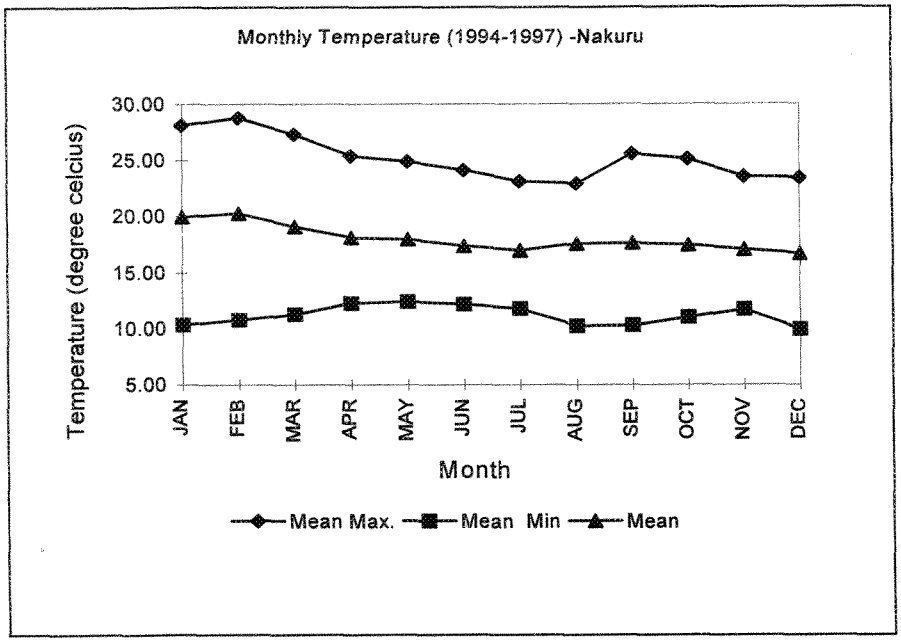

Fig.2.6

Table 2.6 and Fig 2.6 indicate that temperature in the vicinity of Nakuru area is relatively stable with mean monthly temperatures varying between 17 ^{0} C and 20 ^{0} C. Mean minimum temperatures were recorded during the month of December and mean maximum in February. A mean maximum temperatures of 29 ^{0} C was recorded in January and a mean minimum of 10 ^{0} C recorded in January . The mean annual temperature calculated is 18 ^{0} C .

Table 2.7 Maximum, Minimum and Mean Temperatures (^{0} C) Nyeri

Station													
NYERI	Date	JAN	FEB	MAR	APR	MAY	JUN	JUL	AUG	SEP	OCT	NOV	DEC
Mean Max.	1994-1997	25.98	25.75	25.39	23.35	22.10	20.69	19.97	19.37	23.72	24.11	22.29	20.58
Mean Min.	1994-1997	9.81	8.61	11.90	13.23	13.25	12.36	11.99	10.72	12.17	13.36	12.73	9.45
Mean	1994-1997	18.01	18.51	17.86	18.41	17.61	16.71	15.35	15.63	17.27	17.85	16.68	16.24
Highest Max.	1994-1997	27.22	29.25	27.59	25.91	23.38	22.09	20.68	20.48	25.67	25.92	23.86	23.61
Lowest Min.	1994-1997	10.27	10.40	12.73	14.60	14.23	13.37	12.29	12.25	12.47	14.23	13.74	13.74

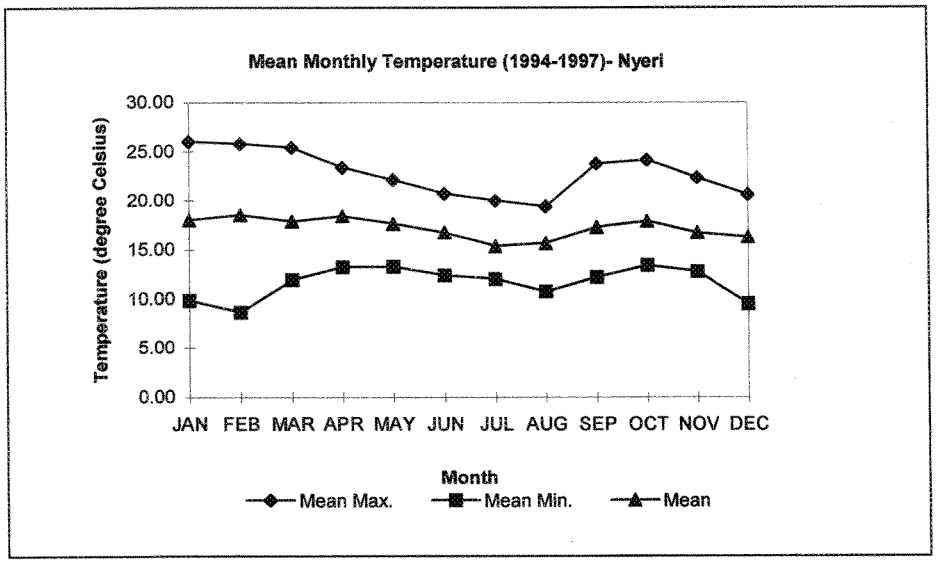

Fig. 2.7

The Station at Nyeri indicate that temperature in this vicinity is relatively stable with mean minimum of about 9 ^{0} C in February and December. Mean maximum temperature varying between 24 and 26 ^{0} C were noted during the months of January, February, September and October. The mean annual temperature as calculated from available data over the specified period is 17 ^{0} C (Fig. 2.7 and Table 2.7).

2.54 Rainfall

Rainfall per annum varies over the area. Long term average annual rainfall shows a variation from 598 mm/year to 1279 mm/year. Rainfall is seasonal and there are primarily two rainy periods per year; the long rains in March, April and May and the short rains in October and November.

2.5.5 Potential Evapotranspiration

Potential Evapotranspiration was calculated using Morton's 1983-CRAE Model.
In the area of the Rift Valley potential evapotranspiration varies from 2117 mm/year to 2251 mm/year. This represents the yearly average from 1994-1997. In the eastern area of the catchment potential evapotranspiration varies from 1947 to 2046 mm/year. There is very little spatial variation, but there is a marked seasonality where Potential Evapotranspiration is highest during dry periods and lowest during rainy periods. This is

expected as rainy periods are characterized by high relative humidity Evapotranspiration also was notably higher in areas where there is little soil cover and low rainfall than in the areas of the upper catchment which is characterized by dense vegetation and higher rainfall.

2.6 Vegetation and Landuse

The Lake Naivasha and its catchment areas represent important ecological sites in Kenya due to the diversity of fauna and flora which are distributed through a range of vegetation zones.

The vegetation in the catchment can be divided into four (4) groups. They are forest, wooded grassland, bushland, and grassland. These vegetation types were categorized into three eco-climatic zones by Pratt and Gwyne ("Monitoring Lakes in Kenya: An Environmental Analysis Methodology for Developing Countries" by Stuttard et al., 1995):

Zone II (Humid to dry semi-humid) featuring natural forests, Montane Acacia woodland and intensive agricultural lands mainly around mountainous areas such as The Aberdares.

Zone III (Dry sub-humid to semi-arid) having high agricultural potential. These are areas which lie to the north of Nakuru and the rainshadow slopes of the mountains and include the Kinangop Plateau areas.

Zone IV (semi-arid) these are described as high potential rangelands which are important for grazing purposes. These areas are located in the rift-valley floor and can be found Southeast of Lake Nakuru and in the vicinity of Lake Naivasha.

The natural forest within the study area is comprised of indigenous hardwood trees and grasses such as bamboos. These are mainly found in the upper section of the catchment area in the Aberdares Forest. These form the main watershed of the lakes. Acacia forests are found beside the lakes. The greatest proportion of the low lying central parts of the catchment are rangelands.

2.6.1 Farming

The study area is situated in an a rural area, thus agriculture is the most important economic activity.
The main farming system in this area is described as mixed farming. Land use patterns can be broadly categorized as follows: rainfed crop production (dominant) and irrigated, mainly horticultural production.

Rainfed agriculture are practiced mainly on the slopes of the Aberdares. Irrigated crop farming is common near Lake Naivasha where wheat, barley, beans and fodder crops are cultivated. Horticulture is also widely practiced in the vicinity of the lake. Main products are flowers, vegetables and fruits.

Extensive or Range Livestock production is mainly practiced in the drier parts of the catchment such as North-north-east of the lake and intensive Livestock production is practiced in areas around Naivasha.

2.7 Water use

Water demand from the Lake Naivasha is primarily for agricultural, geothermal power production and domestic purposes. A water diversion scheme has been implemented in the Malewa catchment which takes water out of the catchment for the supply of Nakuru and Gilgil Town. These competing water uses in addition to the declining lake level make it necessary to quantify the recharge from the Malewa catchment.

2.8 Communication Links

The road from Nairobi to Uganda and Sudan crosses this region. The main road in this region forms part of the Trans-African Highway and the Great North Road. The main line of the East African Railways also passes through the eastern part of the area and is followed closely by the main road from Nairobi to Nakuru. The region is thus the focus of important communication links.

3.0 LAND COVER CLASSIFICATION AND ANALYSIS BASED ON REMOTE SENSING

Remotely sensed data was used for landcover classification and analysis. This methodology was used as different cover types has its unique spectral response in the electromagnetic spectrum.

The objective of this chapter is to identify vegetation cover and landuse type and use it in groundwater recharge assessment.

3.1 Available Data

Data Available for Land Cover Classification and analysis include :

Aerial Photographs (1992), scale 1:50000
Date: 1984

Remotely Sensed Data: Thematic Mapper (TM) Data
Bands: TM1, TM2, TM3, TM4, TM5, TM6 and TM7
Date: 21st January 1995, (Dry Season)
Pixel Size: 30m *30 m
Rows : 2851
Columns : 2885

These images represent the dry season images. This allows the study of vegetation cover analysis and the identification of vegetation cover that is present throughout the year.

3.2 Image Restoration

Digital image processing involves the manipulation and interpretation of digital images with the aid of a computer. Before satellite data can be used for information extraction it has to be corrected for systematic and non-systematic errors. The aim of image rectification and restoration is to correct image data for distortions or degradation that stem from the image acquisition process. The nature of such procedures varied considerably with such factors as the digital image acquisition type and total field of view.

3.21 Haze Correction

Haze compensation procedures are designed to minimize the influence of sensor and viewing conditions, i.e., atmospheric degradation and illumination effects. The atmosphere scatters shorter wavelength which introduces haze in the imagery and reduces image contrast. To improve the interpretability of images haze correction has to be applied. There are two techniques which are usually applied to eliminate haze. There are:

(1) The first method of haze compensation involves the observation of the radiance (Digital Numbers- DN) recorded over target areas of essentially zero reflectance in the near infrared band. Such areas correspond to deep clear water. Any offset (non-zero values on shadow or water bodies) represents the path radiance and this value can be subtracted from all pixels in that band and the other bands.

(2) The second method of haze correction involves the conversion of DN's to absolute radiance values. This entails the calculation of histograms of the digital information for individual bands. The minimum value of the histogram of each band is subtracted from the data set. The histogram is shifted to the origin, and thus the atmospheric effect is subtracted.

The first method was used in carrying out haze correction on the images.

3.22 Geometric Correction

Digital images usually contain geometric distortions due to factors such as variations in the altitude, attitude, earth curvature, atmospheric refraction and relief displacement. The first step in the correction of the image include the georeferencing of the images to UTM Zone 37 coordinate. Secondly 41 well-distributed ground control points (GCPs) were identified in the image and their image coordinates(column, row numbers) recorded. The same (GCPs) were identified on aerial photographs and their coordinates in terms of UTM coordinates Zone 37 (X and Y coordinates) were noted. The entered (GCPs) make it possible to derive a mathematical equation that relates the rows and columns numbers to X and Y coordinates. Affine transformation was carried out to reach the goal. The images were then resampled using the nearest neighbour technique. The error in georeferencing had a sigma of 2.114m.

3.3 Band Selection and Image Interpretation.

In determining the land cover of the study area, a number of spectral band combination were used to produce false colour composites (Red, Blue, Green) that would aid in the identification of the different land cover. This is because different cover types has its unique spectral response in the electromagnetic spectrum(Table 3.3) Principal Component analysis was performed using bands 1,2,3,4,5 and 7 to check the correlation between bands.

Table 3.3 Thematic Mapper Spectral Bands

Band	Wavelength (μm)	Nominal Spectral Location	Principal Applications
1	0.45-0.52	Blue	Soil/vegetation discrimination, forest type mapping
2	0.52-0.60	Green	Vegetation discrimination and vigor assessment
3	0.63-0.69	Red	Aid in plant species differentiation.
4	0.76-0.90	Near Infrared	Determining vegetation types, vigor and biomass content and for soil moisture discrimination
5	1.55-1.75	Mid-infrared	Indicative of vegetation moisture content and soil moisture.
6[a]	10.4-12.5	Thermal infrared	Useful in vegetation stress analysis, soil moisture discrimination and thermal mapping applications.
7[a]	2.08-2.35	Mid-infrared	Useful for discrimination of mineral and rock types. Also sensitive to vegetation moisture content.

Source: Lillesand, T.M. and Keifer, R.W., -1994- Remote Sensing and Image Interpretation

The following band combinations yielded the best results:

NDVI - using Landsat TM (TM4-TM3)/ (TM4+TM3)- for vegetation density mapping
TM bands 4,5,3 -RGB False Colour Composite for Landcover Classification
TM6 (Thermal) Pseudo colour image-temperature mapping/moisture.

3.3.1 Normalized Difference Vegetation Indices (NDVI)

Vegetation has an important effect on water budget because of evapotranspiration losses and rainfall-runoff responses (Meijerink, et al.,1994).

Vegetation indices (VI) are combinations of reflectance of two or more lands, usually in the visible red band and the near infrared band (Meijerink, et al.1994). These bands have been found to be to be sensitive indicators to the presence and vigor of vegetation. Green vegetation has a low reflectance of vegetation in the red band and high reflectance in the

near infrared band. This unique sharp contrast in reflectance makes vegetation separable from other cover types.

The most commonly used vegetation index is the normalized difference vegetation index:

$$NDVI = \frac{(R_{nir} - R_{red})}{(R_{nir} + R_{red})}$$

Where R_{nir} = Reflectance in the Near Infrared Band
R_{red} = Reflectance in the Red Band

The NDVI helps to compensate for changing illumination condition, surface slope, aspect, and other extraneous factors. The index was developed by Rouse et al., (1974) using the Landsat bands 7 and 5 (Meijerink et al., 1994) The NDVI is a bounded ratio which ranges in value from -1 to +1. Vegetated areas generally yield high values for these indexes because of their relatively high near-infrared reflectance and low visible reflectance. Rocks and areas of bare soil have similar reflectance in the two bands and result in vegetation indices near zero. Cloud, water and snow have large visible reflectance than near-infrared thus yielding negative index values.

A scaling factor NDVI'=NDVI *127+128 was used. The offset value of 128 was used to eliminate negative values and the scale of 127 was used to expand the data display. The scale of the map was readjusted to range between 0 and 255.

3.3.1.1 Interpretation of the NDVI Image

Interpretation of the NDVI image of the area (Fig. 3.3.1.1) shows that vegetation in the area is not homogenous and there are distinct areas such as in the highland region of The Aberdares and Kipipiri where the vegetation cover is dense and hence appears red denoting high NDVI values. These areas correspond to woodland and forested areas. Orange areas reflect area of rainfed agriculture commonly practiced on the slopes of the Aberdares and on areas of the Kinangop Plateau. Green color denotes areas where dryland agriculture is practiced. These relatively high NDVI values indicate that dry arable farming uses a lot of soil moisture. Low NDVI values - blue colored areas are classified as rangeland, indicating shallow soil and sparse vegetation cover .

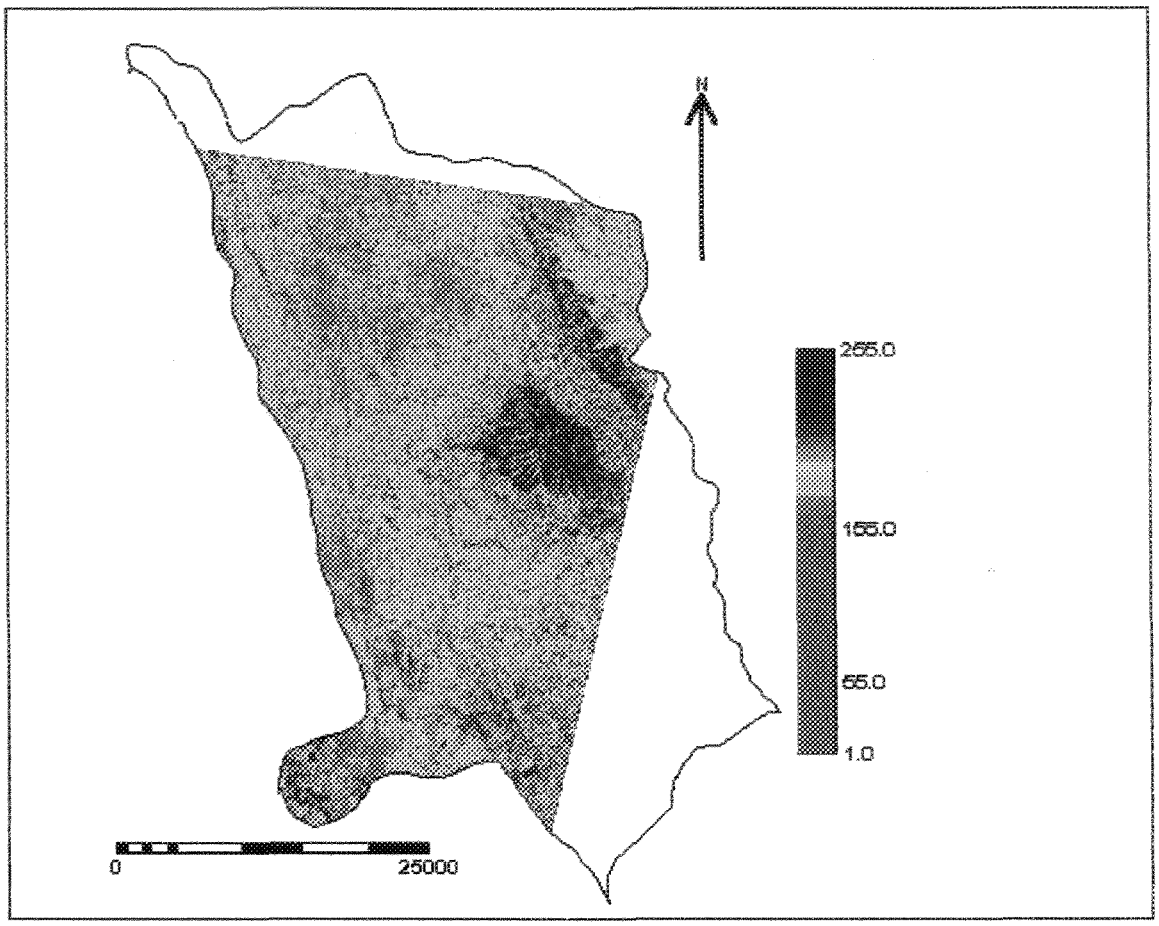

Fig. 3.3.1.1 Landsat TM -NDVI Pseudocolour

3.3.2 Landsat TM Band 6 (Thermal) Pseudocolour

TM band 6 is frequently used in thermal mapping applications for surface temperatures. In pseudo- color shades of blue denotes "cool temperatures" and yellow-orange-red denotes increasingly warmer values (Fig. 3.32). Areas with cooler temperatures were found in thickly forested places occurring at high altitudes such as the Aberdares and the Kipipiri Mountain. These cool areas can be characterized as having high soil moisture content due to the thick vegetative cover and higher rainfall. Areas where rainfed agriculture is practised are indicated in yellow. "Red" areas correspond to those rangelands and areas where dryland farming is practised.

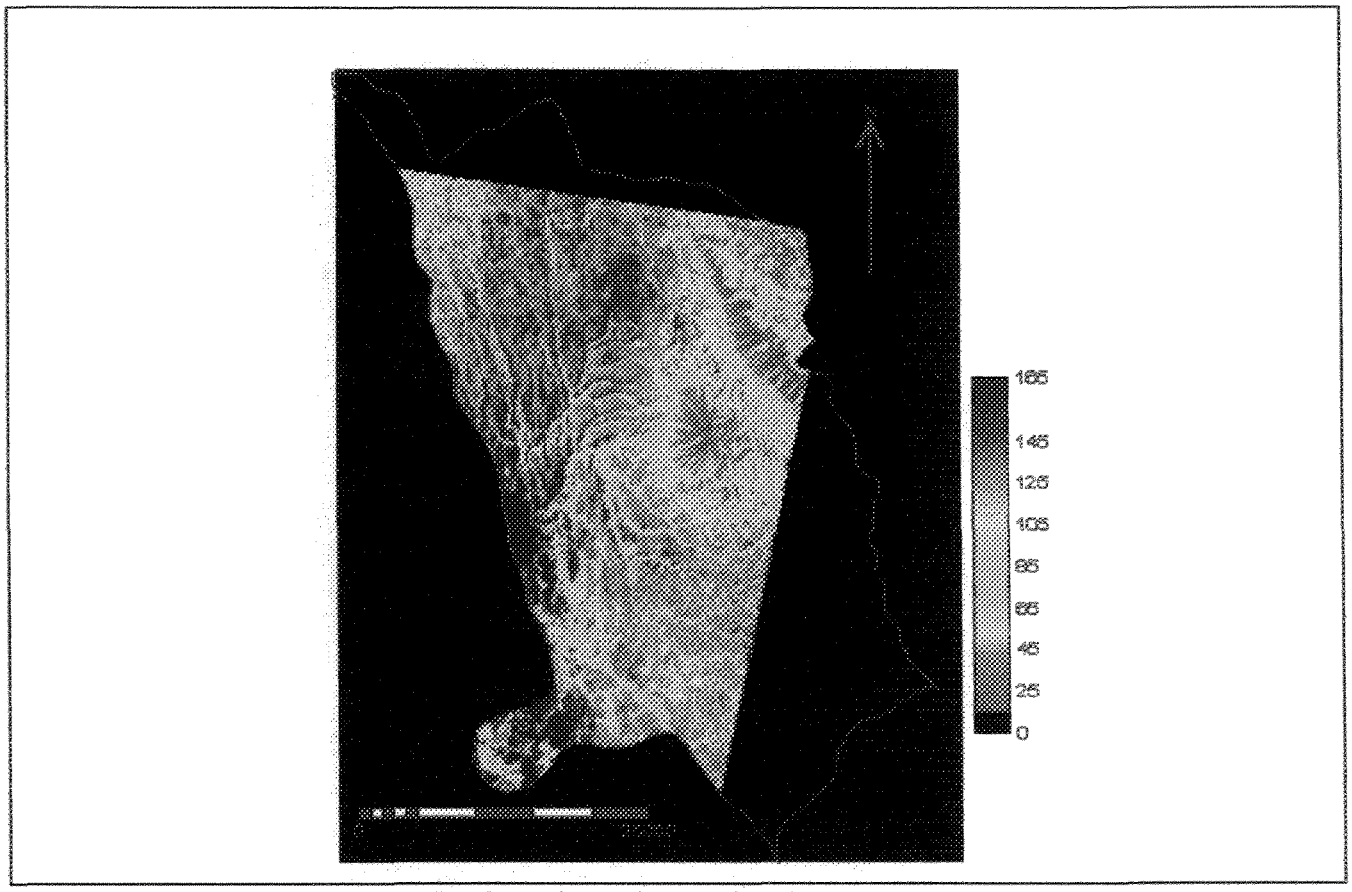

Fig. 3.32 Landsat TM Band 6 (Thermal) Pseudocolour

4.0 GEOLOGY

4.1 Introduction

The Study area is located in the Eastern section of the African Rift Valley (Gregory Rift). The Basin has been subjected to numerous tectonic episodes and is characterized by prominent morphological and structural features. The geology of the area is characterized by volcanic rocks and Quaternary lacustrine deposits. Table 4.1 gives a summarized stratigraphy of the area. The time-scale used is that most generally used in East Africa, with the beginning of the Miocene, Pliocene and Pleistocene epochs being placed at 25, 12, and 2.5 Ma (million years) respectively.

The geology map available only covered a small portion of the study area, hence no geology map and no geological cross-section is included. The geology included here represents a summation of several reports, namely: "Geology of the Naivasha Area" by Thompson and Dodson (1963). "Geological, Volcanological and Hydrogeological Controls on the Occurrence of Geothermal Activity in the Area surrounding Lake Naivasha, Kenya"- Clarke (1990), and "The Vegetation of the Aberdare National Park Kenya" -Schmitt (1991).

The rocks in the Naivasha area are tentatively classified as follows according to their age:-

Holocene volcanics, lake and fluviatile sediments

Upper Pleistocene volcanics and lake sediments

Upper Middle Pleistocene volcanics and lacustrine sediments

Lower Middle Pleistocene (?) volcanics and lake sediments

Miocene-Pleistocene(?) volcanics

TABLE 4.1 SUMMARIZED STRATIGRAPHY

Name of formation(Fmn) or (Mem)	Age	Major Outcrops	Lithology
Simbara Series	Miocene	The Aberdares	Basaltic agglomerates and autobreccias
Kinangop Tuff	3.4-4.5 Ma BP Pliocene-Early Pleistocene	Eastern rift margin	Ignimbrite succession; mostly welded trachytic tuffs, palaeosols and weathered zones at top of most beds
Limuru Trachyte Fmn	1.66-2.65 Ma BP Pliocene-Early Pleistocene	Eastern rift margin	Lava flows of trachyte and rhyolite composition. Some flows have abundant feldspar phenocrysts.
Karati Basalt Fmn	< 1.5 Ma BP Pliocene-Early Pleistocene	Adjacent to North Karati settlement and Naivasha Town	Olivine basalt lava, scoriaeceous blocks and lapilli.
Sattima Series	Pliocene - Middle Pleistocene		Volcanic series; phonolite, olivene alkali-trachyted, mugearites and fissile basalts
Laikipian Basalts	Early Pleistocene-Upper Middle Pleistocene	The Aberdares National Park	non-porphyritic basalts
Lake Sediments		Oserian Farm, Sulmac Estate	Pumiceous granule-pebble gravel, coarse sand, gravely sand , silt and clay.
Alluvial deposits	< 0.45 Ma BP Mid/Late Pleistocene-Holocene	Gullies and small internally draining basins.	Silt, fine sand, some ferruginous coarse sand and boulder gravel.
Eburru pumice	Recent?	Widespread over Western Eburru extending onto the adjacent Mau Escarpment.	Grey pumice lapilli and /or ash beds most of which have a palaeosol and or weathered zone at the top. Blocky pumice deposits occur in the cratered summit area of Eastern Eburru. Pumice accompanied by obsidian and trachyte lava lithics. Occasional beds rich in feldspar crystals and highly feldspar porphyritic lapilli. Some bedded ash deposits low in the exposed succession.

Volcanics

The Simbara Series

The Simbara Series are comprised of basaltic agglomerates and autobreccias. These basalts are exposed in the valleys and on some ridges in the vicinity of The Aberdares. In this series many dykes of basaltic composition outcrop around the highest peaks in the vicinity of the Aberdare National Park.

Kinangop Tuff

This formation is characterized by and ignimbrite succession of mostly welded tuffs. Palaesols and weathered zones occur at the top of most beds. This formation outcrops in the area of the Eastern Rift Valley, namely the Kinangop Plateau. Where exposed, it reaches a maximum thickness of 150m.

Limuru Trachyte Formation

The Limuru Trachyte Formation is comprised of lava flow of trachyte and rhyolite composition. Some flows have abundant feldspar phenocrysts. This formation reaches a maximum thickness of 100m , where exposed, and outcrops in the vicinity of the eastern rift margin. In the vicinity of the Naivasha town, this formations interbeds with the Kinangop Tuff.

Karati Basalt Formation

The Karati Basalt Formation consists of olivine basalt lava, with feldspar and olivene phenocrysts. Scoriaceous and lapilli blocks are also found in the basalt. These basalts are products of Hawaii and/or Strombolian eruption type where lava extrusion is dominant. This formation reaches a maximum thickness of 3m.

Sattima Series

The Sattima Series is comprised primarily of volcanic lava which consists of mostly phonolites, olivine alkali-trachytes, mugearites and fissile basalts.

The Lakipian Basalts

The Laikipian Basalts consists of mainly non-porphyritic basalts. These overlie the trachytes and phonolites of the Sattima Series. The Northern Aberdare Ramp consists of lavas and tuffs of this series.

Lake Sediments

Lake Sediments (ls) form a large part of the floor of the Naivasha basin and are exposed in gullies , road section and small quarries in the vicinity of the Naivasha Town. These sediments consist of pumiceous granule which in turn consists of pebble gravel, coarse sand , gravelly sand, silt and clay and reaches a maximum thickness of 15m at exposed sections. These sediments are thought to be derived from the re-working of pyroclastics in shallow lake areas.

Alluvial deposits (a)

Many of the gullies are have smoothened floors as a result of the deposition of alluvial sediments. These sediments are dominated by sand and gravel. Alluvial deposits associated with the Malewa river are dominated by grayish brown silt and dune sand within which there are intervals of reddish brown ferruginous coarse sand and granule gravel, and pale grey clay. The pale grey clay usually occurs in very thin beds and may have been lake deposited. Large-scale cross-bedding in other parts of the succession indicate deposition in a high energy environment.

Eburru Pumice

The Eburru pumice consists of grey pumice lapilli and or ash beds most of which have a palaeosol and or weathered zone at the top. These deposits also occur as blocky pumice deposits and are often accompanied by obsidian and trachyte lava lithics. Some beds are rich in feldspar crystals and highly feldspar porphyritic lapilli. In the study area this pumice is found in the vicinity of the Kiambogo gully. This pumice is thought to be a result of fall deposits representing the products of plinian eruptions. Thickness of these beds vary between 20-120m.

4.2 Tectonism

The tectonic phases that have determined evolution in the rift valley are represented by major NNW-SSE trending faults and major North-South volcanic alignment of eruption centres and fissures. The study area is located in a geo-dynamic area and hence has various geothermal manifestations such as fumaroles and high-temperature springs. The majority of these are associated with the volcanic complexes in Eburru, Olkaria and Suswa and are currently being exploited for the production of electricity.

4.2.1 Structure

The main structural features in the study area are major NNW-SSE trending faults which define the rift flanks, margin and floor (Fig. 4.2.1). It is proposed that at least three distinct periods of faulting have occurred within the period 0.4 to 4 Ma. Reactivation of some rift margin faults have occurred and may be post 0.4 Ma in age.

In the Naivasha basin, major NNW-SSE faults include the South Kinangop Fault Scarp and the Satima Escarpment. Evidence of the South Kinangop Fault Scarp can be seen where west and south-west of the Kinangop, the rocks that form the plateau have been down-faulted in a series of step faults. Most of these faults are short and die out in several directions. Several of the fault-line scarps suggests slightly curved faults, with the downthrown blocks on the convex side. The Satima Escarpment separates the Aberdare Range from the Kinangop Plateau (Fig.4.2.1).

Analysis of the structural geology of the area shows faulting to be more intensive in the North and Northeastern part of the catchment, in the Kinangop tuff. These faults are mostly North-South oriented and are short.

Faulting occurred prior to the development of the volcanic centers on the rift floor and it is proposed that the bulk of the faulting took place during the late Middle Pleistocene times, possibly along older fault lines.

4.2.2 Volcanism

The development of the Rift Valley is strongly linked to the formation of volcanoes and volcanic eruption. Volcanic eruptions have occurred intermittently since Miocene to Recent times and have given rise to the volcanic mountain of Suswa (Fig. 4.2.2). There is a major North-South volcanic alignment which extends from the Eburru Volcano in the north, Longonot Volcano to the Olkaria Complex in the southern section of the study area. The major Eburru-Olkaria volcanic alignment incorporates the Ndabibi and Akira plains, together with the young eruption centres on Eastern Eburru and in the western part of the Olkaria Volcanic Complex (Fig.4.2.2). A line of vents, and small domes pass through the Olkaria hill and forms a part of the north trending minor alignments of the Olkaria Volcanic Complex. The Longonot major volcanic alignments may extend as far north as Crescent Island to the south-east shore of Lake Naivasha. Minor alignments on Longonot Volcano also include eruption centres situated on fissures radially aligned relative to the summit crater.

4.3 General Hydrogeological Setting

The Rift Valley has its highest elevation the area of Lake Naivasha , generally falling both to the north and south. There is thus a potential hydraulic gradient within the Rift in these axial directions. The boundary escarpments develop the greatest head and lateral flow into the Rift from these highland areas such as the Aberdares and the Kinangop Plateau in the eastern section of the study area. These highlands support well developed tropical rain forest , indicating that local recharge must be higher in these areas than in the rift which has a semi-arid climate.

Rocks in the Naivasha Basin are generally characterized as having a low permeability. Aquifers are normally found in fractured volcanic rocks, or along weathered contacts between different lithological units. These aquifers are often confined or semi-confined with low storage coefficient. There are, however, aquifers with high permeability which are found in sediments around Lake Naivasha. These aquifers are unconfined and have high specific yields. The general groundwater flow direction in the study area can be seen in Fig. 4.2.1

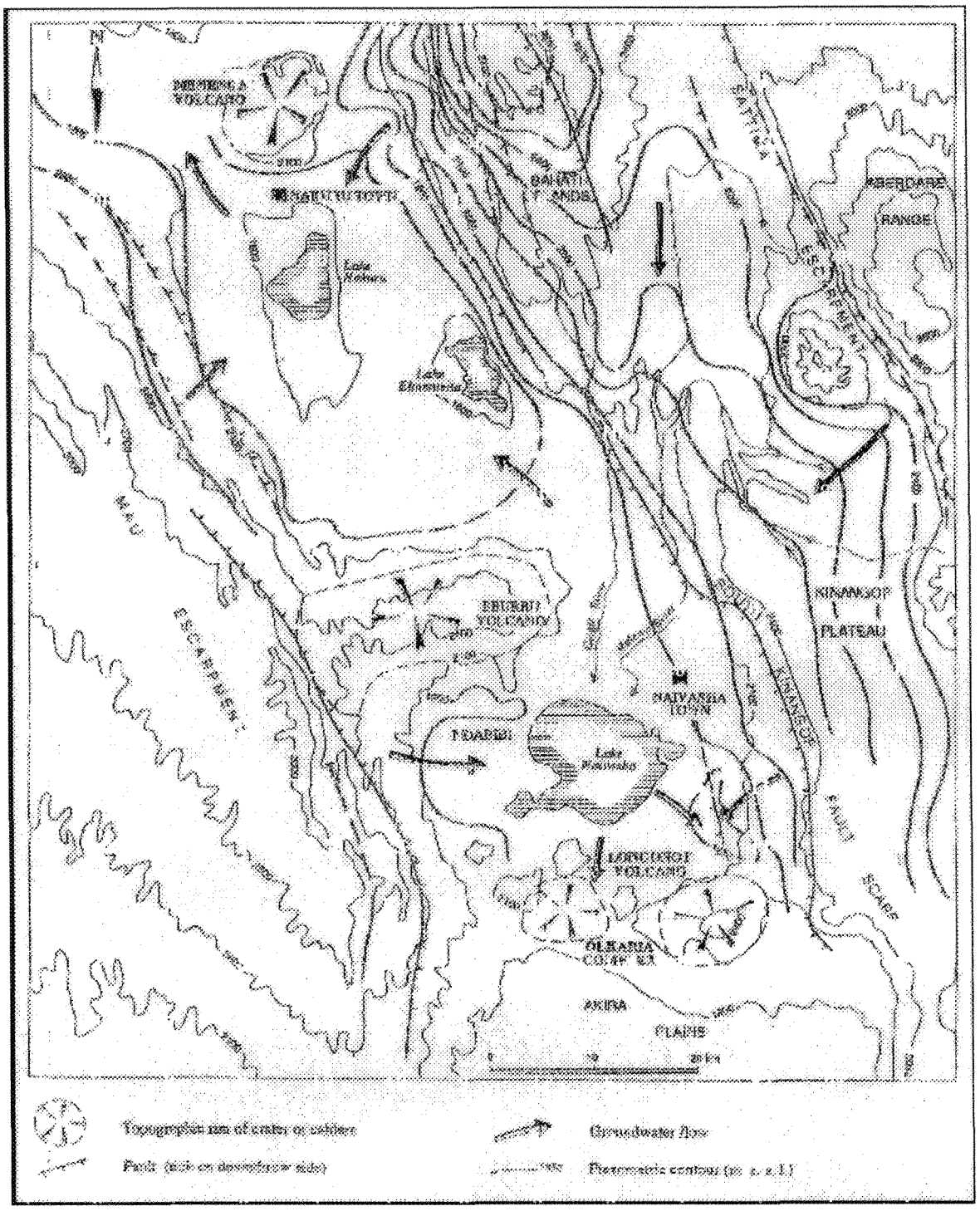

Fig. 4.2.1 Structure and general groundwater flow direction in the study area. (adapted from" Geological , volcanological and hydrogeological control on the occurrence of geothermal activity in the area surrounding Lake Naivasha, Kenya" -Clarke et al., 1990).

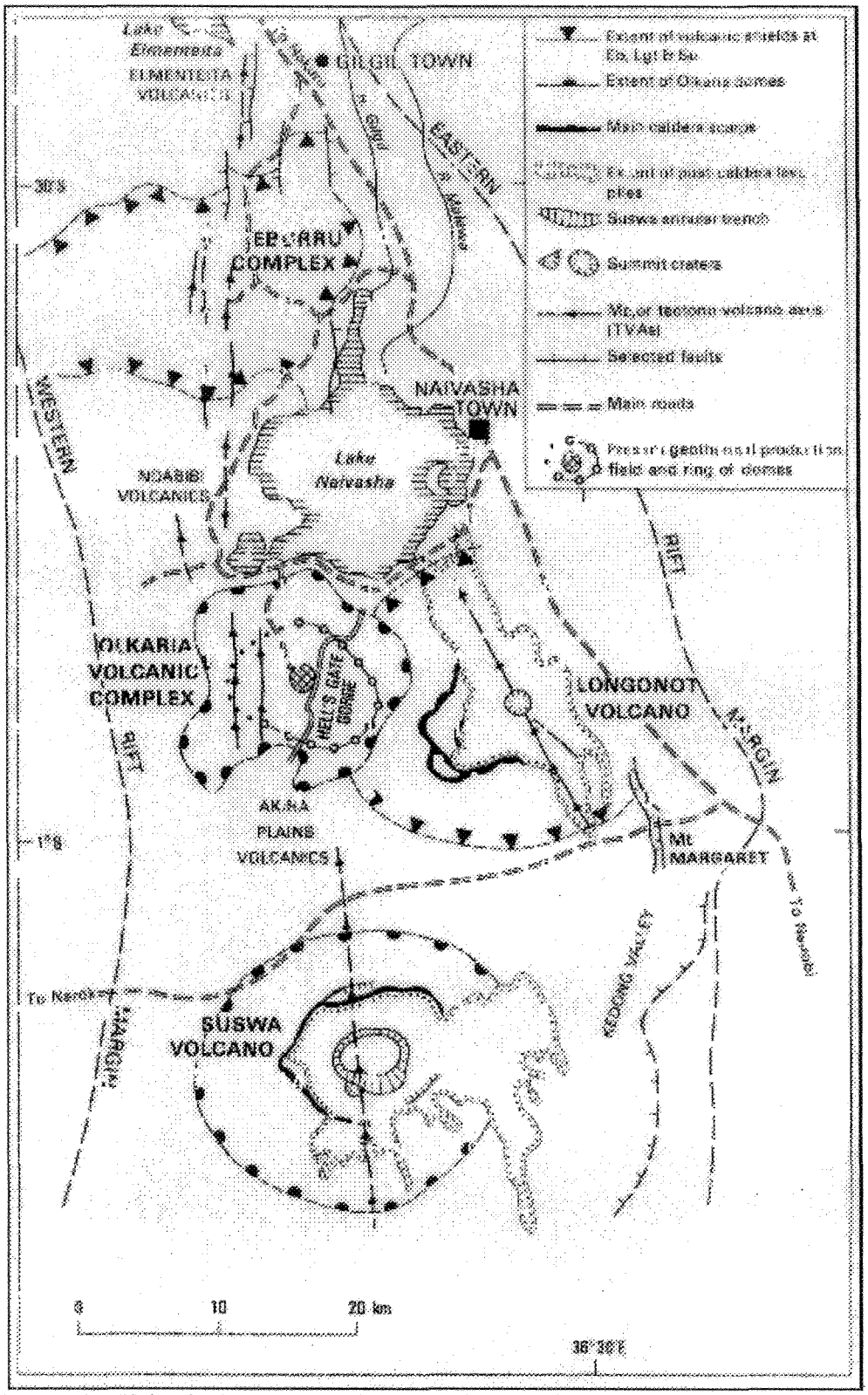

Fig. 4.2.2 Major Volcanic Centres and Alignment (adapted from" Geological , volcanological and hydrogeological control on the occurrence of geothermal activity in the area surrounding Lake Naivasha, Kenya" -Clarke et al., 1990)

5.0 GROUNDWATER RECHARGE USING BASEFLOW ANALYSIS

5.1 Introduction

A streamflow or discharge hydrograph is a graph which shows the flow rate as a function of time at a given location on the stream. In effect, the hydrograph is an "integral expression of the physiographic and climatic characteristics that govern the relations between rainfall and runoff of a particular drainage basin" (Chow,1959)

This chapter aims at quantifying baseflow based on the separation of stream hydrographs.

The dynamics of groundwater discharge to a stream from different water bearing horizons are determined by the occurrence of recharge to the unconfined and confined aquifer in the river basin and groundwater heads relative to stream stage. The following typical relationship between ground and surface water may be identified: (a) aquifer having no hydraulic connection with a stream, where the groundwater table is below the streambed. (b) aquifer having periodic or intermittent influent/ effluent hydraulic relationship with a stream, where the groundwater table is above the streambed during the wet season and below it during the dry season and (c) aquifer having continuous relationship where the discharge is comprised of direct runoff and baseflow.

5.1.1 Hydrograph Separation Techniques

Classical hydrograph analysis involves the decomposition of streamflow into three major components: surface runoff, interflow, and baseflow (groundwater flow). The first two terms are collectively described as direct runoff (quickflow). Surface runoff represents that part of precipitation which flows directly over the land surface into stream channels and interflow is that part which moves laterally through the soil zone and is discharged to streams relatively quickly after infiltration and without reaching the zone of saturation. Groundwater flow is that part of precipitation which reaches the zone of saturation and contributes to groundwater storage. It is clear that this approach is not realistic as the distinctions between interflow and base flow are unclear and involve a certain degree of subjective discrimination. Base flow itself may be composed of a number of components, each of which may vary seasonally, and each with a different recession constant.

During periods of flood streamflow consists of two components: direct runoff and baseflow. A typical flood hydrograph consists of three main elements, the rising limb, the crest segment, a recession curve and a depletion curve (Fig. 5.1.1a).

There are various techniques which are used for separating hydrograph into runoff and baseflow components. The main techniques are based on examination of the hydrograph of total flow. Fig. 5.1.1b-d illustrates some of the techniques that are commonly used.

In Fig. 5.1.1b a straight line has been projected to the point of greatest curvature of the recession limb. This point represents the end of the release of channel storage. In Fig. 5.1.1c the pre-event flow trend is projected until the time of peak. From there the baseflow hydrograph is connected by a straight line that intersects the total-flow hydrograph N days after the peak. In Fig. 5.1.1d a straight line is fitted to the end of the hydrograph recession on the graph and projected backward in time under the peak. From here an estimate is made for the first part of the separation.

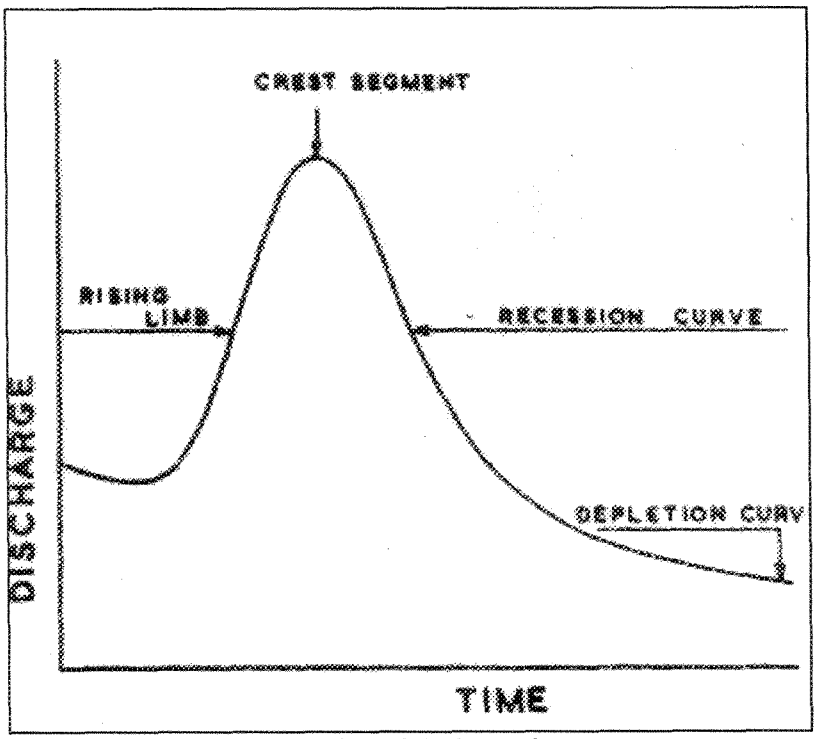

Fig. 5.1.1a The components of a unit hydrograph

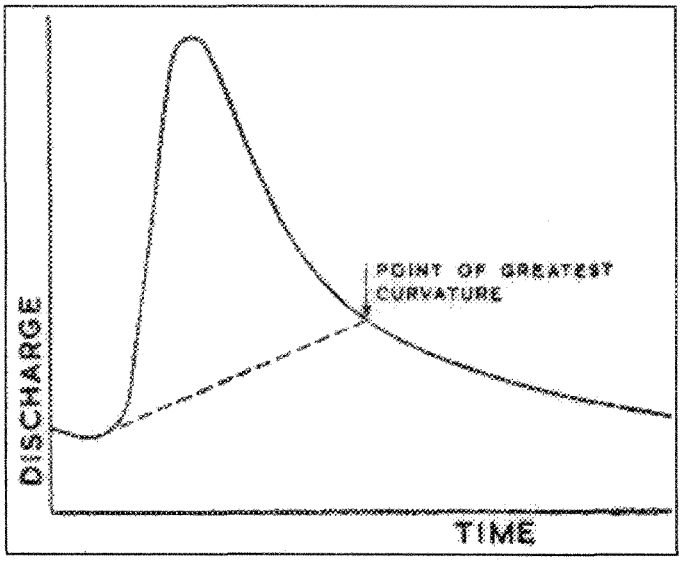

Fig. 5.1.1b

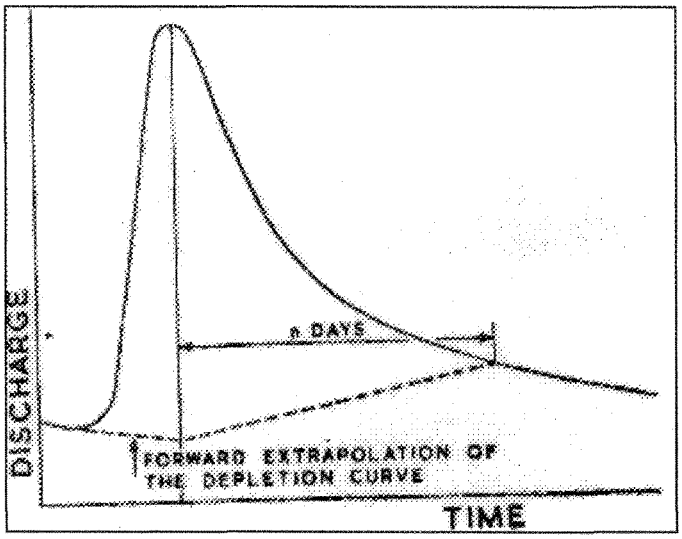

Fig. 5.1.1c

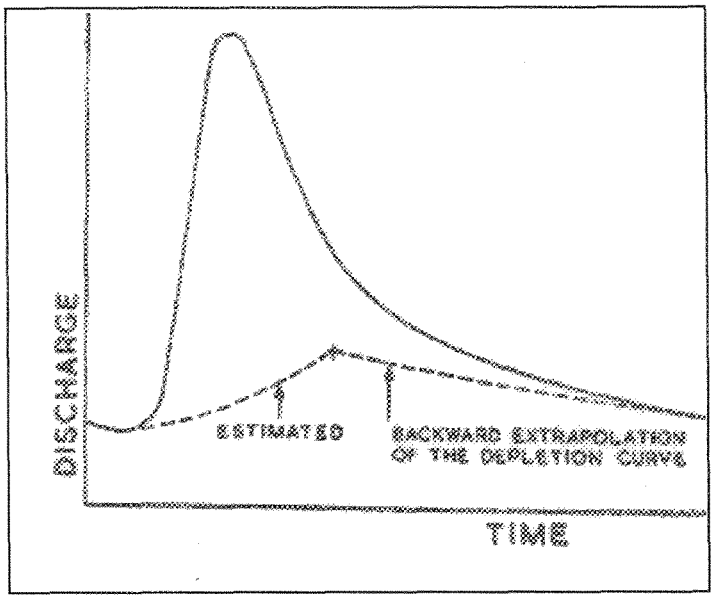

Fig. 5.1.1d

The baseflow separation implemented is based on a recursive digital filter :

$f_k = \alpha f_{k-1} + (1+\alpha)/2 * (y_k - y_{k-1})$

where:

f_k = filtered quick response at the kth sampling instant
y_k = original streamflow
α = filter parameter
$y_k - f_k$ = filtered base flow

The filtering procedure for the data set was done using a spreadsheet. First the original streamflow was filtered and the resulting data subtracted from the original streamflow to obtain the smoothened data. This result was then filtered and the resultant subtracted from the original smoothened data. This procedure was then repeated and results in the original streamflow being filtered three times. The final filtered value represent the baseflow. An α value of 0.925 was used.

The parameter α varies between 0.90 and 0.99 and affects the degree of attenuation and the number of filtering determined the degree of smoothening. The data set was constrained so that the filtered data was not negative or greater than the original streamflow.

The justification for use of this technique rests on the fact that filtering out high-frequency signals is intuitively analogous to the separation of low-frequency base flow from the higher frequencies. This technique, though described as arbitrary as the others, provides an objective repeatable estimate of an index of baseflow which is easily automated (Nathan and McMahon -1990).

Discharge data have been obtained from the following stations on the Malewa river and its major tributaries (Fig.5.1.1e): The data set was available in the form of daily discharge values.

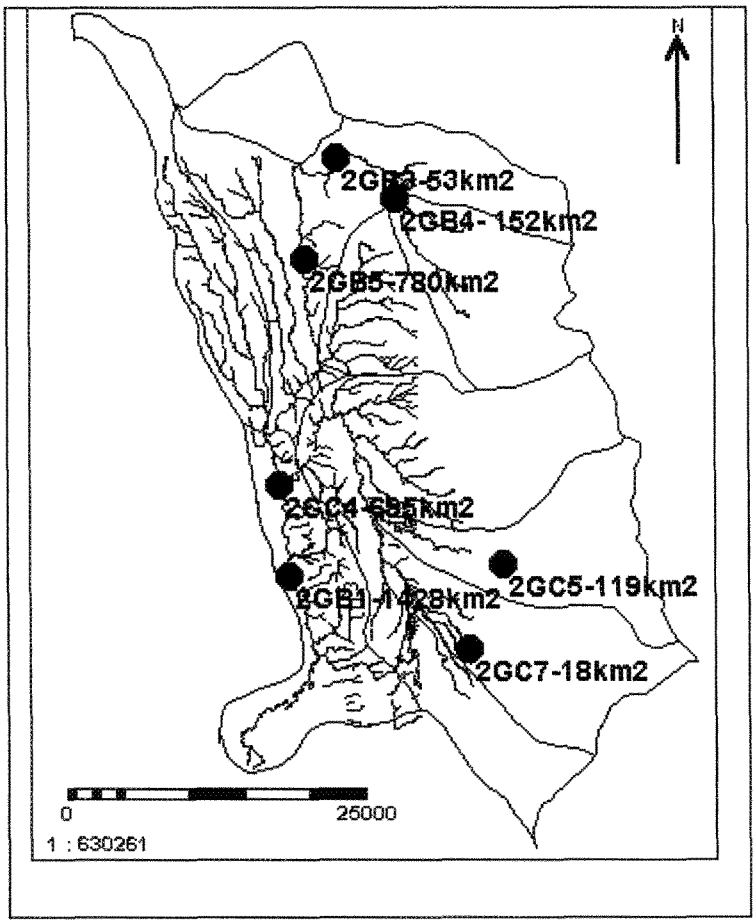

Fig 5.1.1e The Gauged Stations of the River Malewa

Table 5.1 Discharge Data Set

Name and Location of Station	Area (km^2)	Data Years
2GB1 - Lower Malewa	1428	1960-1984
2GB3 - Upper Malewa	53	1960-1992
2GB4 - Upper Malewa	152	1960-1993
2GB5- Upper Malewa	780	1960-1987
2GC4- Turasha	695	1960-1992
2GC5 - Nandarasi	119	1960-1993
2GC7 - Engare Mugutyu	18	1960-1991

The data set was selected from 1960 up to the latest data set (Table 5.1).
The Software SPSS was used to compute missing data. The linear interpolation method was used as this method was already used on the data set received.

From the separation of baseflow, values for average annual baseflow and direct runoff values were obtained (Table 5.1.1). This was done for seven (7) gauged stations on Malewa (Fig. 5.1.1e). An example of the filtered data can be seen in Fig. 5.1.1f. Table 5.11 shows the average annual baseflow, quickflow (direct runoff) and streamflow for all the major gauged stations. Values displayed in mm were obtained by dividing the average annual data by the respective catchment area. Due to differences in the catchment area of the stations, the average annual figures in mm will be used for comparison.

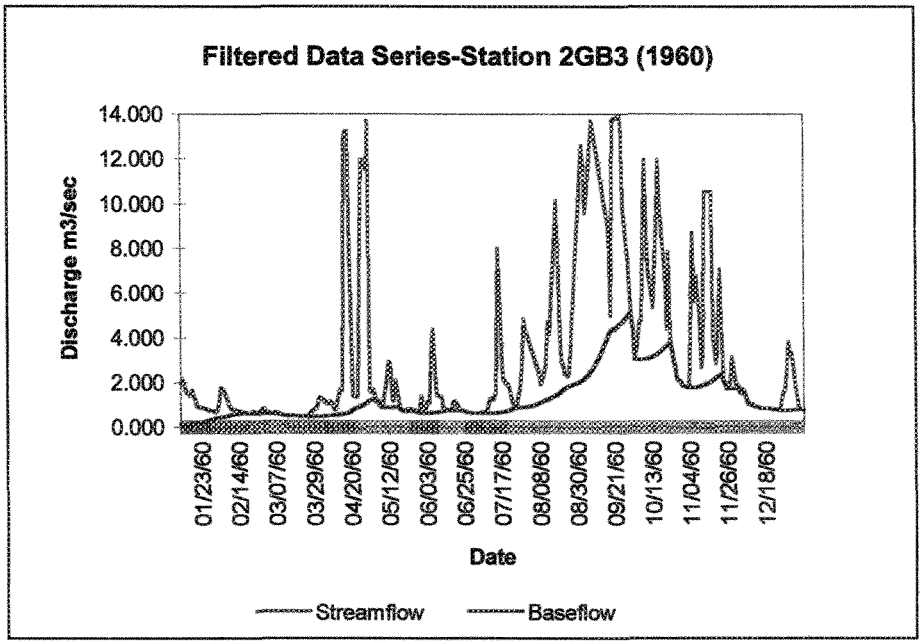

Fig. 5.1.1f

Table 5.1.1 Results of the Filtered Streamflow Data

Stations	Size of Catchment (10^6 m2)	Average Annual Streamflow (m^3s^{-1})	Average Annual Streamflow (mm)	Average Annual Baseflow (m^3s^{-1})	Average Annual Baseflow (mm)	Average Annual Baseflow (m3)	Rainfall Annual Average (mm)	Average Annual Runoff (m^3s^{-1})	Average Annual Runoff (mm)	Runoff Coefficien
2GB3	53	0.249	145	0.192	112	5936000	1114.2	0.057	33	0.03
2GB4	152	3.393	692	1.423	290	4408000	1141.2	1.970	401	0.36
2GB5	780	2.843	113	1.248	49	38220000	767.5	1.594	63	0.08
2GC5	119	0.882	229	0.448	117	13923000	1144.7	0.439	113	0.10
2GC7	18	0.251	432	0.106	182	3276000	1278.7	0.145	249	0.19
2GC4	695	3.778	168	1.547	69	47955000	645.6	2.231	99	0.15
2GB1	1428	6.336	137	2.796	60	85680000	1207.9	3.540	77	0.06

5.1.2 Streamflow Analysis

From Table 5.1.1 it can be seen that station 2GB1 (Fig. 5.1.2a) represents the main gauged station of the river Malewa. This station represents approximately 92 % of the total area of the Naivasha catchment and contributes approximately 137 mm as inflow (baseflow and streamflow) to the Lake.

Station 2GB3 (Fig 5.1.2b) and 2GB4 (Fig. 5.12c) represents the main gauged stations for the upper Northern catchment area. These stations receive contributions from The Aberdares and flow into the main gauged station 2GB5 (Fig. 5.1.2d). Estimated streamflow from the two stations (2GB3&2GB4) totals 3.6 m^3s^{-1} . When this figure is compared with the measured streamflow of 2GB5 (2.8 m^3s^{-1}), it can be seen that there is a loss of 0.8 m^3s^{-1} . This loss may be due to the fact that this may be an area of groundwater recharge and there are numerous hand-dug wells in the area. If the stream is in hydraulic continuity with the aquifer, then this abstraction would result in a decrease in streamflow. The loss in streamflow may also be due to grid-faulting which occurs in the rift floor or to errors in the rating curve used.

Stations 2GC5 (Fig. 5.1.2g) and 2GC7 (Fig. 5.1.2f) represent the streamflow from the eastern catchment areas. These rivers receive contribution from the North and South Kinangop Plateau areas respectively. Both rivers contribute approximately 1.133 m^3s^{-1} to station 2GC4 (Fig.5.1.2e). Measured streamflow at this station is 3.8 m^3s^{-1} . This represents an addition inflow of approximately 2.7 m^3s^{-1} which is thought to represent streamflow contribution from the ungauged section of the catchment. The ungauged area of the catchment represents about 70% of the total streamflow contribution from this area.

The main gauged stations representing the northern and eastern catchment areas, Stations 2GB5 & 2GC4 respectively, flow into the main station of the River Malewa-2GB1. Collective inflows from 2GB5 and 2GC4 represent 6.621 m^3s^{-1} . On comparing this figure to that representing measured streamflow at 2GB1 (6.336 m^3s^{-1}), it can be seen that there is a minor loss of streamflow of 0.285 m^3s^{-1} . As this station represents the main gauged station before the river enters Lake Naivasha, it is assumed that this

represents the gross streamflow contribution to the Lake. However the data used here was not yet corrected. Compare with Podder (1998).

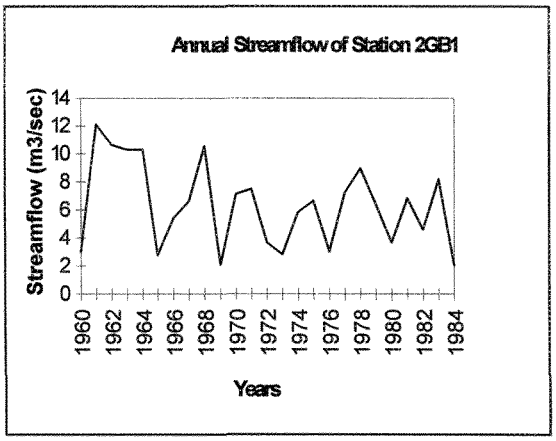

Fig.5.1.2a

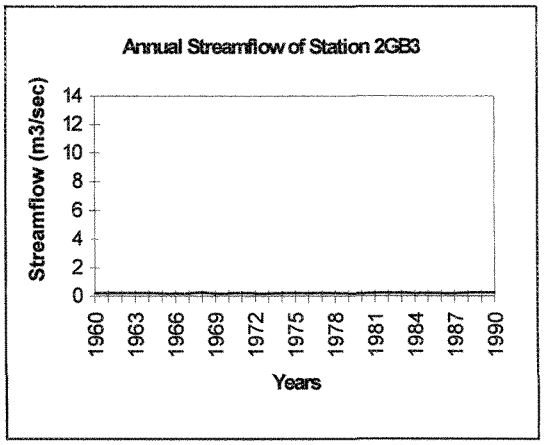

Fig.5.12b

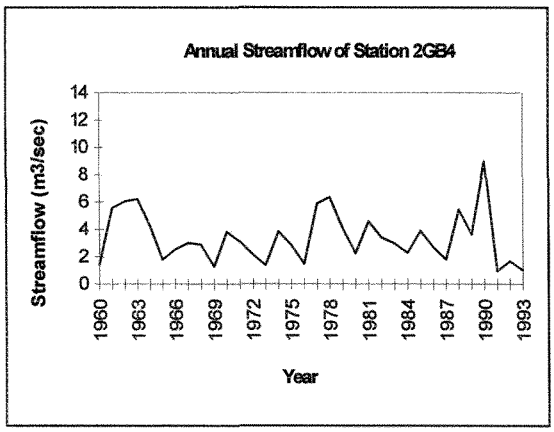

Fig. 5.1.2c

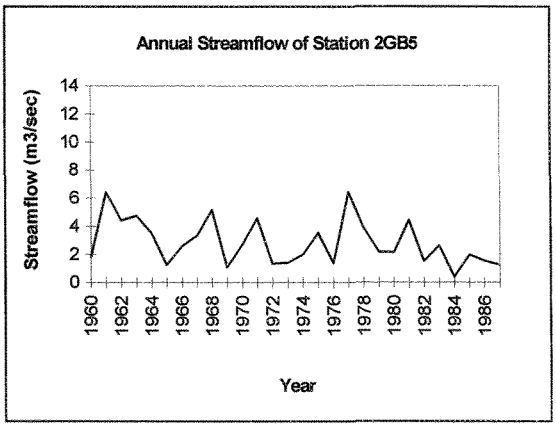

Fig.5.1.2d

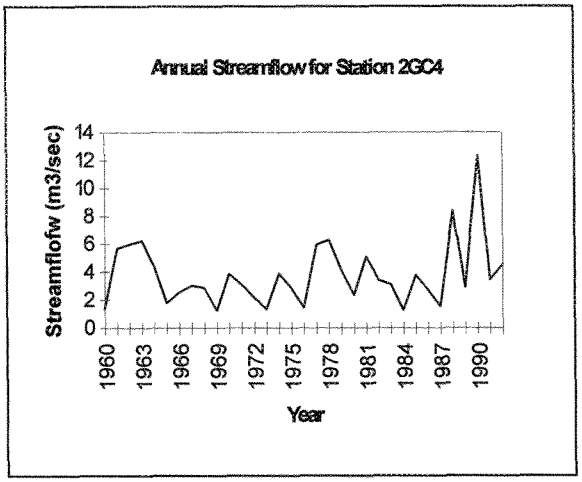

Fig.5.1.2e

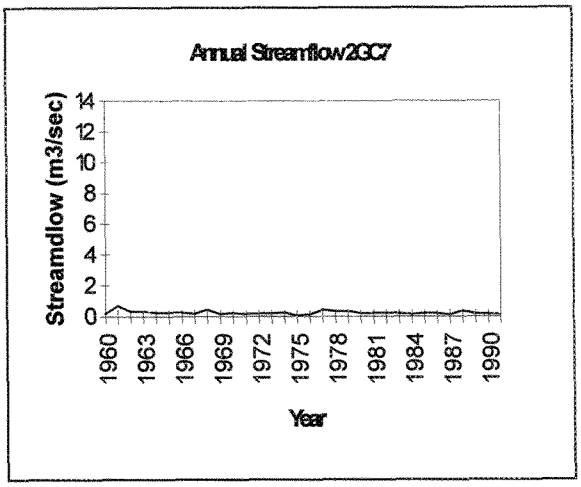

Fig.5.1.2f

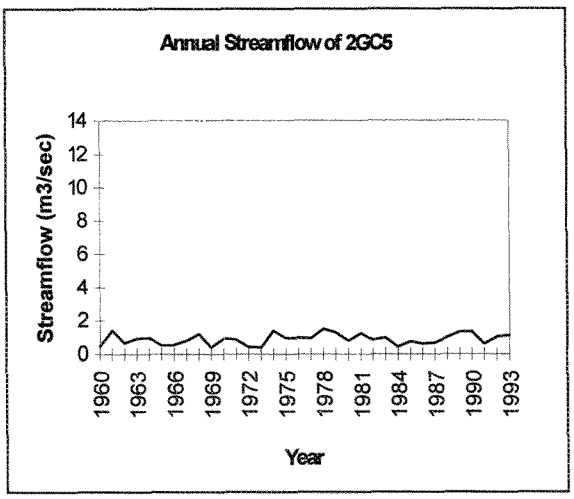

Fig.5.1.2g

5.1.3 Baseflow Analysis

Using this methodology, baseflow contribution represents the potential groundwater recharge.

Average annual baseflow contribution from the gauged sections of the catchment can be seen in Table Fig.5.1.1. Annual Baseflow contribution for the various stations can be seen in Fig 5.1.3a to Fig.5.1.3g.

Baseflow from stations 2GB3(Fig. 5.1.3c) and 2GB4 (Fig. 5.1.3b) represent a total of 1.615 m3/sec or 402 mm. The baseflow calculated at stations 2GB5 was 1.248 m3/sec or

49 mm. This represents a loss in baseflow of 0.367 m3/sec This loss corresponds to the observed decrease in streamflow in the previous section 5.1.2.

For stations 2GC5 (Fig.5.1.3f) and 2GC7 (Fig. 5.1.3e) baseflow contributions amount to 0.554 m3/sec. Measured baseflow at station 2GC4 (Fig. 5.1.3a) represents 1.547 m3/sec or 69 mm. This additional baseflow of 0.993 m3/sec can be attributed to inflow from the ungauged area of this catchment area..

Baseflow contributions from stations 2GB5(Fig. 5.1.3d) and 2GC4 (Fig. 5.1.3g) amounts to 2.795 m3/sec . A baseflow of 2.796 m3/sec or 60 mm was calculated for station 2GB1 (Fig. 5.1.3a). This indicate that there is no loss of baseflow from the stream along the Ol Kalou - Turasha area. This amount is assumed to represent the net groundwater recharge from the Malewa catchment to the Lake.

I t can be seen that most of the groundwater contribution from the Malewa catchment comes from the eastern area of the catchment, primarily the Kinangop Plateau area. The majority of the baseflow contribution comes from the ungauged areas of the catchment. Here baseflow contribution is calculated to be approximately 56 %. 44% of the remaining baseflow contribution comes from the Upper Malewa catchment. These areas are located primarily in the vicinity of stations 2GB4 and 2GB5 which corresponds to the areas of Ol Kalou area.

For the main gauged station at 2GB1 average annual inflow (baseflow and streamflow) to the Lake Naivasha is estimated to be 197 mm.

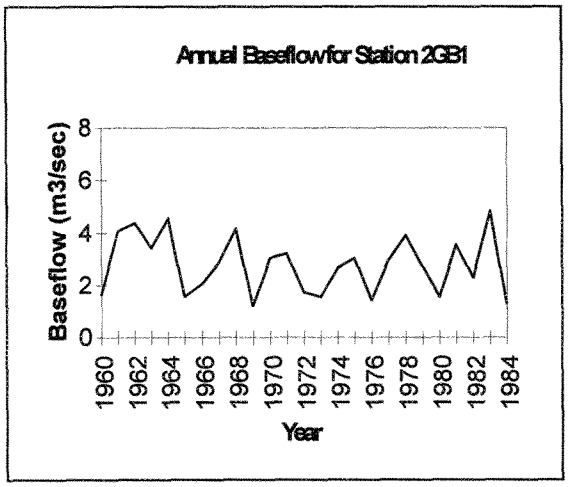

Fig. 5.1.3a

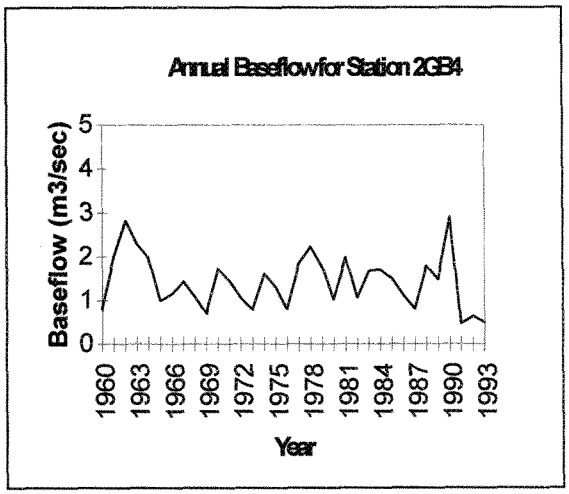

Fig. 5.1.3b

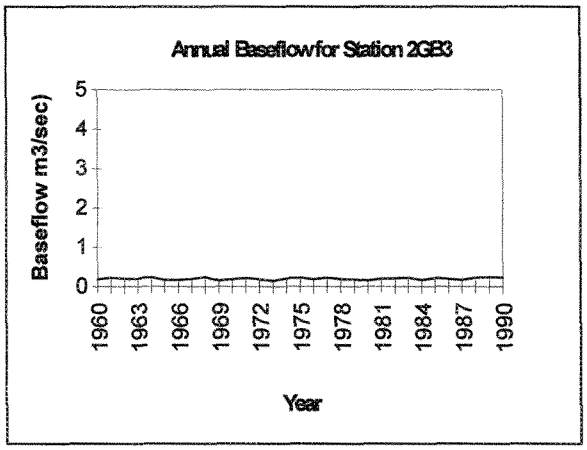

Fig. 5.1.3c

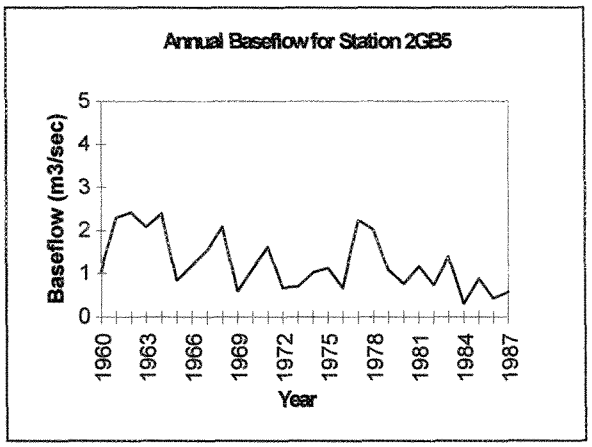

Fig. 5.13d

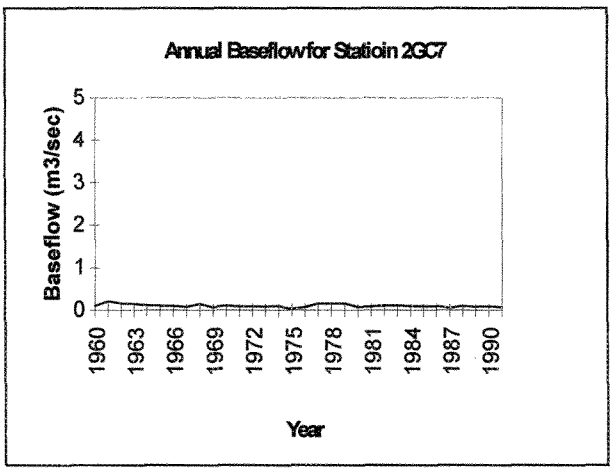

Fig. 5.1.3e

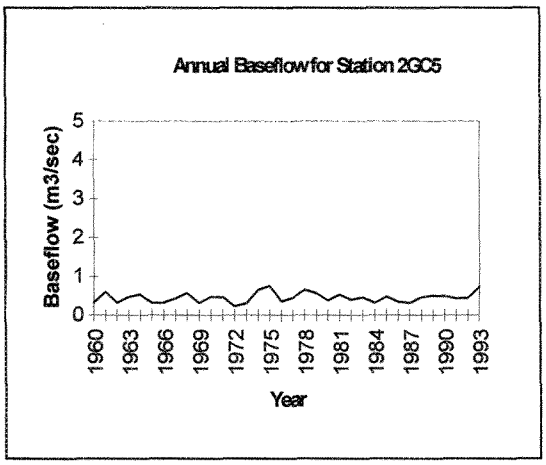

Fig.5.1.3f

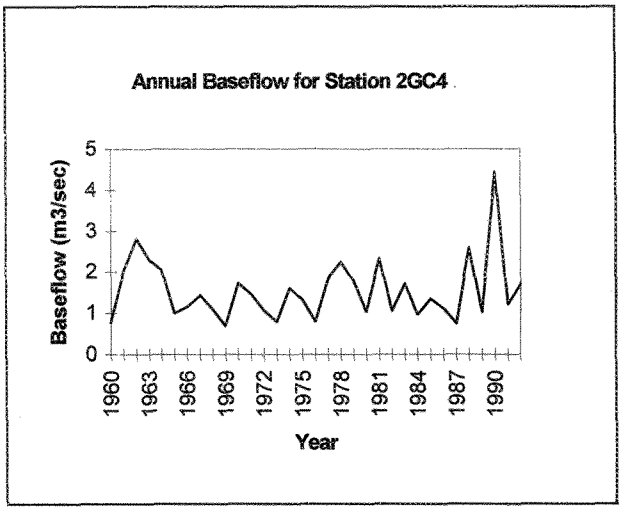

Fig. 5.1.3g

Based on the analysis of baseflow a generalized recharge map was made (Fig. 5.1.3).

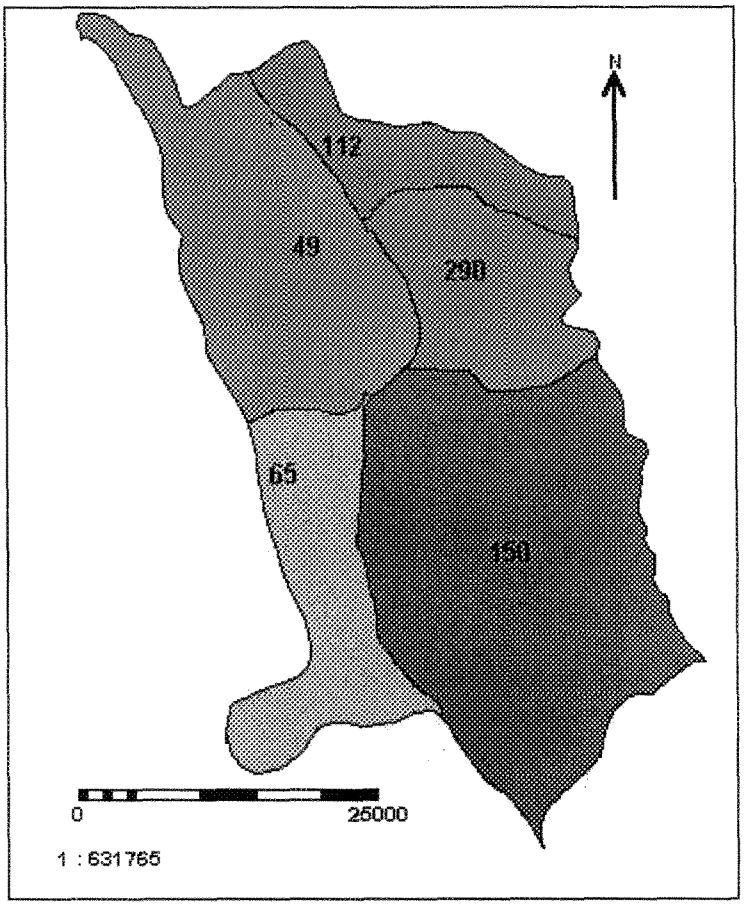

Fig. 5.13 Generalized recharge zonation map in mm/year

5.1.4 Rainfall-Runoff relationship

Effective rainfall is that part of rainfall which is neither retained on the land surface nor infiltrated into the soil. After flowing across the watershed surface, excess rainfall becomes direct runoff at the watershed outlet under the assumption of Hortonian overland flow.

The relation between rainfall and the amount of water transported out of the catchment area is described by the runoff coefficient. This coefficient depends on a number of different factors within the catchment area such as slope, soils, vegetation, evaporation, catchment size and the characteristics of the rainfall. The runoff coefficient was calculated by dividing the average annual baseflow by the area of the catchment and the average annual rainfall (See Equation below)

Runoff coefficient = Average Annual Baseflow/ Area* Average annual rainfall

Average Annual Baseflow (m^3/sec)
Average annual rainfall =mm

The rainfall stations which are thought to contribute most to the streamflow of the gauged stations were selected as representing rainfall from that area of the catchment.

Values for runoff coefficient can be seen in the Table 5.1.1. Fig. 5.14a-g shows the average yearly runoff values for the respective stations.

From Table 5.1.1 it can be seen that station 2GB4 has the highest runoff coefficient from the catchment and that 36% of rainfall contributes to overland flow or quickflow. Runoff coefficient values for the other stations range between 0.03-0.19. An annual average runoff coefficient of 0.06 was calculated for the main gauged station at 2GB1. This is assumed to be representative of the entire catchment.

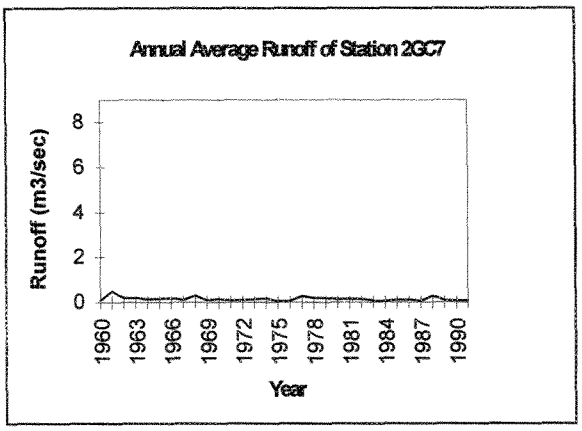

Fig. 5.1.4a

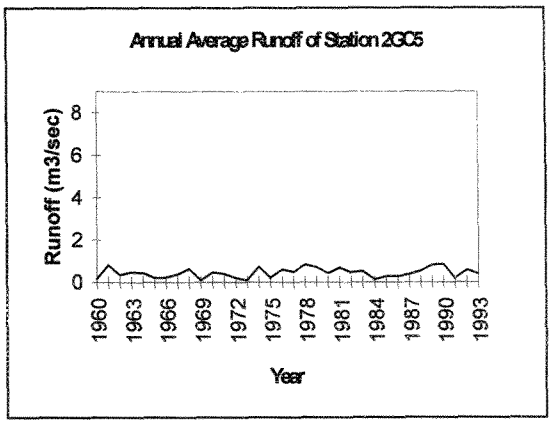

Fig. 5.1.4b

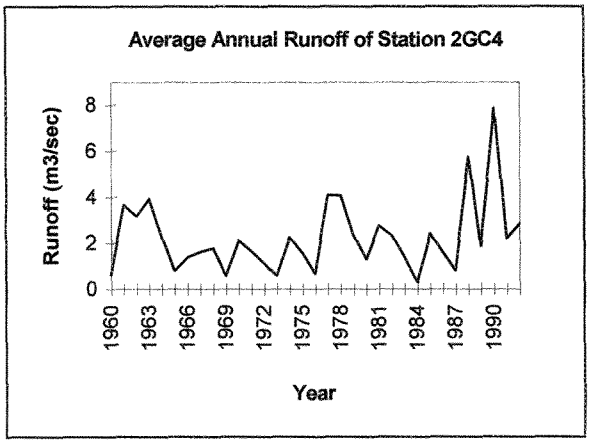

Fig. 5.1.4c

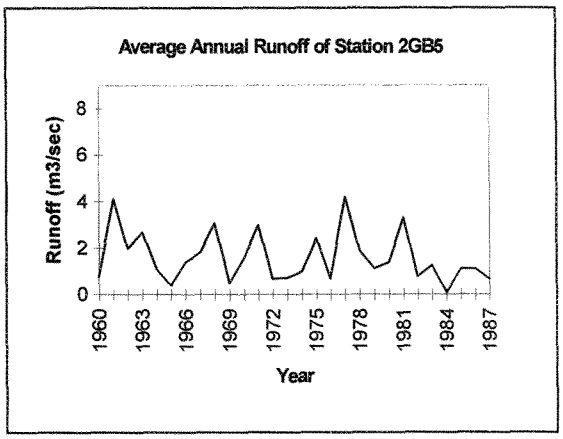

Fig. 5.1.4d

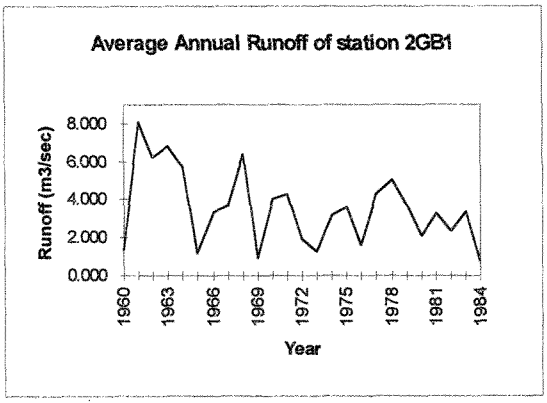

Fig. 5.1.4e

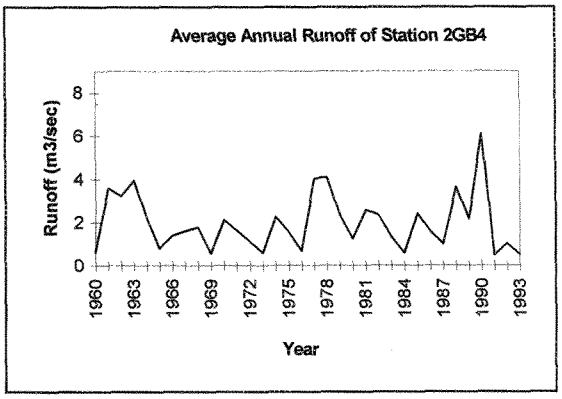

Fig. 5.1.4f

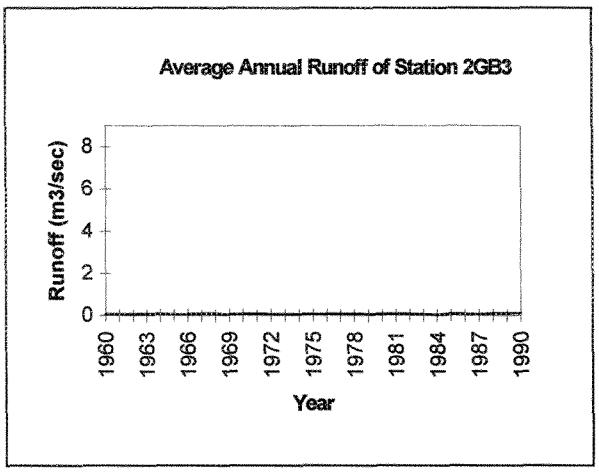
Average Annual Runoff of Station 2GB3
Runoff (m3/sec)
0
2
4
6
8
1960
1963
1966
1969
1972
1975
1978
1981
1984
1987
1990
Year

Fig. 5.1.4g

6.0 CALCULATION OF AREAL EVAPOTRANSPIRATION USING MORTON'S (1983) CRAE MODEL

6.1 Introduction

Evapotranspiration refers to the amount of water that is returned to the atmosphere by the combined effect of evaporation and transpiration. Evapotranspiration is dependent on the availability of energy, temperature, humidity, the availabiility of moisture and complex soil-plant- atmosphere interactions. It represents the component of the hydrologic cycle most directly influenced by land-use and climatic changes.

The potential evapotranspiration is the optimum rate of evapotranspiration possible under the prevailing hydrological conditions. Actual evapotranspiration refers to evapotranspiration under normal conditions. Usually actual evapotranspiration is lower than potential evapotranspiration with the exception of when the crop coefficient value is greater than one.

Different methods based on various meteorological parameters are available for the estimation of evapotranspiration rate. The choice of a calculation method depends upon the availability of data and the applicability of the model to the study area. In this study potential and actual evapotranspiration was calculated using Morton's (1983) CRAE model.

6.2 Mortons Complementary Relationship (CRAE) Model

Morton proposed the Complementary Relationship Areal Evapotranspiration Model (CRAE) concept that a complementary relationship exist between the evapotranspiration from an area (areal evapotranspiraion) and potential evaporation.
Areal evaporation was defined as the evapotranspiration from an area so large that the effects of the evapotranspiration on the temperature and humidity of the overpassing air are fully developed. The potential evapotranspiration is defined as the evapotranspiration that would occur form a hypothetical moist surface with radiation absorption and vapour transfer characteristics similar to those of the area and so small that the effects of the evapotranspiration on the over-passing air would be neglible. He also introduced the concept of Wet environment areal evapotranspiration which he

defined as the evapotranspiration that would occur if the soil-plant surfaces of the area were saturated and there were no limitations on the availability of water.

This concept is opposed to the conventional view that potential evapotranspiration is the areal evaporation that would occur if there were no limitations on the availability of water. Thus in the conventional approach the potential evaporation is regarded as a cause of the areal evaporation whereas in the complementary relationship it is an effect.

The data requirement for this model is mean long-term annual rainfall, mean monthly air and dew point temperatures, and mean monthly observed sunshine hours or net radiation. In addition, the altitude and latitude of the meteorological station considered are required.

6.3 Representation of The Complementary Relationship

The complementary relationship can be represented by:

$$E_T + E_{TP} = 2\,E_{Tw} \quad (1)$$

or by:

$$E_T = 2\,E_{TW} - E_{TP} \quad (2)$$

where:

E_T = areal evaporation, the actual evapotranspiration from an area so large that the effects of upwind boundary transitions are neglible.

E_{TP}= potential evapotranspiration, as estimated from a solution of the vapour transfer and energy-balance equation, representing the evapotranspiration that would occur from a hypothetical moist surface with radiation absorption and vapour transfer characteristics similatr to those of the area and so small that the effects of the evapotranspiration on the overpassing air would be neglible.

E_{TW} = wet environment areal evapotranspiration, the evapotranspiration that would occur if the soil-plant surfaces of the area were saturated and there were no limitations on the availability of water.

Fig.6.3 provides a schematic representation of the relationship between areal potential evapotranspiration under condition of constant radiant-energy supply.

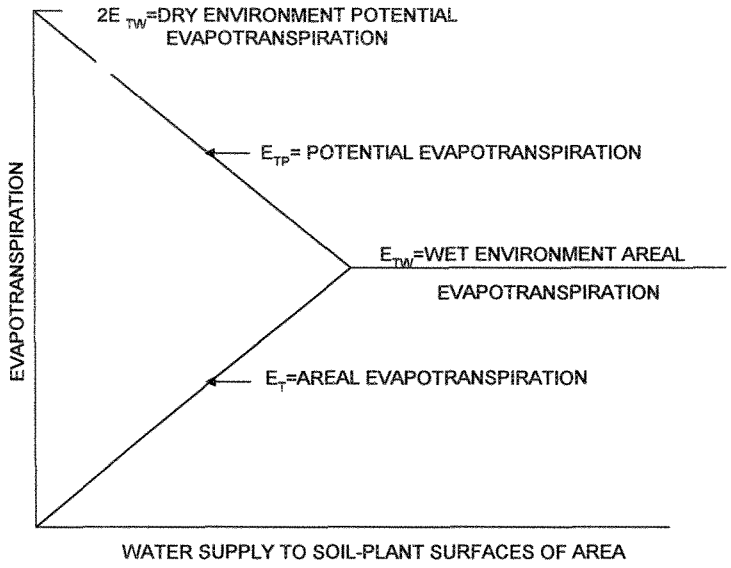

Fig. 6.3 Schematic representation of the complementary relationship between areal and potential evapotranspiration with constant radiant-energy supply.

The ordinate represents evapotranspiration and the abscissa represents the water supply to the soil-plant surfaces to the area, a quantity that is usually unknown.

Under arid conditions(hot and dry), where no water is available for areal evapotranspiration (extreme left of Fig. 6.3) , E_T=0 and E_{TP} is at its maximum rate of $2E_{TW}$ (the dry environment potential evapotranspiration). As the water supply to the soil-plant surfaces of the area increases (moving to the right of Fig.6.3) the resulting equivalent increase in E_T causes the over-passing air to become cooler and more humid, thus resulting in an equivalent decrease in E_{TP}. When the supply of water to the soil-plant surfaces of the area has increased sufficiently, the values of E_T and E_{TP} converge to that of E_{TW}.

6.4 Computation of the main Components

The main components of the Complementary Relationship are Potential Evapotranspiration (E_{TP}) and wet-environment areal evapotranspiration E_{TW}.
E_{TP} computation is accomplished through estimation of potential evapotranspiration equilibrium temperature (T_P) which is done by an iterative process. T_P is the temperature at which the energy balance and the vapour transfer for a moist surface give the same value of potential evapotranspiration, ie. Equations (3) and (4).

$$E_{TP}=R_T-[\gamma p f_T+4\varepsilon\sigma(T_P+273)^3](T_P-T) \quad (3)$$

$$E_{TP}=f_T(\nu_p-\nu_D) \quad (4)$$

where:

T_P =equlibrium temperature (°C)
T =air temperature in (°C)
R_T =net radiation for soil-plant surfaces at air temperature (W/m^2) and is calculated using the net long-wave radiation loss for soil-plant surfaces, incident global radiation and average albedo. The lattter are estimated using air temperature, sunshine hours and atmospheric pressure.
f_T = vapour transfer coefficient (dimensionless)
ε = surface emissivity (dimensionless)
σ = Stephan-Boltzmann constant ($W/m^2/K^4$)
ν_D =saturation vapour pressure at the dew point temperature (mbar)
ν_p = saturation vapour pressusre at T_P (mbar)
γ = psychometric constant (dimensionless)
p =atmospheric pressure (mbar)

The T_P estimate obtained is then used in Eqn. 4 to evaluate E_{TP}. E_{TW} is evaluated as given in Eqn (5):

$$E_{TW}= b_1 + b_2\left[1+\gamma \frac{p}{\Delta p}\right]^{-1} RT_P \quad (5)$$

where:

E_{TW} = wet environment areal evapotranspiration (W/m^2)
b_1, b_2 = constants calibrated by Morton
RT_P = net radiation for soil-plant surfaces at the potential evapotranspiration equilibrium temperature (W/m^2)
Δp = slope of the saturation vapour pressure curve at T_P.

Upon estimation of ET_P the value of E_T can be explicitly determined using the following equation:

$$E_T=2E_{TW} - ET_P \quad (6)$$

The equations outlined above, for estimating ET_P and E_{TW} give daily values expressed in energy flux units (W/m^2). To obtain monthly E_T values in units of evaporation (mm depth), the estimates were divided by the latent heat of vaporization of water and then

multiplied by the number of days in that month. Annual E_T estimates were obtained as the sum of the monthly values.

The procedure to calculate Areal Evapotranspiration is listed as" pseudo-code in a paper (Morton,1983). This was coded using Turbo Pascal 7.0 programming language (Appendix II).

6.5 Model Input Data

For each month the average of maximum and minimum air temperataures in degrees Celsius (T) , average dew-point temperature in degrees Celsius (T_D), ratio of observed to maximum possible sunshine duration (S), the month number (i =1 to 12) and the number of days in the month (n) were input into the model. Station input data such as latitude in degrees (ϕ), altitude above mean sea level (H) and average annual precipitation (P_A)in millimetres were also input into the model (Appendix II). The data covers the period 1994-1997.

The meteorological data required to calculate the potential evapotranspiration (PET) was available for two synoptic meteorological stations near the study area. These are the meteorological stations in Nakuru and Nyeri. The data obtained from the Station at Nakuru is assumed to be representative of the Rift Valley Floor as the climatic conditions are similar. The Nyeri station represents the eastern margin of the catchment namely the Kinangop Plateau and The Aberdares.

6.6 Results of the Model

The resulting values for the Nakuru station can be seen in Table 6.6a

Table 6.6a Morton Potential Evapotranspiration (mm) for Station Nakuru.

Year	Jan	Feb	Mar	Apr	Mar	Jun	Jul	Aug	Sep	Oct	Nov	Dec	Yearly Total
1994	259.30	224.60	223.71	176.88	169.42	165.82	167.19	175.50	184.87	178.62	141.25	184.12	2251.28
1995	241.53	217.11	195.14	171.22	167.72	173.97	169.85	184.63	174.64	162.23	148.22	173.02	2179.27
1996	202.31	214.95	200.09	181.91	171.98	157.08	164.12	170.56	170.14	169.09	147.58	167.41	2117.23
1997	219.18	251.61	227.89	149.63	169.28	167.81	173.04	174.94	177.70	170.36	137.98	156.00	2175.42
Monthly Average	230.58	227.07	211.71	169.91	169.60	166.17	168.55	176.41	176.84	170.08	143.76	170.14	2180.80
Rainfall	30.30	36.90	53.40	116.10	102.20	71.60	73.10	91.90	75.30	86.20	93.00	41.40	871.40

Table 6.6b Morton Areal Evapotranspiration (mm) for Station Nakuru.

Year	Jan	Feb	Mar	Apr	Mar	Jun	Jul	Aug	Sep	Oct	Nov	Dec	Yearly Total
1994	15.49	45.70	67.41	91.25	122.60	131.87	140.68	120.04	104.99	97.97	123.91	67.05	1128.96
1995	30.10	52.99	108.16	106.38	126.44	109.46	133.08	93.83	138.20	145.69	108.02	95.97	1248.32
1996	63.05	62.99	93.89	78.13	115.38	156.79	150.36	136.46	151.39	121.46	108.00	72.78	1310.68
1997	48.76	24.68	65.33	149.63	119.54	126.47	128.38	129.50	136.27	124.70	137.98	156.00	1347.23
Monthly Average	39.35	46.59	83.70	106.35	120.99	131.15	138.12	119.96	132.71	122.45	119.48	97.95	1258.80
Rainfall	30.30	36.90	53.40	116.10	102.20	71.60	73.10	91.90	75.30	86.20	93.00	41.40	871.40

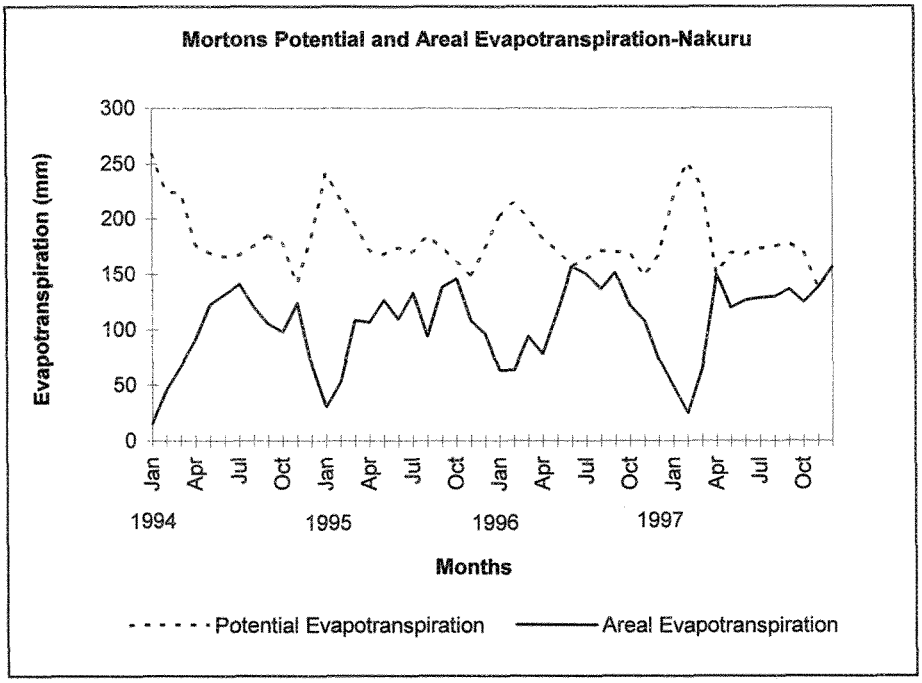

Fig. 6.6a

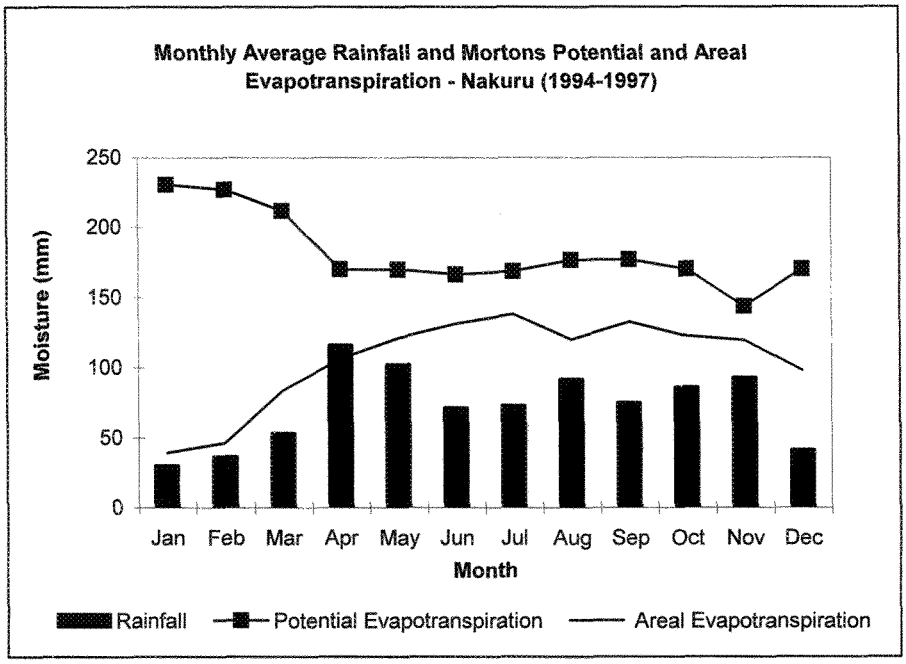

Fig. 6.6b

It can be observed from Table 6.6a and Fig. 6.6a that there is a consistent seasonal pattern over the period 1994-1997. From Fig 6.6b it is evident that potential evapotranspiration is highest during the dry periods and low during the rainy period. This is expected as the rainy months are characterized by lower temperature and higher humidity and dry periods by higher temperature and lower humidity. Annual P.E.T values appear to be fairly constant over this period and an average value of 2180 mm was calculated. The highest P.E.T values were recorded during the months January, February and the beginning of March (dry period) and the lowest values recorded in November during the period of the short rains. It can be seen from Fig 6.6b that potential evapotranspiration decrease with increasing rainfall. This supports Mortons Complementary model where evapotranspiration consumes both energy and water, and result in the cooling and humidifying of the overpassing air. These factor together result in the reduction of P.E.T.

Fig 6.6a indicate that there is no clear consistent pattern of monthly variations in areal evapotranspiration. There is however a high temporal variation where areal evapotranspiration values vary from a low of 40 mm to a high of 138 mm. Low areal evapotranspiration values occur during the months of January and February which corresponds to the dry period and high values occur during the months of June to September (Table 6.6 b). An annual average value of 1258 mm was calculated. Generally it can be said that areal evapotranspiration increases steadily during the month of January to around July where it reaches a maxima. Areal evapotranspiration then decreases through to October, from where it reaches peaks again in November and again decreases in December. Fig. 6.6b indicate that areal evapotranspiration exceeds rainfall throughout the year, except for the month of April (middle of the long rain). This suggests that there is little moisture available for surface runoff, infiltration or groundwater recharge. This is not necesssarily so as daily precipitation may exceed areal evapotranspiration rates, and in the absence of surface runoff, this excess moisture is infiltrated to the groundwater. Generally areal evapotranspiration increase with increasing rainfall.

Fig. 6.6a shows clearly Morton Complementary Relationship between the potential evapotranspiration and the areal evapotranspiration.

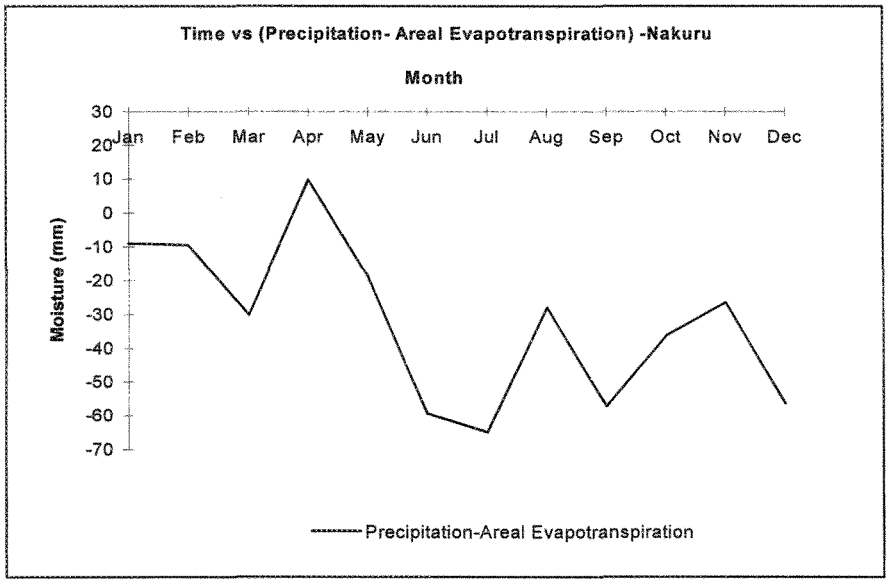

Fig. 6.6c

Fig 6.6c shows a graph of the monthly budget of Precipitation - Areal Evapotranspiration. Here it can be seen that there is a deficit of soil moisture throughout the year excepting for the month of April. The maximum deficit occurs during the dry months of June, July and September.

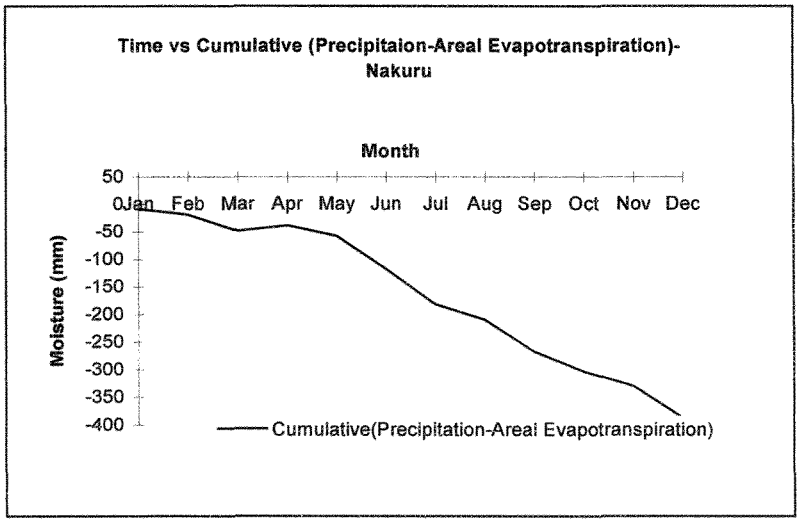

Fig. 6.6d.

Fig. 6.6d shows the accumulative deficit during the year.

The resulting values for the Station located at Nyeri can be seen in Table 6.6c and Table 6.6d.

Table 6.6c Morton Potential Evapotransspiration (mm) for Station Nyeri

Year	Jan	Feb	Mar	Apr	Mar	Jun	Jul	Aug	Sep	Oct	Nov	Dec	Yearly Total
1994	181.84	175.14	188.27	156.08	154.55	152.82	154.93	155.74	173.85	171.48	129.90	163.87	1958.44
1995	183.53	179.32	181.81	158.23	154.47	156.05	157.37	156.24	163.30	157.60	139.57	159.80	1947.29
1996	168.72	169.92	171.32	164.66	160.67	153.77	149.56	158.88	176.78	178.66	143.53	155.04	1951.50
1997	187.71	214.64	202.34	179.32	181.01	157.31	153.58	158.82	165.08	161.13	133.37	152.07	2046.40
Monthly Average	180.45	184.75	185.93	164.57	162.67	154.99	153.86	157.42	169.75	167.22	136.59	157.70	1975.91
Rainfall	58	56	90	130	110	70	36	38	45	96	110	85	924

Table 6.6d Morton Areal Evapotranspiration (mm) for Station Nyeri.

Year	Jan	Feb	Mar	Apr	Mar	Jun	Jul	Aug	Sep	Oct	Nov	Dec	Yearly Total
1994	117.41	120.58	128.40	142.29	154.55	152.82	154.93	155.74	142.20	126.98	129.90	143.37	1669.16
1995	110.91	107.34	155.92	148.29	154.47	156.05	157.37	156.24	163.30	156.32	128.82	150.85	1745.88
1996	158.60	144.18	157.52	132.14	148.81	153.77	149.56	158.88	129.09	100.14	126.35	123.64	1682.67
1997	90.22	62.57	100.91	78.01	77.09	157.31	153.58	158.82	165.08	157.68	133.37	152.07	1486.72
Monthly Average	119.29	108.67	135.69	125.18	133.73	154.99	153.86	157.42	149.91	135.28	129.61	142.49	1646.11
Rainfall	58	56	90	130	110	70	36	38	45	96	110	85	924

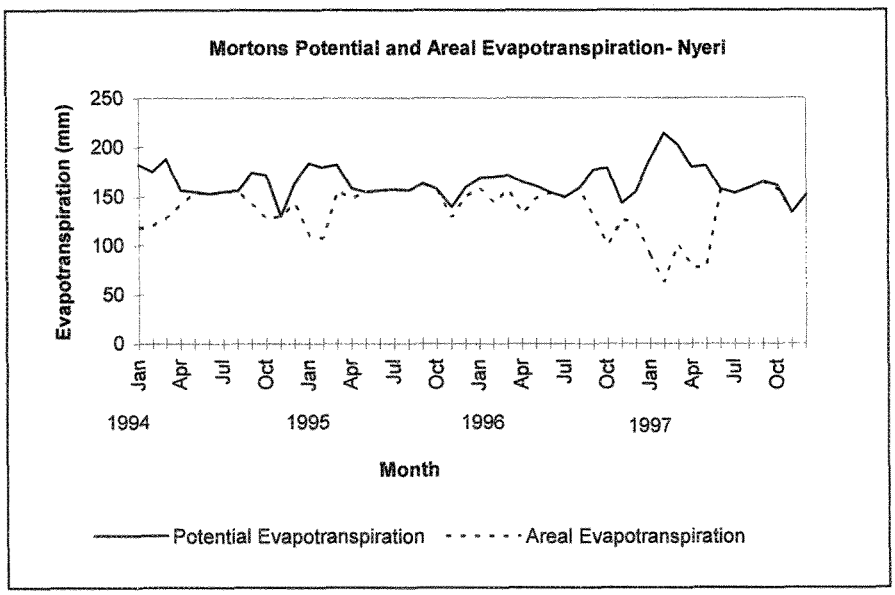

Fig. 6.6e

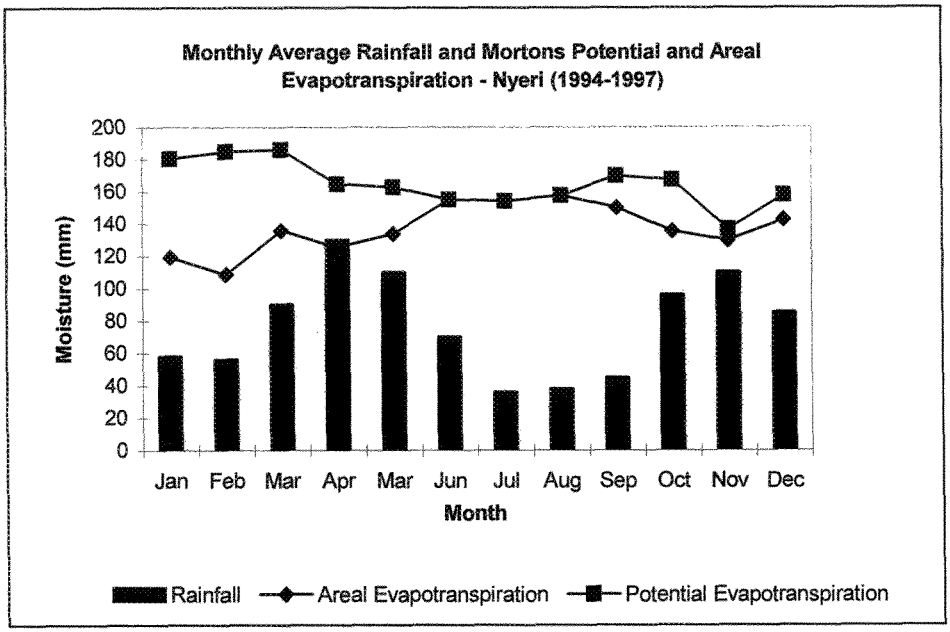

Fig. 6.6f

The monthly variation of Potential Evapotranspiration for the station at Nyeri is shown in Fig 6.6e . Here it can be seen that there is no significant seasonal variation and the pattern of Potential evapotranspiration follows one which is inverse to that of the rainfall (Fig. 6.6f) with periods of low potential evapotranspiration occuring during rainy periods and high Potential evapotranspiration during dry periods. An annual mean P.E.T of 1975mm was recorded between 1994-1997. The monthly mean maximum of 186 mm was recorded in March and a monthly mean minimum of 137 mm in November. Fig 6.6f indicate that rainfall exceeds P.E.T for the entire year. Monthly P.E.T show a definite trend of increasing during the dry months decreasing during the rainy period

Fig. 6.6f indicate a relatively high temporal variation and a general pattern of areal evapotranspiration increasing with increasing rainfall. An annual mean evapotranspiration of 1646 mm was recorded. The monthly mean maximum of 158 mm was recorded in September and the mean minimum of 109 mm was recorded in February. It can be seen from Fig. 6.6f that when the long-term average values were taken, that there is no clear relationship between areal evapotranspiration and rainfall. It can however be seen that areal evapotranspiration is higher than the mean monthly rainfall except for the month of April. This again suggests that there is little moisture available to for surface runoff or groundwater recharge. However daily precipitaion may exceed areal evapotranspiration rates and in the absence of surface runoff , excess moisture may infiltrate to the groundwater.

Fig. 6.6e shows that potential evapotranspiration approximates areal evapotranspiration throughout the months of May -September suggesting also that there is available moisture to replenish soil moisture and groundwater recharge.

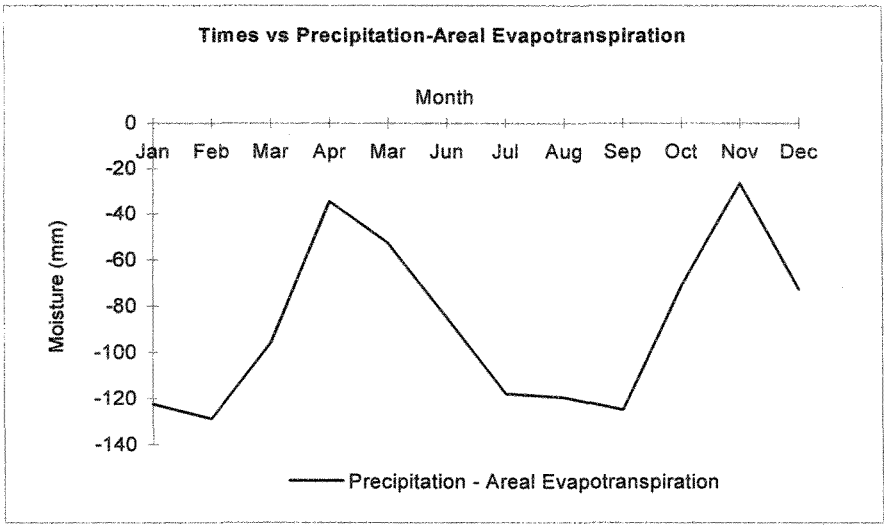

Fig. 6.6g

Fig. 6.6g shows the moisture deficit which ocurs during the year. It can be seen that maximum deficit occurs during the dry months of February and July through to September. Minimum deficit occurs during the wet months of April and November. The budget shows that there is a continuous soil moisture deficit throughout the year.

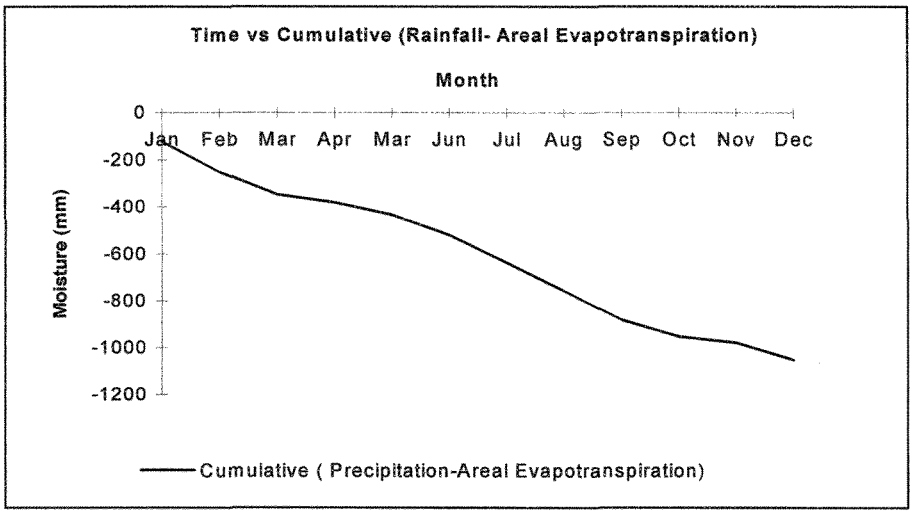

Fig. 6.6h

Fig. 6.6h shows the accumulative soil moisture deficit during the year.

6.7 Advantages of using the CRAE Model

1) The model can be applied, without the need for local optimization of coefficients, to river basins with different climates, vegetation covers, soils and landforms.

2) This approach is advantageous in that it a more realistic representation of reality than the conventional approach in that potential evaporatranspiration is higher in areas short of water than in areas where water is available. This is so as evapotranspiration consumes both energy and water, thereby cooling and humidifying the overpassing air and reducing the potential evaporation.

3) The resultant model permits areal evapotranspiration to be estimated from its effects on routinely observed climatological variables used in the computing potential evapotranspiration, thereby avoiding the complexities of the soil-vegetation system.

4) As a consequence the model is verifiable, so that errors in the associated assumptions and relationships can be detected and corrected by progressive testing over an ever-widening range of environments.

5) The model was calibrated with monthly data under particularly stringent condition, that is, in areas where the dry-environment potential evapotranspiration and the potential evapotranspiration are very large and the areal evapotranspiration is a small residual.

6.8 Limitations of the Model

The CRAE model has the following limitations:

1) It requires accurate humidity data and these are dependent on frequent observations by a skilled personnel.

2) They cannot be used for short intervals (less than five days) because of subsurface heat-storage changes and because of the lag times associated with the change in storage of heat and water vapour in the atmospheric boundary layer after changes in surface conditions or the passage of frontal systems.

3) They cannot be used near sharp environmental discontinuities such as a high-latitude coastline or the edge of an oasis, because of advection of heat and water vapour in the lower layers of the atmosphere.

4) They require input from a climatological station whose suroundings are representative of the area of interest.

5) They cannot be used to predict the effects of natural or man-made changes because they neither use nor require knowledge of the soil-vegetation system. This is considered to be the most serious long-term limitation to the application of the CRAE model.

6) It cannot be applied to deep lakes with large seasonal changes in subsurface heat storage.

The data calculated from the two stations indicate that Morton's areal evapotranspiration was consistently greater than rainfall. This suggests that the rainfall data used was not representative of the study area. This can be verified as studies (Karongo and Sharma-1997) in the adjacent catchments of Kimakia and Ndarugu indicate areal evapotranspiration data,as calculated by Morton, which are within the same range as those calculated in the previous section. The mean annual rainfall data used is however significantly higher, indicating that groundwater recharge occurs. The areal evapotranspiration calculated in the previous section was markedly higher during the dry months than that calcualted for the above-mentioned study. This indictes that that the method as coded here overestimated areal -evapotranspiration by a substantial amount. Discrepancies could also be due to the inaccuracy of the data set.

7.0 GROUNDWATER RECHARGE USING WATER BALANCE-THORNETHWAITE AND MATHER

7.1 Introduction

The water budget is a very essential tool in water resources planning. It provides a very simple, yet effective method of gaining insight into the trends of water deficit and surplus that occur in the area. As it is based on meteorological data it can be used as a tool for the prediction of the effect of man made changes on the hydrology of an area. Here it is used to estimated the groundwater recharge that occur in the study area.

The water balance, calculated for a single soil profile or for an entire catchment, refers to the balance between incoming precipitation and outflowing evapotranspiration, groundwater recharge and streamflow. In its simpliest form the water balance can be expressed as follows:

Inflow-Outflow = Change in storage

Each of the elements of inflow and outflow may include several different items. These are:

Inflow Items which include: surface water inflow, groundwater inflow, precipitation and Imported water

Outflow Items include: surface water outflow, groundwater outflow, evapotranspiration and exported water.

Storage Items include: change in surface water storage, change in groundwater storage and change in soil moisture storage.

The water balance of a basin can be stated by the following equation:

surface inflow +subsurface inflow+precipitation +imported water+ decrease in surface storage+decrease in groundwater store= surface outflow+subsurface outflow+evapotranspiration+exported water+increase in surface storage+increase in subsurface storage

The water budget computation used is based on the water balance computations as developed by Thornethwaite and Mather (1957). This model uses average monthly

of precipitation and average monthly potential evapotranspiration to estimate average monthly actual evapotranspiration. Soil and vegetation characteristics are combined by means of the water holding capacity of the root zone.

The model assumes that the final output is the "moisture surplus"available for runoff into river, streams and lakes.

The Water Balance Model is modified and coded "WTRBLN" by Donker (1988).

7.2 Input Parameters of the Model

The WTRBLN requires the following input data: precipitation, evapotranspiration, water holding capacity of soils, direct runoff, crop coefficient values.

7.2.1 Precipitation (RAIN)

This section analyzes the rainfall in the study area on a long term monthly basis. Stations around and outside of the catchment boundaries were included in order that spatial interpolation would give complete coverage of the project area (Fig. 7.2.1). The long term monthly average precipitation was used in the analysis as this was the only available data (Table 7.2.1).

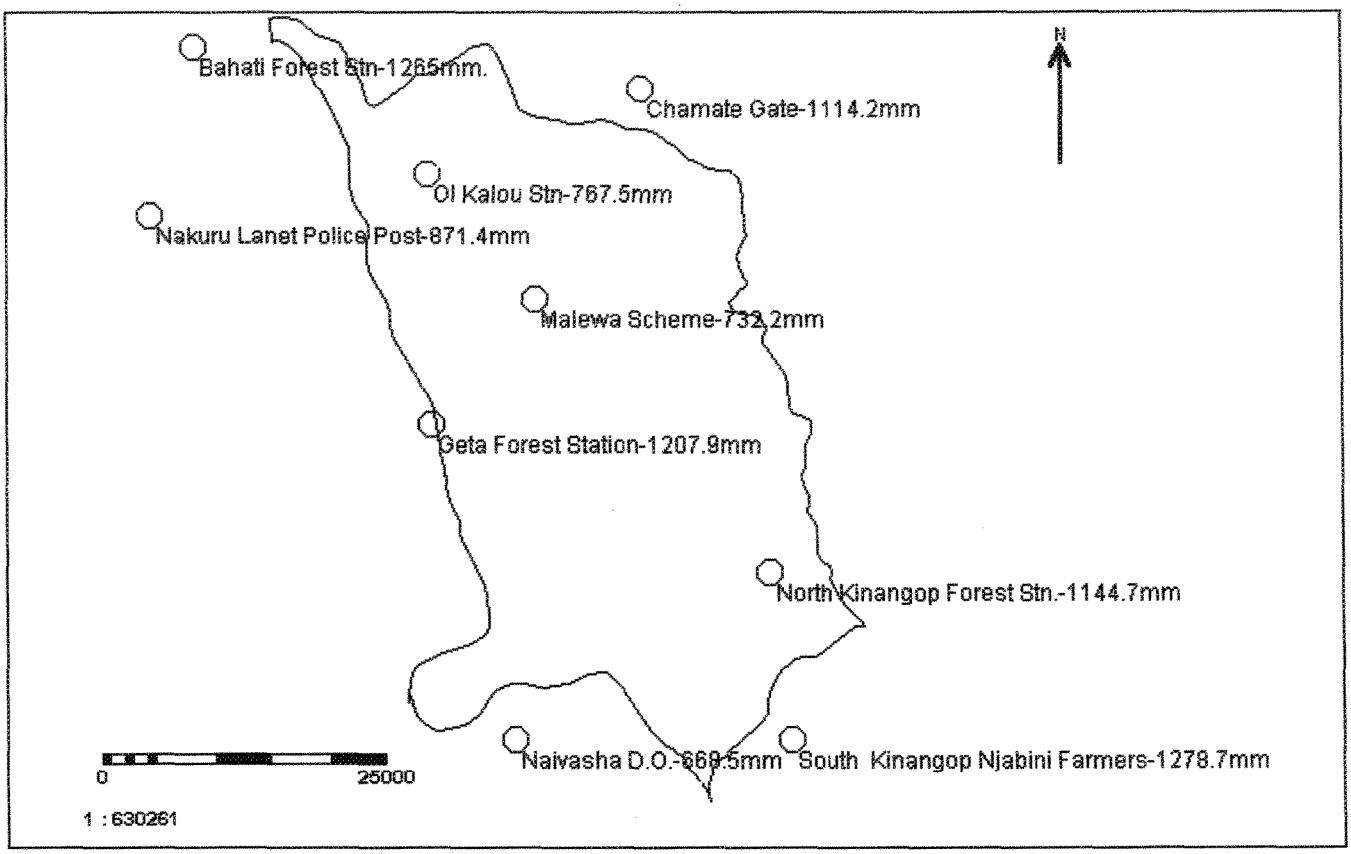

Fig.7.21 Location of the Rainfall Stations in the Study area

Table 7.2.1 Long Term Average Rainfall (mm)

Station Location		Station Name															
X	Y		Height (m)	Jan	Feb	Mar	Apr	May	Jun	Jul	Aug	Sep	Oct	Nov	Dec	years	Rainfall Total (yearly)
214315	9920714	Naivash D.O."	1900.43	25.4	35.7	57.8	112.9	83.8	81.7	34.4	44.6	43	48.7	60.7	39.8	77	668.5
236582	9935474	North Kinangop Forest Station"	2630.42	43.1	50.9	86.9	174	154.4	107.1	75	94.3	102.6	98.9	98.4	59.1	72	1144.7
186444	9981558	Bahati Forest Station	2316.48	25.6	31.8	56.9	163.1	21.0.3	125.9	133.9	164.2	119.9	103.5	91.6	38.3	59	1265
225433	9977875	Chamate Gate	2634.64	35.2	33.5	62.6	145.2	123.1	104.2	111.5	164.6	84.8	69.1	97.9	62.5	11	1114.2
206870	9970497	Ol Kalou Station"	2367.08	20.3	17.8	30.8	99.4	104.8	86.1	106.2	128.2	53.7	46.6	53.3	20.3	50	767.5
238446	9920727	South Kinangop Njabini Farmers Tr Ctr"	2590.80	65.1	66.8	117.3	231.7	173.9	74.3	63.7	65.1	63.6	118.6	132.6	106	38	1278.7
182733	9966803	Nakuru Lanet Police Post	1889.76	30.3	36.9	53.4	116.1	102.2	71.6	83.1	91.9	75.3	86.2	93	41.4	29	871.4
207248	9948369	Geta Forest Station"	2590.80	41.1	45.2	75.1	168.2	168.5	109.9	106.4	116.6	125.2	105.5	91.3	54.9	32	1207.9
216155	9959436	Malewa Scheme"	2316.48	30.2	26	49.8	110.6	107.4	77	64.3	86.1	63.3	53.4	48.4	16.1	14	732.2

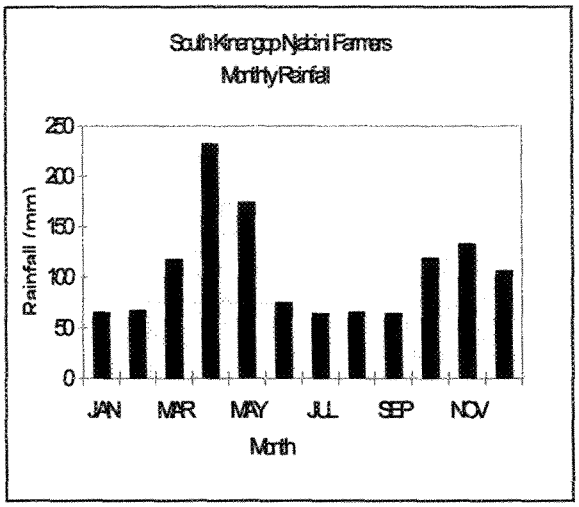

Fig 7.2.1a

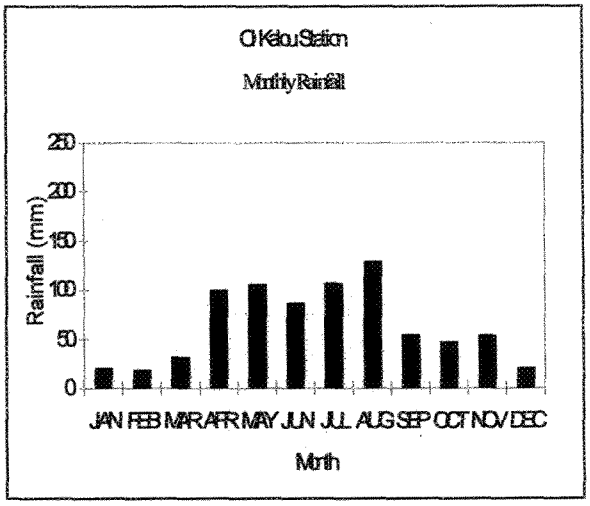

Fig.7.2.1b

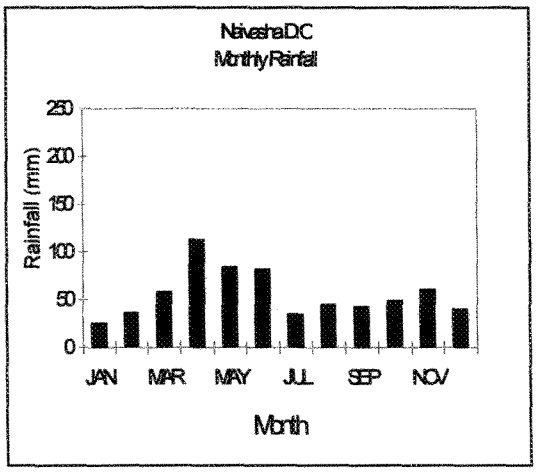

Fig.7.2.1c

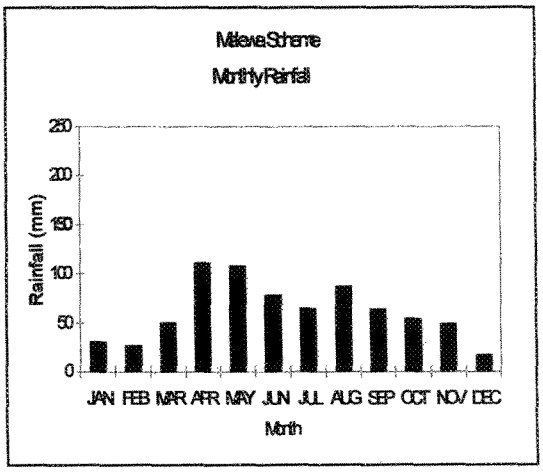

Fig. 7.2.1d

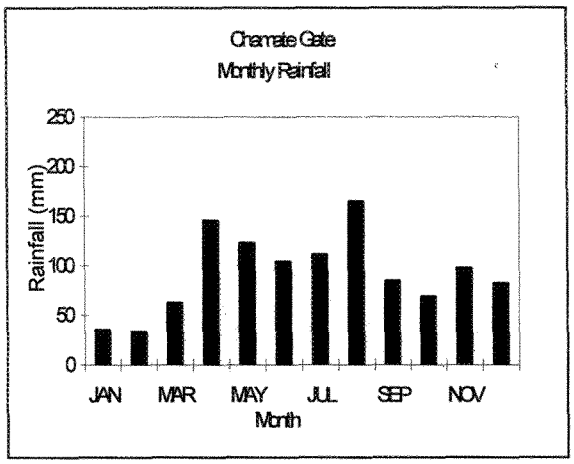

Fig.7.2.1e

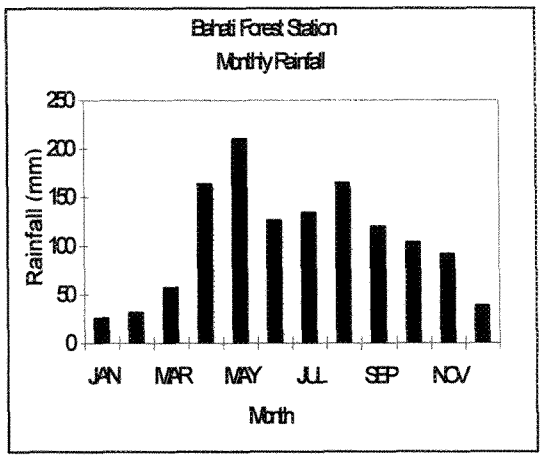

Fig 7.2.1f

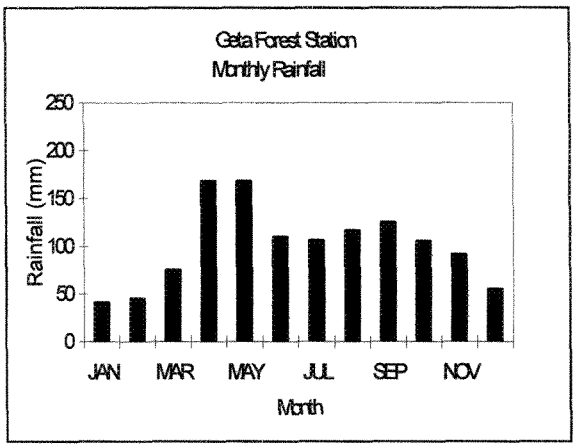

Fig. 7.2.1g

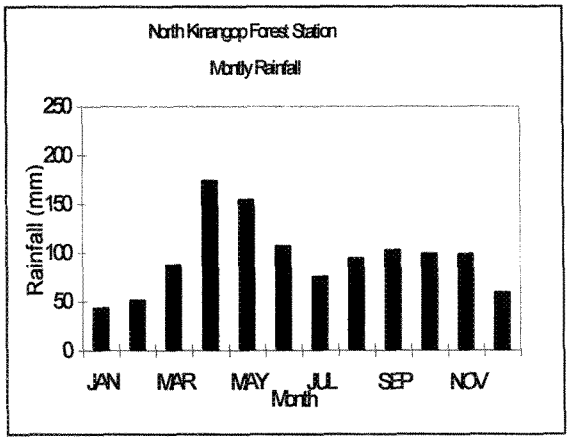

Fig. 7.2.1h

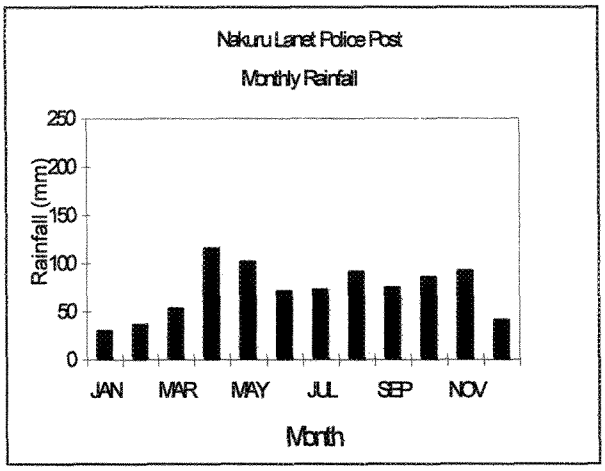

Fig. 7.2.1i

From the graphs (Fig.7.2.1a- Fig. 7.2.1i) it can be seen that the rainfall pattern vary widely across the study area due to orography, with notably higher levels of rainfall occurring at the stations located at higher altitudes compared with those situated on the valley floor. For example, annual variation in precipitation varies from 670 mm/annum in the vicinity of Naivasha which is situated at an elevation of 1900 m amsl, to 1279 mm/annum in the South Kinangop area at an altitude of 2590m amsl. There are primarily two rainy periods per year, the long rains occurring in March, April and May and the short rains, in October and November. This can be observed at stations such as Naivasha D.O., North and South Kinangop. At stations such as Ol Kalou, Chamate Gate, Nakuru Lanet Police Post, Bahati Forest and Geta Forest Station there is well defined rainy season in August. It can be seen that the rainfall pattern within the study area is subject to great spatial and temporal variation.

There is a correlation between altitude and rainfall and a correlation coefficient (R^2) of 0.67 was calculated (Fig. 7.2.1j). The relationship can be expressed as follows:

$$R=0.7160(H)-710.00 \qquad (7.2.1)$$

where R=Rainfall in mm
H=elevation in m.

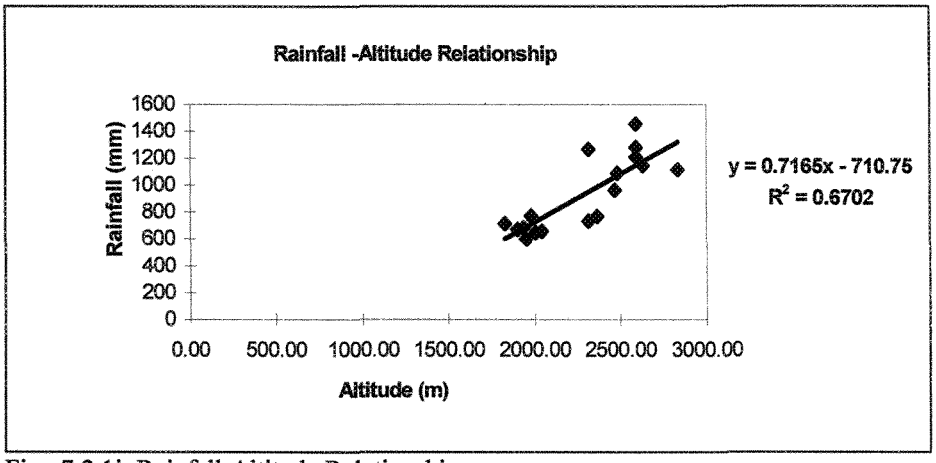

Fig. 7.2.1j Rainfall-Altitude Relationship

7.2.1.1 Spatial Distribution of Rainfall

Based on the relationship described in section 7.2.1. a rainfall distribution map was derived. Fig.7.2.1.1 shows the spatial rainfall distribution map.

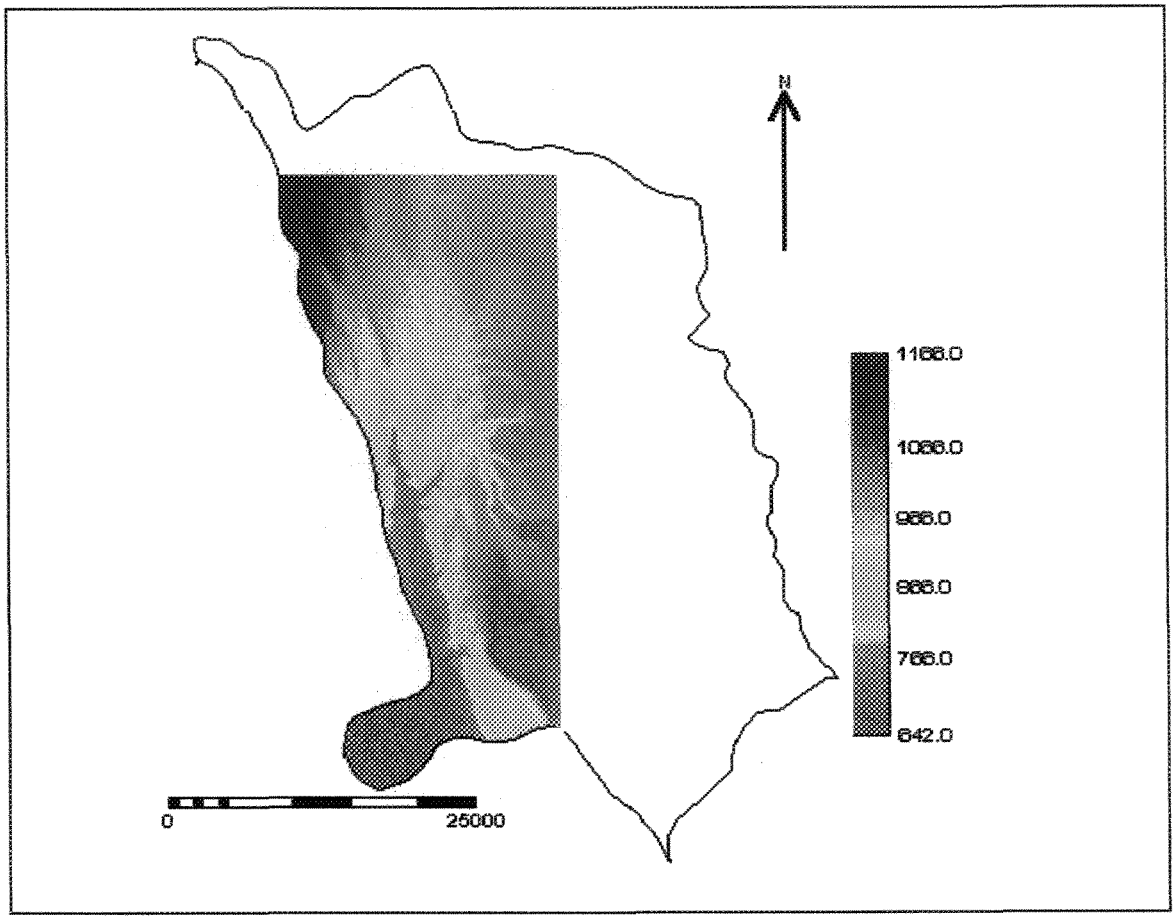

Fig. 7.2.1.1 Spatial rainfall distribution map.

7.2.2 Potential Evapotranspiration

Potential Evapotranspiration as calculated by Morton's (1983) model was input into the program. Data obtained from the Nyeri station is assumed to represent the eastern catchment areas whereas data from Nakuru represents the upper northern catchment areas and the Central Rift Valley (Table 7.2.2).

Table 7.2.2 Monthly Evapotranspiration values for Nakuru and Nyeri

Months	Jan	Feb	Mar	Apr	May	Jun	Jul	Aug	Sep	Oct	Nov	Dec	Yearly Total
Station -Nakuru	230.6	227.0	211.7	169.9	169.6	166.17	168.55	176.41	176.84	170.08	143.76	170.14	2180.8
Station - Nyeri	180.4	184.8	185.9	164.5	162.7	155.0	153.9	157.4	169.8	167.2	136.6	157.7	1976.0

7.2.3 Crop Coefficient (Kc)

This input represents a modification of the original method of Thornethwaite. This factor seeks to correct the evapotranspiration which is defined with as the cover type to a value that represents the dominant cover type in the area under consideration. In the vicinity of Naivasha, the main cover type is wheat and barley. In the Kinangop Plateau area wheat, barley and maize represent the major ground cover. Based on the local crop calendar the following Kc values were applied to the various areas where the WTRBLN Model was used (Table 7.2.3).

Table 7.2.3 KC values of the major ground cover.

Months	Wheat	Barley(Long)	Barley (short)	Maize (Long)	Maize (Short)
Jan	0.35	0.35	1.12	0.25	1.12
Feb	0.35	0.35	1.28	0.25	1.28
Mar	0.35	0.35	0.95	0.25	0.95
Apr	0.35	0.50	0.25	0.40	0.25
May	0.35	0.90	0.25	0.78	0.25
Jun	0.50	1.13	0.25	1.12	0.25
Jul	1.05	1.30	0.25	1.25	0.25
Aug	1.33	1.35	0.25	1.30	0.25
Sep	1.15	1.40	0.25	1.10	0.25
Oct	0.80	1.25	0.25	0.80	0.25
Nov	0.35	1.13	0.40	0.25	0.40
Dec	0.35	0.80	0.78	0.25	0.78

7.2.4 Major Soil Group

The soil pattern in the study area (Fig. 7.2.4) is very intricate due to striking differences in altitude, landforms, geology and climate. The exploratory soil map of Kenya and the data associated with it (Sombroek et al.,1982; scale 1:1,000,000) was used to identify the major soil groups which occur in the study area. This data provided a textural composition for each of the major soil classes identified on the map as occurring within the study area. A depth classification scheme was also included (Table 7.2.4). The descriptive terminology applied is based on the FAO's "Guidelines for soil profile description".

There are seven (7) major soils groups that can be found in the Malewa catchment (Table 7.2.4.1). The soils found in the M group are primarily derived on Mountains and major scarps and slopes. Of this group M2 and M9 soils occur in the study area. M2 soils are generally well drained, very deep (1.20-1.80m),dark reddish-brown to dark brown , very friable and smeary, clay loam to clay , with a thick acid humic topsoil. In places it is shallow (0-50 cm) to moderately deep (50-80 cm) and rocky. These soils are found in the Kipipiri and the Aberdare mountains.

M9 soils can be described as imperfectly drained , shallow(0-50cm) to moderately deep(50-80cm), dark greyish-brown, very friable, acid humic to peaty, loam to clay loam, with rock outcrops in places. These soils are found in the Aberdare Mountains of the study area.

The soils found in the L group are found on plateaus and high-level structural plain (flat to gently undulating). L20, L21 and L22 soils from this group occur in the study area. These soils are developed on ashes and other pyroclastics rocks of Recent volcanoes.

L20 soils are well drained, moderately deep (50-80cm) to very deep (120-180cm), dark brown, friable and slightly smeary. Texture varies from clay loam to clay. These soils are found in the areas of the Kinangop Plateau.

L21 soils have a friable and slightly clay loam texture. They are imperfectly drained, deep (80-120cm) very dark greyish brown to dark brown. These soils are found in the region of the Kinangop Plateau.

L22 soils are a complex of well drained, deep (80-120cm) to very deep (120-180cm), very dark greyish brown to dark brown, friable and slightly smeary, clay loam and imperfectly drained, deep, very dark greyish brown to black, firm, moderately calcareous m cracking clay. The soils are found in the Ol Kalou region.

The soils of the PlP sub-group are developed on sediments mainly from volcanic ashes. Of this group P111 and P17 occur in the study area. P111 is a complex of well drained, moderately deep (50-80cm) to deep (80-120cm) , dark brown, friable and slightly smeary, fine gravely, sandy clay loam to sandy clay, with a humic topsoil and imperfectly drained, moderately deep to deep, strong brown, mottled, firm and brittle, sandy clay to clay. These soils are found in the vicinity of the lake Naivasha.

P17 soils consists of imperfectly drained to poorly drained, very deep, dark greyish brown to dark brown, firm to very firm, slightly to moderately calcareous, slightly to moderately saline, moderately to strongly sodic, silt loam to clay; in many places, with a humic topsoil; subrecent lake edges of the Central Rift Valley. These soils are found along the main road from Naivasha to Gilgil.

The H group is comprised of soils which are developed on basic igneous rock (serpentines, basalts, nepheline phonolite, older basic tuffs included). Of this group H9 is located in the study area. It is well drained, shallow, dark reddish brown, friable, very calcareous, bouldery or stony with a loam to clay loam texture. In many places it is saline. In the study area it is found in the graben areas of the rift.

Ux group are soils developed in the uplands area undifferentiated levels (undulating to rolling; altitudes and base level variable). This group is further divided into several sub-groups which include the UxBP soil group. This group is comprised of soils developed on basic igneous rocks (basalt), but with influence of volcanic ash predominant. Ux3 is a well drained deep to very deep, dark reddish brown to dark red, firm clay; with inclusions or imperfectly drained, moderately deep, dark greyish brown clay. These soils are found in the upper northern area of the Malewa catchment in the vicinity of Ol Kalou.

UxV are soils developed on undifferentiated volcanic rocks. Of this group Ux5 is located in the vicinity of the Kipipiri Mountains. Ux5 soils are described as well drained, very deep, dark reddish brown to very dark greying brown, friable and slightly smeary clay, with a humic topsoil.

The R group are soils developed on volcanic footbridges (dissected lower slopes of major older volcanoes and mountains; undulating to hilly). Of this group R1 is found in the upper catchment area of The Aberdare Forest. This consists of well drained , extremely deep, dark reddish brown to dark brown friable clay , with an acid humic topsoil (ando-humic Nitisols; with humic Andosols).

The F group consists of soils developed on colluvium from various volcanic rocks (mainly basalts). They are mainly found on footslopes (gently sloping to sloping: slopes 2-8%) such as the escarpment at the foot of the Aberdares and at the base of the Kipipiri Mountain where the F7 group is mainly found. These soils can be described as well drained, deep to very deep, reddish brown, friable clay, with an acid humic topsoil (ando-humic Acrisols).

Table 7.2.4 Soil Depth Scheme

Depth	Description
50cm	shallow
80 cm	shallow to moderately deep
95 cm	moderately deep
110cm	moderately deep to deep
120cm	deep
150 cm	deep to very deep
180 cm	very deep
250 cm	extremely deep

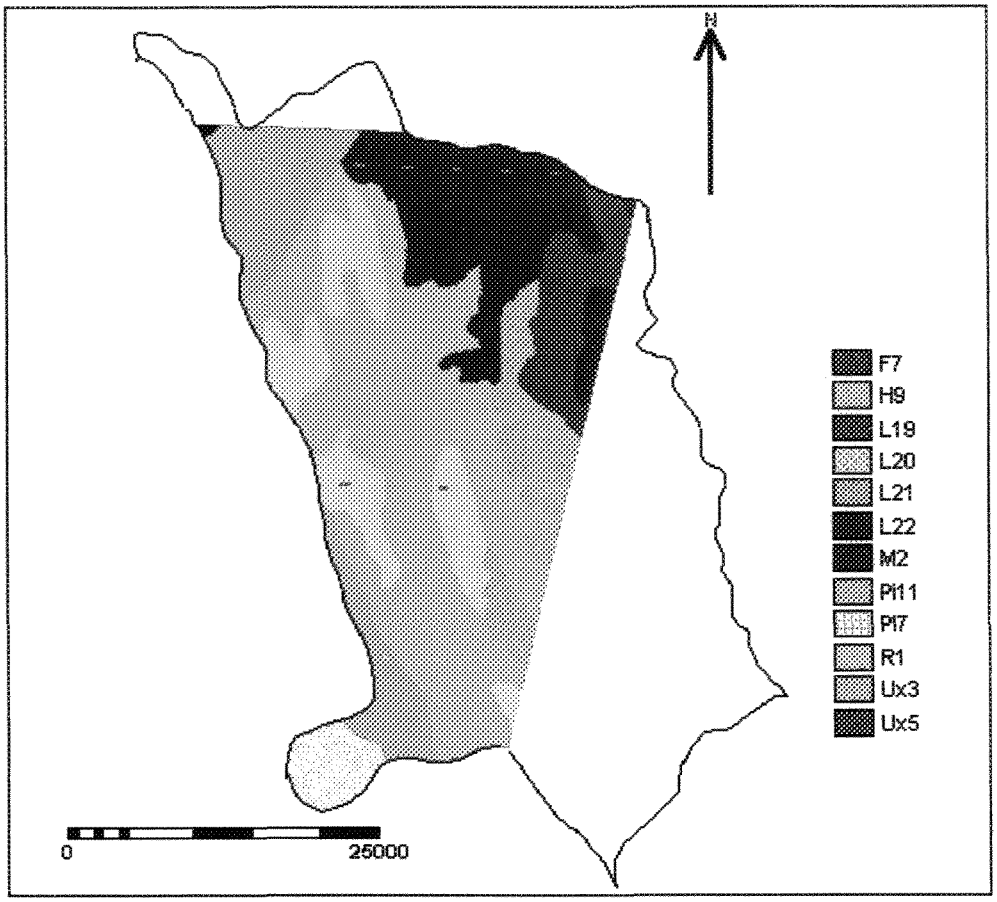

Fig. 7.2.4 Soil Map of the Study Area

7.2.4.1 Available Water Capacity

The available water capacity is the quantity of water that can be held by the soil per unit area and is a function of the soil texture, structure, organic matter content, density and soil depth. The calculation of available water capacity was made by using the soil texture to obtain the water holding capacity of the soil and the rooting depth of the major vegetation type. Table 7.2.4.1 shows the major soil group, their texture and available water holding capacity.

In the vicinity of Naivasha, Kinangop Plateau and the slopes of the Aberdares, the main crops grown are wheat, barley and fodder crops. These crops have a rooting depth of 1.0-1.7m. From field observations the Kikuyu grass found abundantly throughout the study area attains a maximum rooting depth of 2.5 m. In The Aberdares which consists of a mixed mature forest of pine and bamboos and hardwood species. Deep auguring revealed a rooting depth of 5.0 m for the pine trees. This value was also applied to South Kinangop region where mature pine forests are found. The maximum rooting depths of the above soil cover was used.

The available water holding capacity of these soils were obtained using the following formula:

AWC (mm) = Available Water (%volume)* Rooting Depth (m)

Table 7.2.4.1 Water Holding Capacity of the Major Soil Groups in the Study Area.

Soil Type	Texture	Depth of soil (cm)	Available Water Capacity (%vol)	Rooting Depth (m)	Available water capacity of root zone (mm)
M2	clay loam to clay	120-180	19-23	5.0	950-1150
M9	loam to clay loam	0-50	17-19	5.0	850-950
L20	clay loam to clay	50-180	19-23	5.0	950-1150
L21	clay loam	80-120	19	5.0	950
L22	clay loam	80-180	19	5.0	950
Pl11	sandy clay loam	80-180	17	2.5	425
Pl7	silt loam to clay	120-180	20-23	2.5	500-575
H9	loam to clay loam	0-50	17-19	2.5	425-475
Ux3	firm clay	80-180	20	2.5	500
Ux5	slightly smeary clay	120-180	23	5.0	1150
R1	friable clay	>180	23	5.0	1150
F7	friable clay	80-180	23	5.0	1150

7.2.5 Direct Runoff /Storm Runoff (SR)

Direct Runoff represents the percentage of rainfall that does not enter the soil but is lost by direct surface runoff or storm runoff. The values for direct runoff (runoff coefficient) (Table 7.2.5) was obtained by baseflow separation using the available records.

Table 7.25 Runoff Coefficient Values

Stations	Size of Catchment (km2)	Runoff Coefficient
2GB3	53	0.03
2GB4	152	0.36
2GB5	780	0.08
2GC5	119	0.10
2GC7	18	0.19
2GC4	695	0.15
2GB1	1428	0.06

7.2.6 Partitioning Rule (Groundwater runoff delay coefficient)-(C2)

A partitioning rule was introduced by Thornethwaite and Mather (1957). This is as the groundwater store acts as a buffer and causes a delay in the groundwater runoff. Therefore not all the water in storage will become part of the groundwater in the same month. Only a certain fixed percentage will runoff in the same month; the rest is detained till the next month. Partitioning rule used varied between 30 and 50 %.

7.3 Method of Computation of the Soil Moisture Model

The calculation method used in program "Wtrbln" is based on Thornethwaite and Mather who developed a simple book-keeping model that uses average monthly values of precipitation and average monthly potential evapotranspiration to estimate average monthly actual evapotranspiration.

The process of computation of the program "WTRBLN" is described as follows:

1. The programs first subtracts the surface runoff or direct storm runoff (SR) (which is a fixed percentage of the rainfall-C1) from the (RAIN) to arrive at the effective rainfall. With the input of the KC and the PET values the program calculates the crop PET (CPET). The CPET is then subtracted from the effective rainfall and the remaining part (SRECH) is available for infiltration into the soil. When the soil is not at its water holding capacity (WHC) and (SRECH) is positive, SRECH will then be utilized by the soil for replenishment (SM)

2. When the soil reaches its water holding capacity (WHC), the excess moisture (GRECH) contributes to groundwater recharge. If SRECH is negative the excess moisture will be utilized by the plants to replenish soil moisture. This results in an exponential soil moisture depletion and there is an accumulated potential water loss (APWL)of the soil. In this case the Actual Evapotranspiration (EA) is less than CPET.

3. If GRECH is added to water which is still present in the ground, the groundwater store will be act as a buffer and there will be a delay in groundwater runoff. The partitioning rule (C2) is then used in the computation of the total available surplus as not all the water in the store will become part of the groundwater flow in the same month. The rest will be detained (DET) until the next month.

4. Finally the total outflow to the catchment is calculated. This includes both storm runoff (SR) and groundwater runoff.

   The model was calculated on a monthly basis.

A graphic representation of the model can be seen in Fig. 7.3.

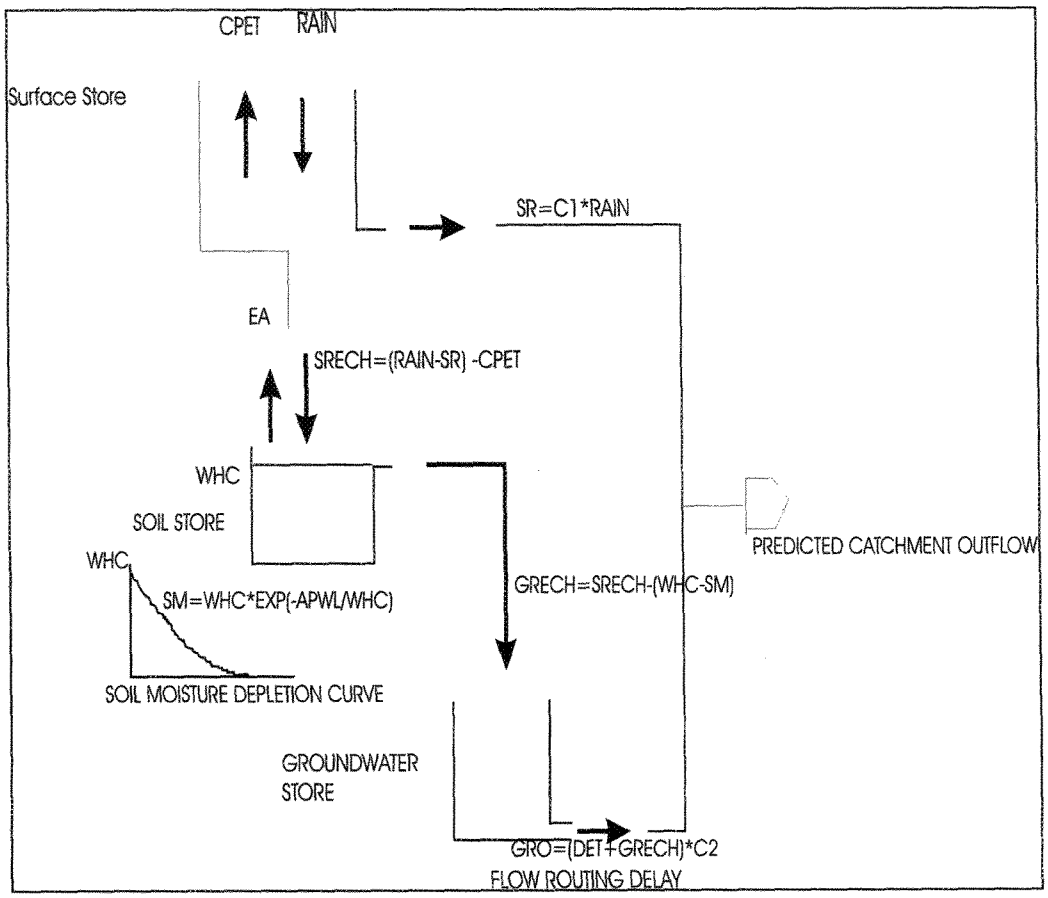

Fig. 7.3 Graphic Representation of The Water Balance Model (adapted from Introduction to The use of Geographic Information systems For Practical Hydrology by Meijerink et al., -1994)

7.4 Calculation Results

Water balance calculation using WTRBLN were done at seven (7) localities (Fig. 7.4a) which were selected as rainfall data and streamflow data was available for these areas. These were also the areas in which baseflow analysis was performed. Waterbalance calculations were done at the following locations: 2GB1, 2GB3, 2GC7 and 2GC5, 2GB4, 2GB5 and 2GC4. The input and ouput values for stations 2GB1 and 2GC5 will be discussed.

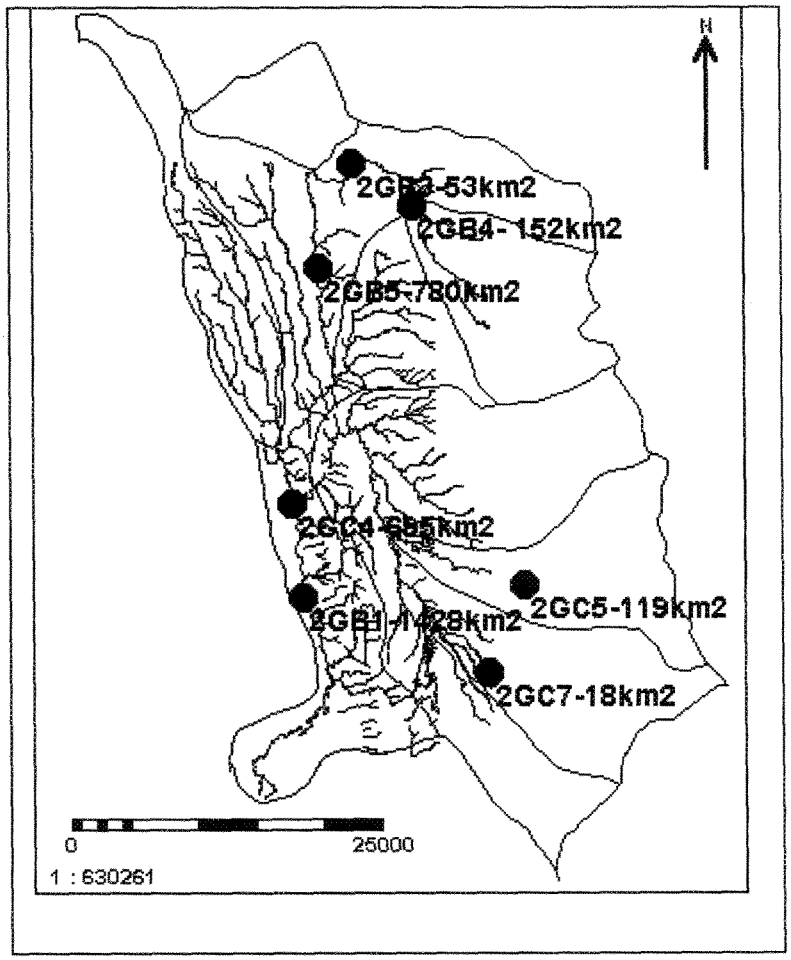

Fig.7.4a Locations where the Waterbalance was calculated.

Input data for the area located in the vicinity of 2GB1 is shown below in Table 7.4a.

Table 7.4a Input Data for the Area of 2GB1

Example 1 Standard Method.
Geta Forest Stn. area of catchment 1428km2-Station 2GB1

1	41	2	231	0.35
2	45	3	227	0.35
3	75	5	212	0.35
4	168	10	170	0.43
5	169	10	170	0.63
6	110	7	166	0.82
7	106	6	169	1.18
8	117	7	176	1.34
9	125	8	177	1.28
10	91	5	170	1.03
11	55	3	144	0.74
12	106	6	170	0.58

A water holding capacity of 425 mm was estimated for the soils in this catchment area.

Column 1: Month number
Column 2: Average Montlhy Rainfall (mm)
Column 3: Average Montlhy overland flow figures(mm)
Column 4: Average monthly potential evapotranspiration
Column 5: Crop coefficent (Kc) values

The results of the waterbalance calculation can be seen in Table 7.4b below.

Table 7.4b Long-term Average Monthly Water balance Calculation for Station 2GB1-Calculation by Standard Method

J	F	M	A	M	J	J	A	S	O	N	D	Y
Rain:												
41	45	75	168	169	110	106	117	125	91	55	106	1208
Overland Flow:												
2	3	5	10	10	7	6	7	8	5	3	6	72
Effective Rain:												
39	42	70	158	159	103	100	110	117	86	52	100	1136
Ref.Pot.Evp.:												
231	227	212	170	170	166	169	176	177	170	144	170	2182
Kc values :												
0.3	0.3	0.3	0.4	0.6	0.8	1.2	1.3	1.3	1.0	0.7	0.6	
Crop Pot.Evp.:												
81	79	74	73	107	136	199	236	227	175	107	99	1593
Rain - Evpt.:												
-42	-37	-4	85	52	-33	-99	-126	-110	-89	-55	1	-457
Ac. Pot. Water Loss:												
-42	-79	-83	0	0	-33	-133	-258	-368	-457	-512	0	
Soil Moisure:												
385	353	349	425	425	393	311	231	179	145	128	129	
Difference in Soil Moisture:												
256	-32	-3	76	0	-32	-82	-80	-53	-34	-17	1	
Actual Evapotranspiration:												
295	74	73	73	107	135	182	190	170	120	69	99	1587
Moisture Deficite:												
-214	5	1	0	0	1	17	46	57	55	37	0	5
Moisture Surplus:												
0	0	0	9	52	0	0	0	0	0	0	0	61

Longterm Average Monthly Water Balance Table. All values in mm.

Example 1 Standard Method.
Geta Forest Stn. area of catchment 1428km2

Soil-water storage capacity: 425 mm.

Standard calculation method.

The soil moisture has not attained the maximum capacity during the last month(s) of the wet priod(s). This causes erroneous results since the standard procedure assumes that at the end of the wet period(s) the soil-water storage is at maximum. In this case: USE THE SUCCESSIVE APPROX. METHOD.

Month Number:	Soil Moisture(mm):	Soil-water storage capacity(mm):
12	129	425
5	425	425

Input data for the area located in the vicinity of 2GC5 is shown below in Table 7.4c.

Table 7.4c Input Data for the Area of 2GC5

Example 1 Standard Method.
N. kinangop Stn. area of catchment 119km2-Station 2GC5

1	43	4	180	0.30
2	51	5	185	0.30
3	87	9	186	0.30
4	174	17	165	0.38
5	154	15	163	0.57
6	107	11	155	0.81
7	75	8	154	1.15
8	94	9	157	1.32
9	103	10	170	1.13
10	99	10	167	0.80
11	98	10	137	0.30
12	59	6	158	0.30

A water holding capacity of 950 mm was estimated for the soils in this catchment area.

The resulting output table can be seen below in Table 7.4d below.

Table 7.4d Long-term Average Monthly Water balance Calculation for Station 2GC5- Calculation by Standard Method

J	F	M	A	M	J	J	A	S	O	N	D	Y
Rain:												
43	51	87	174	154	107	75	94	103	99	98	59	1144
Overland Flow:												
4	5	9	17	15	11	8	9	10	10	10	6	114
Effective Rain:												
39	46	78	157	139	96	67	85	93	89	88	53	1030
Ref.Pot.Evp.:												
180	185	186	165	163	155	154	157	170	167	137	158	1977
Kc values :												
0.3	0.3	0.3	0.4	0.6	0.8	1.1	1.3	1.1	0.8	0.3	0.3	
Crop Pot.Evp.:												
54	56	56	63	93	126	177	207	192	134	41	47	1245
Rain - Evpt.:												
-15	-10	22	94	46	-30	-110	-122	-99	-45	47	6	-215
Ac. Pot. Water Loss:												
-15	-25	0	0	0	-30	-140	-262	-361	-406	0	0	
Soil Moisure:												
935	926	948	950	950	921	820	721	650	620	667	672	
Difference in Soil Moisture:												
263	-9	22	2	0	-29	-101	-99	-71	-30	47	6	
Actual Evapotranspiration:												
302	55	56	63	93	125	168	184	164	119	41	47	1417
Moisture Deficite:												
-248	0	0	0	0	0	9	23	28	15	0	0	-172
Moisture Surplus:												
0	0	0	92	46	0	0	0	0	0	0	0	138

Longterm Average Monthly Water Balance Table. All values in mm.

Example 1 Standard Method.
N. kinangop Stn. area of catchment 119km2

Soil-water storage capacity: 950 mm.

Standard calculation method.

The soil moisture has not attained the maximum capacity during the last month(s) of the wet priod(s). This causes erroneous results since the standard procedure assumes that at the end of the wet period(s) the soil-water storage is at maximum. In this case: USE THE SUCCESSIVE APPROX. METHOD.

Month Number:	Soil Moisture(mm):	Soil-water storage capacity(mm):
12	672	950
5	950	950

Applying the standard calculation method results in the situation where the Actual Evapotranspiration is higher than the effective rainfall for both areas. This error is due to the fact that eqn 1 which is used to calculate soil moisture during the dry months, assumes that at the end of the wet period the water capacity of the rootzone is achieved. However this is not the case for the two examples shown above for stations 2GB1 and 2GC5. In

both cases at the end of the wet period the rootzone has not achieved maximum water capacity. This is due to the fact that Actual Evapotranspiration 1587 mm is higher than effective rainfall 1136mm for station 2GB1, and Actual Evapotranspiration 1417 mm is higher than effective rainfall (1030 mm) for station 2GC5. Even though the tables indicate a moisture surplus at the end of the water year, this figure is erroneous as the formula does not work under such situations and it actually creates water when in fact there is none.

$$S_M = W.\exp(-La_M/W) \qquad (1)$$

where:

S_M = soil moisture during month M (mm)

La_M = accumulated potential water loss at month M (mm)

W = available water capacity of the rootzone (mm)

Use had to be made of the succesive approximation method (Dunne and Leopold 1978) to fulfil the conditions related to the formula to obtain soil moisture for the dry months.The successive approximation method was used in both situations. This method seeks to equate yearly evapotranspiration with yearly rainfall. Besides this the water capacity of the root zone (W) had to be set to considerable lower values (145 mm for Station 2GB1 and 250 mm for Station 2GC5) than that previously esitmated from the combined field observations and tables. Tables 7.4e and Fig. 7.4b shows the corrected water balance for the area of station 2GB1 and Tables 7.4f and Fig. 7.4c shows the corrected water balance for the area of station 2GC5.

Table 7.4e Long-term Average Monthly Water balance Calculation for Station 2GB1- Calculation by the Successive Approximation Method

J	F	M	A	M	J	J	A	S	O	N	D	Y
Rain:												
41	45	75	168	169	110	106	117	125	91	55	106	1208
Overland Flow:												
2	3	5	10	10	7	6	7	8	5	3	6	72
Effective Rain:												
39	42	70	158	159	103	100	110	117	86	52	100	1136
Ref.Pot.Evp.:												
231	227	212	170	170	166	169	176	177	170	144	170	2182
Kc values :												
0.3	0.3	0.3	0.4	0.6	0.8	1.2	1.3	1.3	1.0	0.7	0.6	
Crop Pot.Evp.:												
81	79	74	73	107	136	199	236	227	175	107	99	1593
Rain - Evpt.:												
-42	-37	-4	85	52	-33	-99	-126	-110	-89	-55	1	-457
Ac. Pot. Water Loss:												
-513	-550	-555	0	0	-33	-133	-258	-368	-457	-512	-471	
Soil Moisure:												
4	3	3	88	140	115	58	24	11	6	4	6	
Difference in Soil Moisture:												
-1	-1	-0	85	52	-25	-57	-34	-13	-5	-2	1	
Actual Evapotranspiration:												
40	43	70	73	107	128	157	144	130	91	54	99	1136
Moisture Deficite:												
40	36	4	0	0	9	42	92	97	84	53	0	457
Moisture Surplus:												
0	0	0	0	0	0	0	0	0	0	0	0	0

Longterm Average Monthly Water Balance Table. All values in mm.

Example 1 Standard Method.
Geta Forest Stn. area of catchment 1428km2

Soil-water storage capacity: 145 mm.

Successive Approximation Method.

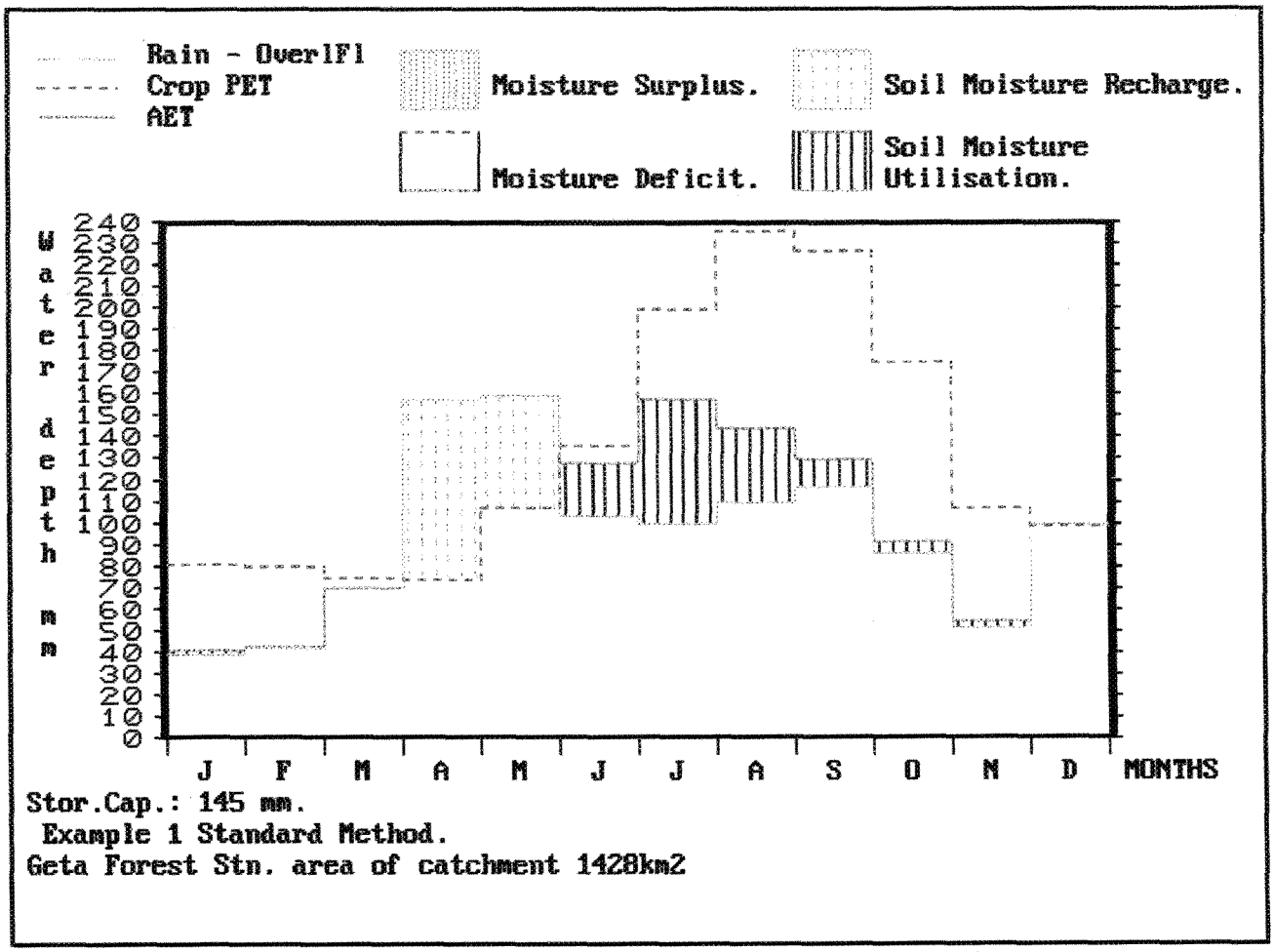

Fig. 7.4b Results of a Monthly Water Balance Calculation using the Successive Approximation Method- Station 2GB1.

Table 7.4f Long-term Average Monthly Water balance Calculation for Station 2GC5
Calculation by the Successive Approximation Method

J	F	M	A	M	J	J	A	S	O	N	D	Y
Rain:												
43	51	87	174	154	107	75	94	103	99	98	59	1144
Overland Flow:												
4	5	9	17	15	11	8	9	10	10	10	6	114
Effective Rain:												
39	46	78	157	139	96	67	85	93	89	88	53	1030
Ref.Pot.Evp.:												
180	185	186	165	163	155	154	157	170	167	137	158	1977
Kc values :												
0.3	0.3	0.3	0.4	0.6	0.8	1.1	1.3	1.1	0.8	0.3	0.3	
Crop Pot.Evp.:												
54	56	56	63	93	126	177	207	192	134	41	47	1245
Rain - Evpt.:												
-15	-10	22	94	46	-30	-110	-122	-99	-45	47	6	-215
Ac. Pot. Water Loss:												
-240	-250	0	0	0	-30	-140	-262	-361	-406	0	-225	
Soil Moisure:												
96	92	114	209	250	222	143	88	59	49	96	102	
Difference in Soil Moisture:												
-6	-4	22	94	41	-28	-79	-55	-29	-10	47	5	
Actual Evapotranspiration:												
45	50	56	63	93	124	146	140	122	99	41	47	1025
Moisture Deficite:												
9	6	0	0	0	2	31	67	70	35	0	0	220
Moisture Surplus:												
0	0	0	0	5	0	0	0	0	0	0	0	5

Longterm Average Monthly Water Balance Table. All values in mm.
Example 1 Standard Method.
N. kinangop Stn. area of catchment 119km2
Soil-water storage capacity: 250 mm.
Successive Approximation Method.

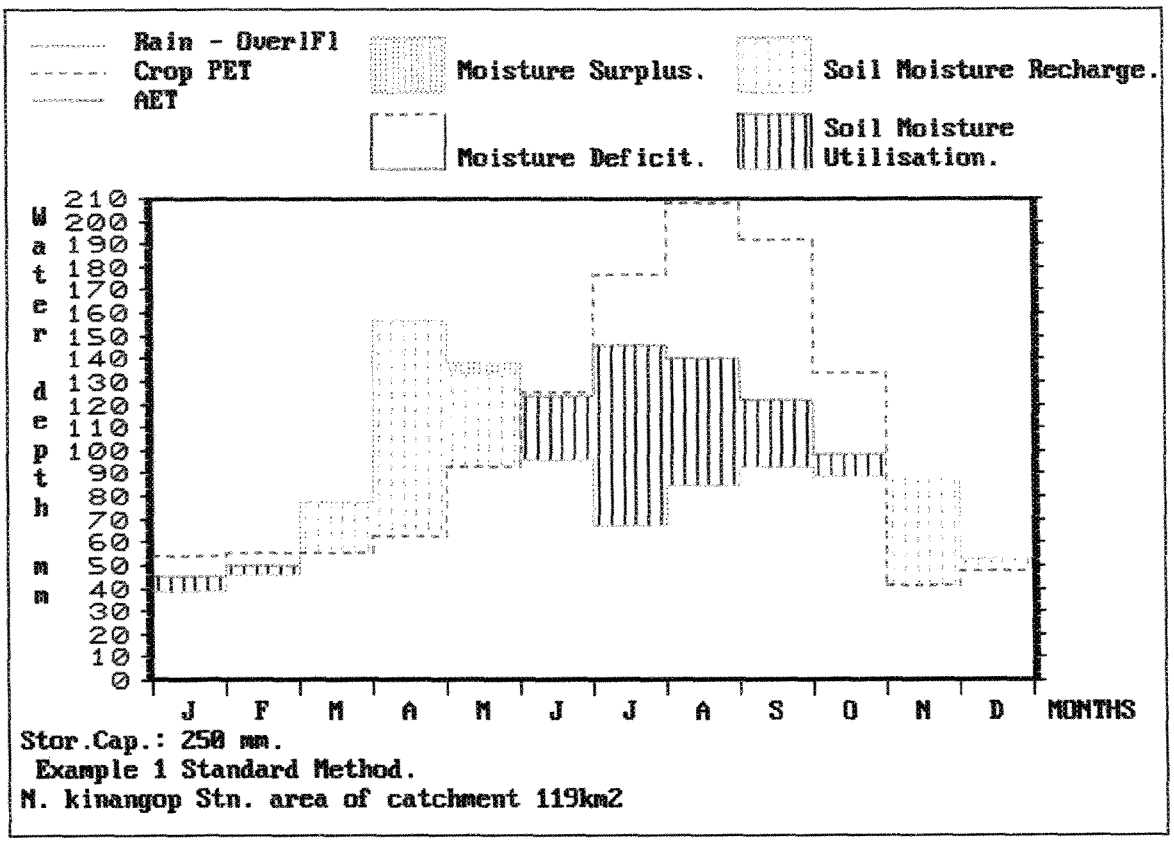

Fig. 7.4c Results of a Monthly Water Balance Calculation using the Successive Approximation Method- Station 2GC5.

Even though the results are mathematically correct, they did not match field evidence of observed recharage such as runoff and streamflow. It is noted that even though the successive approximation method was used there was no soil moisture surpus was generated and hence there was no groundwater recharge. A similar situation occured in the other areas where the waterbalance was calculated. As this situation does not represent the true seasonal water budget of the areas of interest the successive approximation method was not applied at these locations.

The fact that no moisture surplus was generated indicates that it is likely that the Reference Potential Evapotranspiration values as calculated by Mortons Model was too high. As stated previously in Chapter 6, the method as coded here overestimates Areal Evapotranspiration. Hence it can also be stated that the Potential Evapotranspiration is subject to the same error. The overestimation of runoff values could also lead to the non-generation of moisture surplus as this reduces the effective rainfall, making less moisture available for soil replenishment and moisture surplus generation.

8.0 ELECTRICAL CONDUCTIVITY (EC) ROUTING

8.1 Introduction

Water quality parameters are useful tools for the detection and hydrological interpretation of source areas. It is also useful for tracing flowpaths of water through catchment areas. Chemical gauging by means of existing (natural) quality variations is often attractive, especially at the confluence of streams with different chemical characteristics, or to calculate groundwater inflow with a different composition from the stream (Appelo et al., 1983).

8.2 Electrical Conductivity (EC) routing.

Electrical Conductivity is a popular and easily measurable quality parameter in hydrology. When chemical variations are sufficiently great, changes in EC along the longitudinal profile permit calculation of groundwater contributions (lateral inflow in general) (Appelo et al.,1982) see Fig. 8.2a

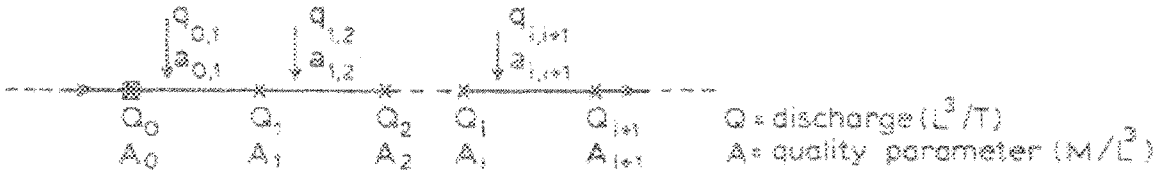

Fig. 8.2a Stream reaches that receive inflow of different quality can be coupled in a routing procedure.

The calculation of groundwater contributions starts with the continuity equation:

$$Q_i \cdot A_i + q_{i,\,i+1} \cdot a_{i,i+1} = Q_{i+1} * A_{i+1} \qquad (1)$$

where:
Q = discharge in the main stream
A = water quality in the main stream
q = discharge in the contributing stream, springs or seepage zones
a = water quality in the contributing stream, springs or seepage zones

$$Q_{i+1} = Q_{i+}q_{i,i+1} \quad (2)$$

when solving for channel discharge in a downstream direction, eqns 1 and 2 are combined to give

$$Q_{i+1} = Q_i \,.\, [(A_i - a_{i,i+1})/(Ai+1-a_{i,i+1})] = Q_i \,.\, R_{i+1} \quad (3)$$

and for the side inflow:

$$q_{i,i+1} = Q_i \,.\, [(A_{i+1} - A_i)/(a_{i,i+1} - A_{i+1})] = Q_i, S_{i,i+1} \quad (4)$$

From the above formulas groundwater recharge can be represented by the following equation:

EC of river upstream . discharge of river upstream + EC groundwater . groundwater inflow = (discharge of river . groundwater inflow) . EC of river downstream.

Groundwater inflow (Qgr) is the parameter which is unknown.

This method requires that the stream be divided into a number of individual reaches in which the homogeneity of transverse profiles with respect to the measured water quality is assured. The homogeneity of the profile depends on the spacing and type of contributing sources and tributaries, and on mixing characteristics of the stream course.

During fieldwork a number of EC routing in the Malewa catchment was done. The routing was comprised of measuring the EC in the main Malewa river, its tributaries, springs and seepage zones. The discharge of the river, where not measured, was estimated from available records. The EC of groundwater water was also estimated in places where data was not available. Because measurement was done during low flow regime the direct runoff parameter was not included in the calculations. The values obtained are shown in Table 8.2 and Fig. 8.2b.

8.3 Groundwater Inflow Calculation and Results

Calculation of groundwater inflow for varying areas of the catchment was made.

For the calculation of groundwater recharge from the upper northern catchment- Ol Kalou area (Stations, 2GB3, 2GB4 and 2GB5), to the area of Station 2GC4. The following parameters were input:

EC of the groundwater = 601µs/cm
EC of the surface water upstream = 85µs/cm
EC of the surface water downstream =104µs/cm
Discharge of the river upstream =537 l/sec
Area of Catchment = 985 *$10^6 m^2$

The calculation procedure is as follows:

85* 537 + 601 * Qgr = (537 + Q gr) * 104
5645 + 601 Qgr = 70884 + 104 Qgr
497 Qgr = 25239
Qgr = 51 l/sec
Qgr = .05 m^3 /sec
Qgr = 1.6 mm/year

Groundwater inflow from the upper northern catchment area to the area os Station 2GC4 was estimated to be 0.05 m^3/sec.

Input parameters for the estimation of the groundwater inflow from the eastern section of the catchment area (Kinangop area- Station 2GC5 and 2GC7) to the area of Station 2GC4 are as follows:

EC of the groundwater = 550µs/cm
EC of the surface water upstream = 84µs/cm
EC of the surface water downstream = 85µs/cm
Discharge of the river upstream = 437 l/sec
Area of Catchment = 137*$10^6 m^2$
The calculation is as follows:

84* 437 + 550 * Qgr = (437 + Q gr) * 85
36708 + 550 Qgr = 37145 + 85 Qgr
465 Qgr = 437
Qgr = 0.94 l/sec
Qgr = .0009m^3 /sec
Qgr = 0.21 mm/year

Estimated parameters for the estimation of groundwater inflow from the upper northern and eastern catchment (Ol Kalou and the Kinangop Plateau- Stations 2GB3, 2GB4 and 2GB5) to the area of 2GB1 are as follows:

EC of the groundwater = 550µs/cm
EC of the surface water upstream = 80 µs/cm
EC of surface water downstream = 132µs/cm
Discharge of river upstream = 400 l/sec.
Estimated area of catchment = $1817*10^6 m^2$
The calculation is as follows:

80* 400 + 550 Qgr = (400 + Q gr) * 132
32000 + 550 Qgr = 45200 + 132 Qgr
418 Qgr = 13200
Qgr = 31.6 l/sec
Qgr = .031 m^3 /sec
Qgr = 0.538 mm/year

Here it is estimated that groundwater recharge from the northern and eastern area of the catchment is approximately 0.030 m^3/sec.

Input Parameters Estimation of groundwater inflow along for the main Malewa river from the area of Turasha- Station 2GC4 to the Naivasha area (2GB1) are as follows:

EC of the groundwater = 550µs/cm
EC of the surface water upstream = 85µs/cm
EC of the surface water downstream = 132µs/cm
Discharge of the river upstream = 1258 l/sec
Estimated area of catchment = $1817*10^6 m^2$

The calculation is as follows:

85* 1258 + 550 Qgr = (1258 + Q gr) * 132
106930 + 550 Qgr = 166056 + 132 Qgr
418 Qgr = 59126
Qgr = 141.4 l/sec
Qgr = 0.141 m^3 /sec
Qgr = 2.45 mm/year

Fig. 8.3 shows the location of areas where the calculations were done.

8.4 Analysis of Results

From the following calculations of groundwater inflow into the Malewa river during the dry period (October 1997), it can be seen that there is more contribution of groundwater inflow (0.05 m3/sec or 1.6 mm/year from the northern section of the catchment than for the eastern section (0.0009m3/sec or 0.2 mm/year). For the eastern section of the catchment groundwater inflow is practically nil. Average groundwater inflow from the upper northern and eastern area was estimated to be 0.031 m3/sec or 0.5 mm/year. A groundwater inflow value of 0.141 m3/sec or 2.45 mm/year was calculated for the area of Turasha station -2GC4 to the area of station 2GB1.

On comparing the average groundwater inflow from northern and eastern catchment (1.8 mm) with that groundwater inflow calculated for both areas (0.5mm), it can be seen that there is a decrease in groundwater inflow of 1.3 mm/year along these tributaries. This could be attributed to grid faulting along the rift floor which acts as conduits and channel flow along the rift floor. However there is indication of groundwater inflow along the main tributary of the Malewa and there is an increase in inflow of 1.9 mm/year. This additional inflow is presumed to come from the area of the Kinangop Plateau where there is groundwater inflow from springs and seepage zones. These springs and seepage zones are thought to be the result of faulting which have offset relatively high permeability zones. Groundwater inflow is also possible from the areas west of the lake , such as the Mau Escarpment. There is also the possibility of groundwater inflow from adjacent catchments.

8.5 Errors and Limitation

One of the potential source of error could be due to the fact that the direct runoff component of streamflow was not considered in the calculations. This would lead to an overestimation of groundwater inflow.

The low values calculated along the major Malewa river and its tributaries could be attributed to the fact that the computations were done during the dry season where the rivers were at low-flow regime. Hence groundwater inflow would be expected to be minimal.

Values calculated could also be erroneous due to the fact the parameters such as the Ec of groundwater and discharge figures were estimated at localities where measurement was not done.

During calculation it was noted that sometimes there was very little differences between the Ec of the main river and the contributing streams. This situation increases the margin

for errors in the calculation of groundwater inflow. The use of Ec as a quality parameter is questionable as inflow of groundwater upstream from springs or seepage zones may not be reflected downstream due to the effect of dilution.

One of the main limitations in the hydrochemical method is that the chemical concentrations used for the shallow groundwater may not adequately represent the water that actually contributes to the stream during the storm. The chemistry of shallow groundwater obtained from wells near streams is commonly quite spatially variable (Freeze and Cherry -1979).

Table 8.1 EC values of surface water

X	Y	EC-value (us/cm)
209093	9926345	132
212845	9929674	126
210653	9941729	119
208823	9971118	132
212153	9971774	86
219850	9969405	73.7
219911	9969406	73
223373	9963150	71.9
225098	9961674	106
229089	9957905	70.9
230296	9955421	93.2
232058	9952852	69
234660	9945824	89.3
220819	9936896	130
220760	9936994	83.6
220693	9936914	84.3
226175	9939694	90.3
228370	9939051	83.5
223534	9931201	101
229736	9926996	72.3
210244	9945288	104
212998	9947832	85

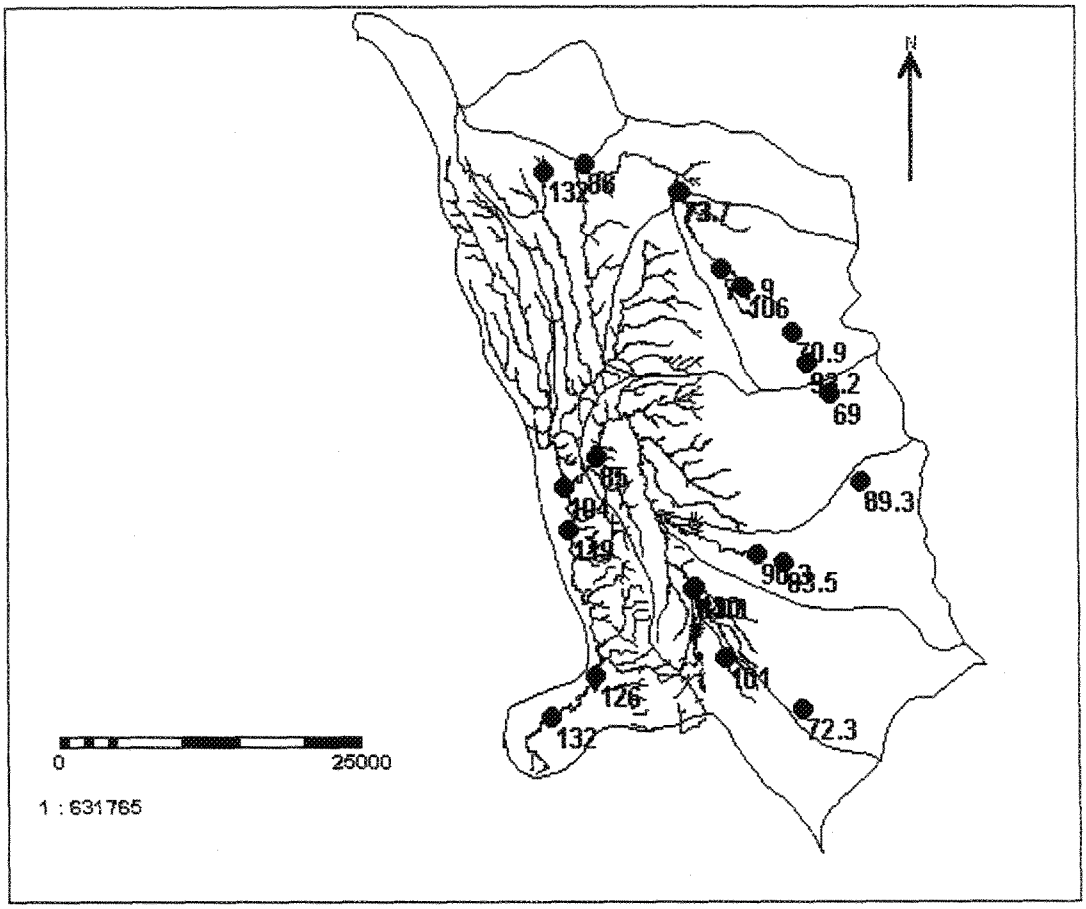

Fig. 8.2b Sites of Surface water EC measurements.

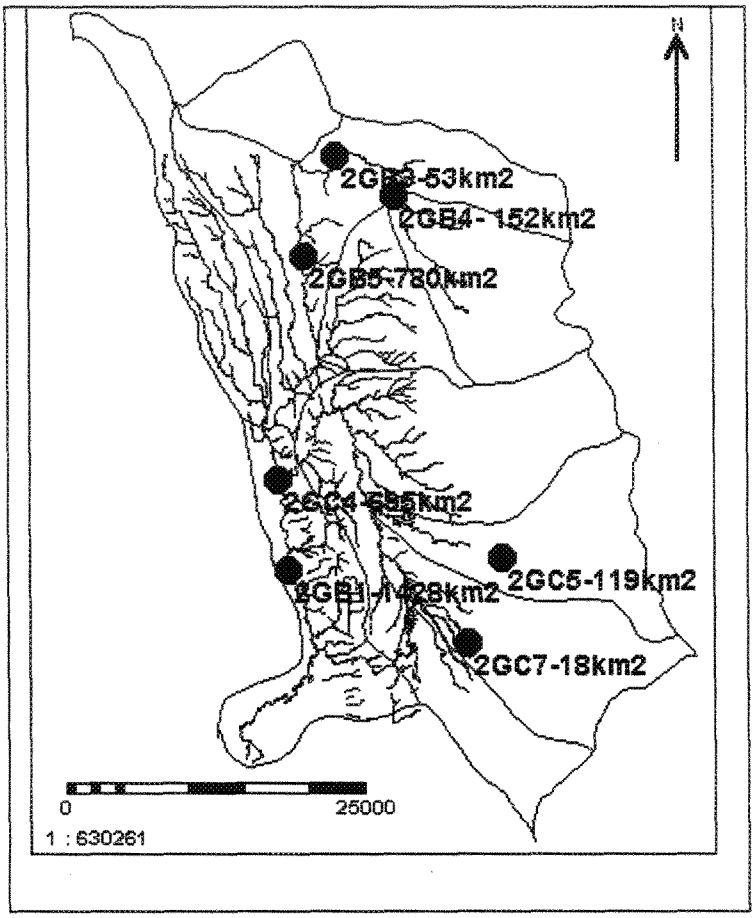

Fig. 8.3 Location of Areas where the Calculation of Groundwater Inflow was done.

9.0 DISCUSSION AND CONCLUSION

The study area presents an area which is quite diverse due to considerable differences in altitude and landforms. These give rise to variable climatic conditions ranging from semi-arid to humid. The variable annual rainfall (598-1279 mm) which was consistently lower than the Areal Evapotranspiration gave the impression that recharge does not occur. The Morton Model as coded here overestimates Areal Evapotranspiration for the catchment area. This is substantiated by the fact that studies carried out in adjacent study area, using Morton CRAE Model, indicate lower values than those calculated here. This discrepancy observed could be due to the inaccuracy of the data set used or errors in the programming codes used.

The resulting values of Potential Evapotranspiration and Areal Evapotranspiration are based on a data set from 1994-1997. This data set does not necessarily reflect the long term annual trends. Furthermore data was only available for two stations which lie outside the study area and hence it is questionable as to whether these station can accurately represent the diverse climatic conditions which exist inside the study area. Considering the large differences where yearly precipitation is less than Areal Evapotranspiration, the applicability of this method under these conditions needs to be further studied.

Groundwater recharge based on Streamflow Analysis indicate that recharge primarily comes from the upper catchment areas of Ol Kalou. There however is some loss of groundwater in the vicinity of Ol Kalou which could be attributed to the abstraction of groundwater from wells or to grid faulting along the rift floor which acts as conduits which channel flow along the rift floor. Baseflow across the Kinangop Plateau area did not show any evidence of being affected by faults which are found in this area. These faults are thought to act as barriers to groundwater flow and have offset zones of relatively high permeability. This is also substantiated by the fact that there are a number of springs and seepage zones in this vicinity. There was no evidence of loss of flow from the upper northern catchment areas and baseflow analysis estimate an annual average recharge value of 60 mm/year. Groundwater recharge over the catchment areas appears to be quite variable and it was observed that recharge primarily occurred over the areas which are at a higher elevation and which have relatively high rainfall. These areas correspond to the rift margins of the Kinangop Plateau and The Aberdares where groundwater recharge ranges from 112 to 290 mm/year. In the Rift Valley where semi-arid conditions exist , recharge was significantly less and varied between 49 to 69 mm /year. Total recharge over the River Malewa is estimated to be 137 mm/year.

Estimation of groundwater recharge using the" WTRBLN" model did not yield any reliable results. This could be due to either an overestimation in the Potential Evapotranspiration values or to an overestimation in the values calculated for direct runoff. Either situation would result in the Potential Evapotranspiration being greater than effective rainfall. In these situations no moisture surplus would be generated and

hence there would be no groundwater recharge. We however know that groundwater recharge does occur as evident by field observation and baseflow analysis. It was observed that even after the water capacity of the rooting zone was reduced , no moisture surplus occurred. It can be said that the "WTRBLN" method as calculated here did not yield results which are representative of the study area. However field verification of the input parameters, such as runoff and water capacity of the rootzone, during wet and dry periods would probably yield results which are indicative of the existing conditions.

Electrical conductivity (EC) routing done during the month of October indicate a groundwater inflow of 1.6 mm/year from the northern areas of the catchment such as the area of Ol Kalou and its environs. Calculations indicate that groundwater inflow from the area of the Kinangop Plateau was minimal (0.2 mm/year). This method verifies the results obtained by baseflow analysis and indicates that there is inflow of groundwater along the major Malewa river from Turasha to the main gauged station at 2GB1. This additional inflow is presumed to come from the area of the Kinangop Plateau through springs and seepage zones which is thought to occur as a result of extensive faulting which displaces relatively high permeability zones. Other sources of inflow could be from the Mau Escarpment (west of the study area), or from adjacent catchment. The point recharge estimation method used here assumes that the stream is homogeneous with respect to its water quality and its transverse profile. It also assumes that the mixing characteristics of the stream and its tributaries are known. Calculations as performed here assumes that the required conditions of the stream were met. In addition to this a number of parameters such as Ec of the groundwater and streamflow, were estimated. The fact that the direct runoff component was also omitted from the calculated implies that the method as applied here has a large degree of uncertainty. Despite these limitations in its applicability in this study, it however gives some indication of areas of groundwater inflow.

It can be concluded that in the absence of any other data, streamflow data can be used to quantify groundwater recharge at any location within a catchment area. The approach to baseflow separation, though subjective, can be estimated with some degree of accuracy. Although the results were not verified by any of the other methods, the data set used is considered to be fairly reliable and the filtering technique used has a fair degree of accuracy.

Variations in the recharge rates estimated by the above methods should not be viewed as a failure of any particular methodology but reflects the different constraints and the applicability which are inherent in each of the methodology used.

10.0 LIMITATIONS AND RECOMMENDATIONS

Despite arriving at a reasonable recharge rate using the method of baseflow separation, several limitations prohibited a more detailed analysis. They are as follow:

1) Meteorological data was not available for localities within the study area and had to be extrapolated from adjacent areas.

2) The soil map available was at a scale of 1:1,000,000 and only gave a general overview of soil which occur in the study area. Even though soil samples analyzed gave some indication of texture, given that the area is large, the soil map had to be used in conjunction with this data. The soil water holding capacity for the various areas is therefore subject to errors.

3) The Satellite Images and the Geology Map did not cover the entire study area and areas such as the Kinangop Plateau and the Aberdares were excluded

It is recommended that the necessary meteorological data be obtained and that the semi-permanent logging station be maintained in order to derive a more accurate climatological coverage of the study area. With this data, the "WTRBLN" model could be refined to arrive at an accurate estimate of recharge. It is suggested that field verification of the input parameters of the "WTRBLN" Model be done to obtain a value which accurately represents the waterbalance of the area. It is suggested that a groundwater recharge potential zonation map be derived to give a better spatial variation of recharge.

REFERENCES

Appelo C. A. J, Becht R, Van de Griend A. A and Sprierings T. C. M (1983). Buildup of discharge along the course of am mountain stream deduced from water-quality routings (EC routings). Journal of Hydrology, 66, pp 305-318.

Ase L. E, Sernbo K. and Syren P. (1986). Studies of Lake Naivasha, Kenya and its Drainage Area. Naturgeografiska Institutionen Stockholms Universteit, Forskningsrapport 63. 75 pp, Illustr.

Chow V. T (1964). Handbook of Applied Hydrology. Mc.Graw-Hill Book Co, London.

Clarke A. C. G, Allen D, Darling G. (1990) Geological, volcanological and hydrogeological Controls on the Occurrence of Geothermal Activity in the Area Surrounding Lake Naivasha, Kenya. Ministry of Energy, Republic of Kenya.

Donker N. H. W (1997). Water Balance Calculation of the Thornethwaite Type. Users Manual; 1-20.

Dune ,T., and Leopold, L.B.,(1978) Water in environmental Planning: W. H. Freeman and Co., San Francisco,818p.

Freeze R. A and Cherry J. A (1979). Groundwater. Prentice-Hall, Inc. Engle-wood Cliffs, N. J. USA, pp 222-224.

Karongo S. K and Sharma I. C (1997). An Evaluation of Actual Evapotranspiration in Tropical East Africa. Hydrological Processes, Vol. 11, pp 501-510.

Lake Naivasha Riparian Owners Association (1993). A Three Phase Environmental impact Study of Recent Developments Around Lake Naivasha, Phase 1, Executive Summary. John Goldson Associates, P.O. Box 70560, Nairobi Kenya (unpublished).

Lake Naivasha Riparian Owners Association (1996) . Lake Naivasha Management Plan. Incorporating Amendment List No.1.

Lillesand T. M and Kieffer R. W (1994). Remote Sensing and Image Interpretation, Third Edition. John Wiley and Sons, Inc. Canada.

Meijerink A. M. J, de Brouwer H. A. M, Mannaerts C. M, Valenzuela C. R, (1994) Introduction to The Use of Geographic Information Systems For Practical Hydrology, Unesco International Programme, IHP-IV M 2.3, International Institute of Aerospace Surveys and Earth Sciences (ITC). Publication Number 23.

Morton F. I., (1983). Operational Estimates of Areal Evapotranspiration and significant and Practice of Hydrology. Journal of Hydrology, pp 661-676.

Nathan.R.J., and MCMahon, T.A., (1990). Evaluation of Automated Techniwues for Base Flow ansd Recession Analyses. Water Research , Vol.26, No.7, Pages 1465-1473.

Podder. A. (1998) Estimation of Long-term Inflow into Lake Naivasha from the Malewa Catchment, Kenya. Msc. Thesis. ITC,Enschede, The Netherlands.

Schmitt K.(1991). The vegetation of the Aberdare National Park, Kenya. Innsbruck: Univ. - Ver l. Wagner, Hochgebirgsforschong; Vol. 8.

Sombroek W. G, Brown H. M. H and van der Pouw B. J. A (1982). Exploratory soil map and AGRO-CLIMATIC ZONE MAP OF KENYA (1980). Exploratory Soil Survey Report E1, Kenya Soil Survey, Nairobi.

Stuttard M. J, Narciso G, Oroda A, Hayball J. B, Suppo M, Isavwa L, Baraza J, Carizi G and Catani R (1995). Monitoring Lakes in Kenya: An Environmental Analysis Methodology for Developing Countries, Final Report to European Commission, contact No. TS3*-CT92-0016.

Thompson A. O and Dodson R. G (1963). Geology of Naivasha Area. Report Geol. Surv. Kenya 55.

Thornethwaite, C. W. and Mather, J.R.,(1957). Instructions and Tables for Computing Potential Evapotranspiration and the Waterbalance: Publ. Climatology, Lab. Climatology, Centeron, New Jersey, v.10 no3,244p.

Appendix I: Monthly Temperature Data- Nakuru and Nyeri

Station- Nakuru
Latitude-0016S
Altitude- 1901 m
Average Maximum, Minimum and Mean Temperature(oC)

Year		Jan	Feb	Mar	Apr	Month May	Jun	Jul	Aug	Sep	Oct	Nov	Dec
1994	max	83.8	84.8	85.8	86.8	87.8	88.8	89.8	90.8	91.8	92.8	93.8	94.8
	min	51.9	52.9	53.9	54.9	55.9	56.9	57.9	58.9	59.9	60.9	61.9	62.9
	mean	21.3	20.7	20.0	19.1	18.2	17.4	16.6	17.1	17.6	18.0	16.4	18.4
1995	max	83.1	83.4	80.2	80.0	77.3	79.0	74.2	77.7	77.4	76.0	76.8	76.4
	min	49.8	51.6	54.0	54.2	54.6	54.3	53.3	52.4	52.5	51.7	51.8	48.5
	mean	20.3	20.0	19.0	18.9	17.9	18.5	16.9	17.6	17.2	16.9	17.4	17.1
1996	max	81.4	83.6	82.0	79.9	77.5	70.4	73.5	75.4	77.1	78.5	75.8	69.3
	min	49.4	52.5	54.4	53.9	55.4	53.3	52.9	51.8	51.0	50.4	51.7	42.9
	mean	18.5	20.0	19.3	19.3	18.3	16.0	16.3	17.0	16.6	16.9	17.1	13.9
1997	max	82.2	84.5	78.4	70.7	76.4	76.3	70.6	63.8	78.7	76.5	73.4	73.4
	min	51.4	49.4	48.7	52.5	52.5	53.3	51.6	42.6	49.0	54.3	56.7	56.7
	mean	19.7	20.5	18.0	15.3	17.5	17.6	18.1	18.6	19.1	18.0	17.5	17.5

Station- Nyeri
Latitude-0030S
Altitude- 1759 m
Average Maximum, Minimum and Mean Temperature(oC)

		Month											
Year		Jan	Feb	Mar	Apr	May	Jun	Jul	Aug	Sep	Oct	Nov	Dec
1994	max	83.8	84.8	85.8	86.8	87.8	88.8	89.8	90.8	91.8	92.8	93.8	94.8
	min	51.9	52.9	53.9	54.9	55.9	56.9	57.9	58.9	59.9	60.9	61.9	62.9
	mean	21.3	20.7	20.0	19.1	18.2	17.4	16.6	17.1	17.6	18.0	18.4	18.4
1995	max	83.1	83.4	80.2	80.0	77.3	79.0	74.2	77.7	77.4	76.0	76.8	76.4
	min	49.8	51.6	54.0	54.2	54.6	54.3	53.3	52.4	52.5	51.7	51.8	48.5
	mean	20.3	20.0	19.0	18.9	17.9	18.5	16.9	17.6	17.2	16.9	17.4	17.1
1996	max	81.4	83.6	82.0	79.9	77.5	70.4	73.5	75.4	77.1	78.5	75.8	69.3
	min	49.4	52.5	54.4	53.9	55.4	53.3	52.9	51.8	51.0	50.4	51.7	42.9
	mean	18.5	20.0	19.3	19.3	18.3	16.0	16.3	17.0	16.6	16.9	17.1	13.9
1997	max	82.2	84.5	78.4	70.7	76.4	76.3	70.6	63.8	76.7	76.5	73.4	73.4
	min	51.4	49.4	48.7	52.5	52.5	53.3	51.6	42.6	49.0	54.3	56.7	56.7
	mean	19.7	20.5	18.0	15.3	17.5	17.6	16.1	16.6	19.1	18.0	17.5	17.5

Appendix II : Code of Mortons (1983) CRAE Model and Input Meteorological data for Stations- Nakuru and Nyeri.

Program Mortons 1983 CRAE Model written by A.S.M. Gieske

```
Program Morton3;  {Morton, J. Hydr., 1983, version 1.0, 26/3/1998}
{$R+}          {Nyeri1.dat}     {TURBO 7.0 PASCAL}
{$N+}
uses graph,crt,printer;
var
  i,n,nit: integer;
  phi,H,Pa,ps,pps,azd,T,Td,S,vd,v,DELTA,theta,cosZ,cosOM,OM,sinOM: double;
  alfa,beta,phir,thetar,OMr,tanOM,coszz,eta,GE: double;
  sinZ,azz,upl1,cz,az,azero,z,W,c1,j,term1,term2,term3,tau,ta: double;
  bz,gamps,gamp,fz,ft,lam,dtp,tp,vp,Gz,G,a,c2,eps,rho,B,RT,RTC: double;
  dp,zeta,ETP,RTP,ETW,ET,ltheat: double;
  datfile,outfile: text;
  fn,fn1,title: string[80];
  xc,yc,ii,ndata,graphdriver,graphmode: integer;
  color: word;
  art,apet,aet: array[1..100] of double;
begin
  {Station data}
  phi:=-0.30;  {latitude degrees}
  phir:=pi*phi/180.0;
  H:=1759.0;  {elevation, m}
  Pa:=924.0;  {avg precipitation, mm}
  ps:=1013;    {standard pressure mbar at sea level}
  pps:=exp(5.256*ln((288-0.0065*H)/288));                    {C-1}
  azd:=0.26-0.00012*Pa*sqrt(pps)*(1+abs(phi/42)+(phi/42)*(phi/42));   {C-2}
  if azd>0.17 then azd:=0.17;
  if azd<0.11 then azd:=0.11;
  fn1:='out2.dat';
  assign(outfile,fn1); rewrite(outfile);
  writeln(outfile,'number  radiation   potential    actual');
  {Monthly input}
  fn:='nyeri1.dat';
  assign(datfile,fn); reset(datfile);
  ndata:=48;
  readln(datfile,title);
  for ii:=1 to ndata do begin
   readln(datfile,i,n,Td,T,S);
  {Computations}
  if T>=0.0 then alfa:=17.27 else alfa:=21.88;
  if T>=0.0 then beta:=237.3 else beta:=265.5;
  vd:=6.11*exp(17.27*Td/(Td+237.3));     {C-3}
  v:=6.11*exp(alfa*T/(T+beta));          {C-4}
  DELTA:=alfa*beta*v/((T+beta)*(T+beta)); {C-5}
  theta:=23.2*sin(pi*(29.5*i-94)/180.0);  {C-6}
  thetar:=pi*theta/180.0;
  cosZ:=cos(phir-thetar);                {C-7}
  sinZ:=sin(phir-thetar);  {needed in Eqn C-15}
  if cosZ<0.001 then cosZ:=0.001;        {C-7a}
```

```
if sinZ<0.001 then sinZ:=0.001;
cosOM:=1-cosZ/(cos(phir)*cos(thetar)); {C-8}
if cosOM<-1 then cosOM:=-1;          {C-8a}
sinOM:=sqrt(1-cosOM*cosOM);
tanOM:=abs(sinOM/cosOM);
OMr:=arctan(tanOM);
OM:=180.0*OMr/pi;
if cosOM<0 then begin OMr:=pi-OMr; OM:=180.0-OM; end;
coszz:=cosZ+(sinOM/OMr-1.0)*cos(phir)*cos(thetar);  {C-9}
eta:=1+(1.0/60.0)*sin(pi*(29.5*i-106)/180.0);       {C-10}
GE:=(1354.0/(eta*eta))*(OM/180)*coszz;              {C-11}
azz:=azd;                                  {C-12}
if azz<0.11 then azz:=0.11;
  upl1:=0.5*(0.91-vd/v);
if azz>upl1 then azz:=upl1;                        {C-12a}
cz:=v-vd;                                  {C-13}
if cz>1 then cz:=1.0;
if cz<0 then cz:=0.0;                          {C-13a}
az:=azz+(1-cz*cz)*(0.34-azz);                      {C-14}
Z:=180.0*arctan(sinZ/cosZ)/pi;
{both sinZ and cosZ>0}
azero:=az*(exp(1.08)-(2.16*cosZ/pi+sinZ)*exp(0.012*Z))/
   (1.473*(1-sinZ));                       {C-15}
W:=vd/(0.49+T/129);                            {C-16}
c1:=21.0-T;                                {C-17}
if c1<0.0 then c1:=0.0;
if c1>5.0 then c1:=5.0;                        {C-17a}
j:=(0.5+2.5*coszz*coszz)*exp(c1*(pps-1));          {C-18}
  term1:=exp(0.75*ln(pps/coszz));
  term2:=exp(0.90*ln(j/coszz));
  term3:=exp(0.60*ln(W/coszz));
tau:=exp(-0.089*term1-0.083*term2-0.029*term3);     {C-19}
  term1:=exp(0.3*ln(W/coszz));
ta:=exp(-0.0415*term2-sqrt(0.0029)*term1);          {C-20}
  upl1:=exp(-0.0415*term2-0.029*term3);
if ta<upl1 then ta:=upl1;                      {C-20a}
Gz:=GE*tau*(1.0+(1.0-tau/ta)*(1+azero*tau));       {C-21}
G:=S*Gz+(0.08+0.30*S)*(1-S)*GE;                {C-22}
a:=azero*(S+(1-S)*(1-Z/330));                  {C-23}
c2:=10.0*(vd/v-S-0.42);                        {C-24}
if c2>1.0 then c2:=1.0;
if c2<0.0 then c2:=0.0;                        {C-24a}
rho:=0.18*((1-c2)*(1-S)*(1-S)+c2*sqrt(1-S))/pps;    {C-25}
eps:=5.22e-08;
term1:=eps*(T+273)*(T+273)*(T+273)*(T+273);
B:=term1*(1-(0.71+0.007*vd*pps)*(1+rho));          {C-26}
if B<0.05*term1 then B:=0.05*term1;            {C-26a}
RT:=(1-a)*G-B;                                 {C-27}
RTC:=RT;                                   {C-28}
if RTC<0.0 then RTC:=0.0;                      {C-28a}
bz:=1.0;  {1.0 for the CRAE model}
if T>=0.0 then fz:=28.0 else fz:=28.0*1.15;
if T>=0.0 then gamps:=0.66 else gamps:=0.66/1.15;
gamp:=gamps*pps;
zeta:=0.28*(1.0+vd/v)+DELTA*RTC/(gamp*bz*fz*(v-vd)/sqrt(pps)); {C-29}
```

```
if zeta>1.0 then zeta:=1.0;                          {C-29a}
ft:=fz*zeta/sqrt(pps);                               {C-30}
lam:=gamp+4*eps*(T+273)*(T+273)*(T+273)/ft;          {C-31}
{iterative procedure to estimate tp,vp and dp}
{initial values}
tp:=T;
vp:=v;
dp:=DELTA;
nit:=0;
repeat
  dtp:=(RT/ft+vd-vp+lam*(T-tp))/(dp+lam);
  tp:=tp+dtp;
  vp:=6.11*exp(alfa*tp/(tp+beta));
  dp:=alfa*beta*vp/((tp+beta)*(tp+beta));
  nit:=nit+1;
until (abs(dtp)<0.01);                               {C-32 to C-35}
{POTENTIAL EVAPOTRANSPIRATION}
ETP:=RT-lam*ft*(tp-T);                               {C-36}
{NET RADIATION AT THE EQUILIBRIUM TEMP TP}
RTP:=ETP+gamp*ft*(tp-T);                             {C-37}
{WET ENVIRONMENT AREAL EVAPOTRANSPIRATION}
ETW:=14.0+1.20*RTP/(1+gamp/dp);                      {C-38}
if ETW>ETP then ETW:=ETP;
if ETW<0.5*ETP then ETW:=0.5*ETP;                    {C-38a}
{AREAL EVAPOTRANSPIRATION}
ET:=2.0*ETW-ETP;                                     {C-39}
{UNIT CONVERSION FROM W/m2 TO mm}
if T>=0.0 then ltheat:=28.5 else ltheat:=28.5*1.15;
RT:=RT*n/ltheat;
  art[ii]:=RT;
ETP:=ETP*n/ltheat;
  apet[ii]:=ETP;
ET:=ET*n/ltheat;
  aet[ii]:=ET;
writeln(outfile,ii:5,' ',RT:10:3,' ',ETP:10:3,' ',ET:10:3);
end;
close(datfile);
close(outfile);
graphdriver:=detect;
initgraph(graphdriver,graphmode,'c:\tp\bgi');
line(10,0,10,300);
line(10,300,510,300);
{plot PET}
setcolor(yellow);
xc:=20; yc:=300-trunc(apet[1]);
moveto(xc,yc);
for ii:=2 to ndata do begin
  xc:=10+10*ii;
  yc:=300-trunc(apet[ii]);
  lineto(xc,yc);
end;
{plot AET}
setcolor(red);
xc:=20; yc:=300-trunc(aet[1]);
moveto(xc,yc);
```

```
  for ii:=1 to ndata do begin
    xc:=10+10*ii;
    yc:=300-trunc(aet[ii]);
    lineto(xc,yc);
  end;
  readln;
  closegraph;
end.
```

Input Data for Station-Nyeri (1994-1997)

Month#	n	Tdew	Tmean	S	ϕ	H	Pa
1	31	11.9	18.1	0.728	30	1759	924
2	28	11.7	18.0	0.774			
3	31	11.6	17.8	0.696			
4	30	12.7	16.8	0.618			
5	31	13.8	16.9	0.678			
6	30	13.5	16.3	0.788			
7	31	12.8	15.6	0.761			
8	31	12.6	15.4	0.7			
9	30	12.0	17.1	0.709			
10	31	13.3	18.5	0.607			
11	30	12.4	15.0	0.528			
12	31	13.2	17.5	0.674			
1	31	11.9	18.4	0.725			
2	28	11.8	18.8	0.773			
3	31	13.9	18.6	0.684			
4	30	15.0	18.8	0.614			
5	31	15.3	18.0	0.678			
6	30	13.8	17.0	0.79			
7	31	12.8	15.9	0.762			
8	31	11.4	14.7	0.706			
9	30	12.0	15.7	0.7			
10	31	12.8	16.4	0.599			
11	30	12.8	16.5	0.528			
12	31	12.7	16.6	0.671			
1	31	12.6	16.7	0.714			
2	28	12.9	17.9	0.768			
3	31	10.5	15.0	0.687			
4	30	14.5	19.2	0.621			
5	31	13.9	17.8	0.68			
6	30	13.4	16.4	0.787			
7	31	12.8	14.9	0.76			
8	31	12.3	15.7	0.696			
9	30	12.0	17.7	0.699			
10	31	12.0	18.6	0.605			
11	30	13.8	17.7	0.529			
12	31	8.2	13.3	0.691			
1	31	11.2	18.7	0.716			
2	28	8.0	19.4	0.792			
3	31	12.3	20.0	0.709			
4	30	11.2	18.9	0.616			
5	31	10.0	17.8	0.682			
6	30	13.8	17.2	0.790			
7	31	11.8	14.9	0.758			
8	31	13.7	16.7	0.690			
9	30	15.5	18.5	0.692			
10	31	14.3	17.9	0.600			
11	30	15.2	17.5	0.519			
12	31	15.2	17.5	0.649			

Input Data for Station Nakuru (1994-1997)

Month #	n	Tdew	Tmean	S	ϕ	H	Pa
1	31	6.5	21.3	0.599	16	1901	871
2	28	8.1	20.7	0.655			
3	31	9.6	20.0	0.580			
4	30	12.1	19.1	0.510			
5	31	12.9	18.2	0.583			
6	30	12.4	17.4	0.704			
7	31	11.9	16.6	0.671			
8	31	11.2	17.1	0.597			
9	30	10.4	17.6	0.600			
10	31	11.2	18.0	0.494			
11	30	12.4	16.4	0.418			
12	31	10.1	18.4	0.564			
1	31	7.1	20.3	0.599			
2	28	8.1	20.0	0.655			
3	31	11.8	19.0	0.580			
4	30	12.8	18.9	0.510			
5	31	12.8	17.9	0.583			
6	30	12.3	18.5	0.704			
7	31	11.8	16.9	0.671			
8	31	10.2	17.6	0.597			
9	30	11.9	17.2	0.600			
10	31	12.7	16.9	0.494			
11	30	12.5	17.4	0.418			
12	31	10.4	17.1	0.564			
1	31	8.9	18.5	0.599			
2	28	9.2	20.0	0.655			
3	31	11.3	19.3	0.580			
4	30	11.5	19.3	0.510			
5	31	12.6	18.3	0.583			
6	30	12.3	16.0	0.704			
7	31	12.1	16.3	0.671			
8	31	12.0	17.0	0.597			
9	30	12.0	16.6	0.600			
10	31	11.4	16.9	0.494			
11	30	12.2	17.1	0.418			
12	31	5.9	13.9	0.564			
1	31	8.7	19.7	0.599			
2	28	4.4	20.5	0.655			
3	31	6.6	18.0	0.580			
4	30	11.8	15.3	0.510			
5	31	12.0	17.5	0.583			
6	30	12.3	17.6	0.704			
7	31	12.8	18.1	0.671			
8	31	13.3	18.6	0.597			
9	30	13.8	19.1	0.600			
10	31	12.7	18.0	0.494			
11	30	14.4	17.5	0.418			
12	31	14.4	17.5	0.564			

Where:

Month# = month number
n = number of days in the month
Tdew = average dew-point temperature in degree Celsius
Tmean = mean temperature in degree Celsius
S = ratio of observed to maximum possible sunshine duration
ϕ = latitude in degrees
H =altitude above mean sea level
P_A = average annual precipitation